THE MECHANISMS OF pMHC RECOGNITION BY THE AHIII T CELL RECEPTOR

Peter J. Miller

A dissertation submitted to the faculty of the University of North Carolina at Chapel Hill in partial fulfillment of the requirements for the degree of Doctor of Philosophy in the Department of Biochemistry and Biophysics.

Chapel Hill
2008

Approved by:

Advisor: Edward J. Collins, Ph.D.

Reader: Barry Lentz, Ph.D.

Reader: Gary Pielak, Ph.D.

Reader: Dale Ramsden, Ph.D.

Reader: Matthew Redinbo, Ph.D.

Reader: Roland Tisch, Ph.D.

ABSTRACT

Peter J. Miller

THE MECHANISMS OF pMHC RECOGNITION BY THE AHIII T CELL RECEPTOR

Cytotoxic T lymphocytes (CTL), or $CD8^+$ T cells, are responsible for clearing infected or diseased cells from the body. Diseased cells label themselves through presentation of non-self, or antigenic, peptides on the exterior of the cell. Both healthy and infected cells present peptides on the surface. These self and non-self peptides are presented by the class I major histompatibility complex molecule, or MHC. The class I peptide-MHC (pMHC) complex is the ligand for the T cell receptor (TCR), which is expressed on the surface of CTLs. TCR discrimination between self and non-self pMHC is the critical event in determining whether or not the CTL will be activated and lyse the antigen presenting cell. It remains unclear through what mechanism(s) the recognition of different pMHC by the TCR translates into qualitatively different activation signals in the T cell.

The AHIII12.2 (AHIII) TCR recognizes and is activated by its cognate pMHC, p1049 in HLA-A2(A2) Activation of AHIII T cells is inhibited by the peptide p1058 when presented by A2. Through mutation of residues in both the peptides and MHC, we present here further support for the affinity model of T cell triggering, that AHIII T cell activation correlates with TCR-pMHC binding affinity. Interestingly, mutations in the

peptide seem to be more deleterious to binding than mutations in the MHC. Crystal structures of A2 mutants bound to the AHIII TCR were determined, and showed that the K66A mutation in the MHC can influence the conformation of a TCR CDR3 loop, which is generally thought of as being restricted to peptide recognition. Thermodynamic analysis of AHIII-p1049/A2(K66A) binding confirmed that the loop movement results in a loss of H-bonds. Thermodynamic analysis of the AHIII TCR binding to wild-type p1049/A2 determined that binding occurs through favorable enthalpy and favor entropy, which contradicts the favored thermodynamic TCR-pMHC binding model of enthalpically driven and entropically apposed binding. Finally, we present here a streamlined protocol to express and purify soluble TCR from singly isolated T cells directly *ex vivo*.

ACKNOWLEDGEMENTS

One of the reasons that I joined the laboratory of Dr. Edward Collins was because of its smaller size. I had been out of school for a few years and felt that I would benefit from more one-on-one guidance from my Principal Investigator, and I truly have. His door was always open, he was always eager to discuss science (or anything for that matter), he guided my research through the years, and taught me how to think critically and approach questions scientifically. Over the years Ed also became a friend, which I value as much as all the scientific training I will take from his lab.

With many roles to fill and fewer people to fill them, a smaller lab also forces you to count more on your colleagues. There is no way that I would have been able to complete the work presented in this dissertation if it were not for the help of Dr. David Riddle in the Collins lab. David has taught me most of what I know about cell culture, molecular biology techniques, and general immunology. He has also become a great friend during the last five years, and I will miss our morning chats over lab-brewed Café Americano.

The other individual from the Collins laboratory I would like to acknowledge individually is Dr. Yael Pazy. Yael was a part of the Collins lab the first two years of my graduate career. I worked directly with her on the crystallization and data collection of the molecules presented in Chapter 2. Together with Ed, she taught me most of the x-ray crystallography skills that I have today.

I would like to thank all of the members of the Frelinger lab, with whom we had lab meeting every week, especially Dr. Jeff Frelinger and Dr. Shaomin Tian. Even though some members would glaze over when I talked about diffraction patterns, van der Waals contacts, and thermodynamics, they were always willing to help with suggestions on cell culture, FACS, and kept me focused on the real goal of my experiments: T cell immunology. I would also like to thank the other members of my committee: Dr. Barry Lentz, Dr. Gary Pielak, Dr. Dale Ramsden, Dr. Matthew Redinbo, and Dr. Roland Tisch, for their support and guidance in the classroom and with my research. Special thanks goes to Dr. Ashutosh Tripathy for his help with all the ITC and SPR experiments and Dr. Laurie Betts for her help with x-ray data collection.

Finally, I would like to thank the members of my family. First, my parents, Charles and Susan Miller, who instilled in me a passion for learning and always encouraged me to do well in school. Most importantly, I want to thank my beautiful wife, Elizabeth Coble, who met me when I had a "real" job and yet supported my decision to leave that and follow my dream to pursue a Ph.D. She may not have always understood what I told her when she asked about my day, but she has been there through all the ups and downs of my research, and will continue to be there for me always.

TABLE OF CONTENTS

Page

LIST OF TABLES

Table

LIST OF FIGURES

Figure

LIST OF ABBREVIATIONS AND SYMBOLS

α	alpha
A (Ala)	alanine
Å	angstrom
APL	altered peptide ligand
APC	antigen presenting cell
ATP	adenosine tri-phosphate
β	beta
β_2m	beta-2-microglobulin
C (Cys)	cysteine
°C	degrees Celsius
Cα	constant domain of TCR alpha chain, or α carbon of peptide backbone
Ca^{2+}	calcium
cal	calorie
CO_2	carbon dioxide
Cβ	constant domain of TCR beta chain, or β carbon of peptide backbone
CCP4	Collaborative Computational Project 4
CD	cluster of differentiation
cDNA	coding deoxyribonucleic acid
CDR	complementarity determining region

^{51}Cr	radioactive chromium
CTL	cytotoxic T lymphocyte, $CD8^+$ T cell
Da	Dalton
D (Asp)	aspartic acid
D	diversity gene segment
ΔG	change in Gibbs free energy
ΔH	change in enthalpy
ΔS	change in entropy
ΔC_p	change in heat capacity at constant pressure
δ	delta
DMSO	dimethyl sulfoxide
E (Glu)	glutamic acid
ε	epsilon
E. coli	Escherichia coli
EDTA	ethylene diamine tetraacetic acid
ELISA	enzyme-linked immunosorbet assay
ER	endoplasmic reticulum
F (Phe)	phenylalanine
FACS	fluorescence-activated cell sorting
FITC	fluorescein isothiocyanate
g	gram
G (Gly)	glycine
γ	gamma

H (His)	histidine
H-2	histocompatibility-2 (murine MHC)
H-bonds	hydrogen bonds
HCl	hydrochloric acid
HEPES	4-(2-hydroxyethyl)-1-piperaineethane sulfonic acid))
HLA	human leukocyte antigen (human MHC)
HPLC	high performance liquid chromatography
HRP	horseradish peroxidase
I (Ile)	isoleucine
IFNγ	interferon gamma
Ig	immunoglobulin
IL	interleukin
IPTG	isopropyl-β-D-thiogalatopranoside
J	joining gene segment
ITAM	immunoreceptor tyrosine-based activation motif
K (Lys)	lysine
K	kelvin
K_a	association constant
K_d	dissociation constant
k_{on}	kinetic on-rate
k_{off}	kinetic off-rate
k	kilo
L (Leu)	leucine

L or l	liter
ln	natural log
m	milli
M (Met)	methionine
M	molarity
μ	micro
MFI	mean fluorescence intensity
$MgCl_2$	magnesium chloride
MHC	major histocompatibility complex
$MnCl_2$	manganese chloride
mol	mole
N (Asn)	asparigine
NaCl	sodium chloride
ND	not determined
NK	natural kill cells
P (Pro)	proline
PBS	phosphate-buffered saline
Q (Gln)	glutamine
R (Arg)	arginine
RU	response unit
s (sec)	second
S (Ser)	serine
σ	sigma (standard deviation)

SDS-PAGE	sodium dodecyl sulfate – polyacrylamide gel electrophoresis
SPR	surface plasmon resonance
T (Thr)	threonine
$t_{1/2}$	half-life
TBS	tris-buffered saline
TCR	T cell receptor
TNFα	tumor necrosis factor alpha
Tris	tris[hydroxymethyl]aminomethane
V (Val)	valine
V	variable gene segment
Vα	TCR alpha chain variable domain
Vβ	TCR beta chain variable domain
vdW	van der Waals
W (Trp)	tryptophan
WT	wild-type
χ	chi
Y (Tyr)	tyrosine
ζ	zeta

CHAPTER 1

INTRODUCTION

1.1 Overview

Cytotoxic T lymphocytes (CTL), or $CD8^+$ T cells, are a critical component of the adaptive immune response to infection. They are required for the elimination of infected host cells, which are harboring virus or intracellular bacteria. CTL are also responsible for the recognition and elimination of aberrant self-cells like cancers. These infected or cancerous cells are labeled as such by self-presentation of non-self, or antigenic, peptides on the exterior of the cell. Both healthy and uninfected cells present self-peptides on the surface. These self and antigenic peptides are presented in the context of the class I major histompatibility complex molecule, or MHC. The class I peptide-MHC (pMHC) complex is the ligand for the T cell receptor (TCR), which is expressed on the surface of CTLs. If a TCR recognizes the peptide in the MHC as antigenic, the CTL will be activated, lysing the target cell and secreting immunostimulatory cytokines. The interaction between the pMHC and the TCR is paramount; it determines whether or not the CTL will respond to a target cell. Surprisingly, after almost two decades of research it is still unclear through which mechanism(s) of molecular recognition the TCR discriminates a self from a foreign pMHC. The work presented here attempts to answer

what mechanism(s) are involved in the AHIII recognition of its cognate pMHC molecules.

1.2 Presentation of Peptide in the Context of MHC

1.2.1 Properties of Class I MHC

Class I major histocompatibility complex (MHC) molecules are heterotrimeric complexes comprised of a ~44 kDa heavy chain, a non-covalently bound 12 kDa protein, β_2-microglobulin (β_2m), and peptide (Figure 1a). Nomenclature for class I MHC is H-2 in mice and Human Leukocyte Antigen (HLA) in humans. The α1 and α2 α helices of the MHC along with the beta sheet floor create a peptide-binding cleft (Figure 1b). Class I MHC molecules are constitutively expressed on the plasma membrane of all nucleated cells, and typically present endogenous self-peptides. The presence of class I MHC molecules with those endogenous peptides on the surface of the cell is required for $CD8^+$ T cell homeostasis (Kieper and Jameson, 1999).

Class I MHC is polygenic, having three alleles A, B, and C in humans. The MHC is also the most polymorphic gene family known in vertebrates. Increasing diversity even more, MHC genes are co-dominantly expressed, meaning humans may have up to six different class I isoforms (Parham et al., 1995). However, the crystallographic structures of class I MHC molecules are similar regardless of the isoform, allotype, or species of origin (Collins et al., 1995; Fremont et al., 1992; Garrett et al., 1989; Guo et al., 1992; Kjer-Nielsen et al., 2002; Madden et al., 1991; Meijers et al., 2005; Saper et al., 1991; Zhang et al., 1992; Zhao et al., 1999). This is because the distribution of polymorphic residues is not randomly scattered through the molecule, but rather they are located in the

a.

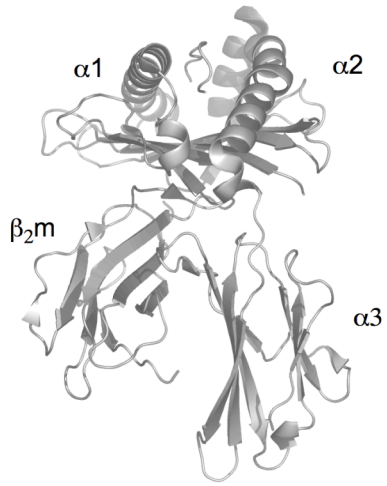

b.

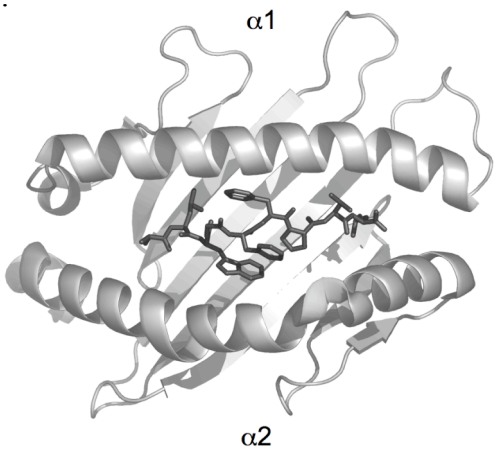

c.

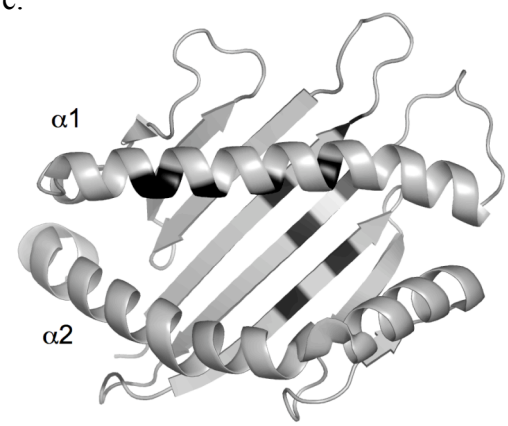

d.

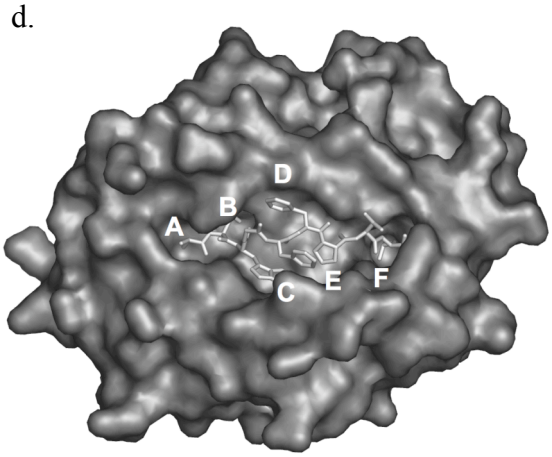

e.

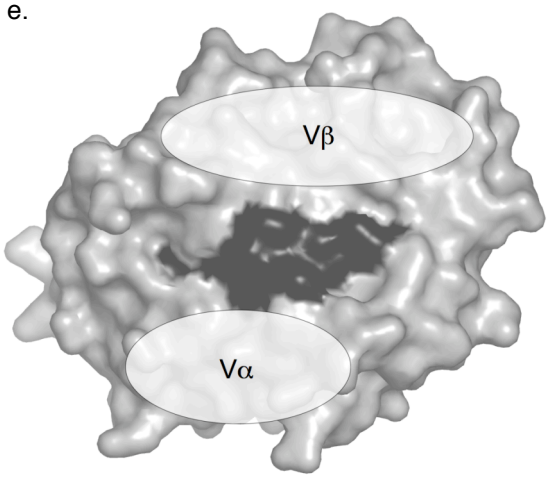

Figure 1. Class I MHC molecule. (a) Heterotrimeric complex composed of MHC class I heavy chain, β_2m, and peptide. The peptide binding cleft created by the α1 and α2 α helices and the beta sheet floor is easily seen from the side. (b) A top view of the peptide binding cleft of the class I MHC molecule. Bound peptide, p1049 (ALWGFFPYL), is colored black. (c) The polymorphic regions of the class I MHC molecule, shaded black, reside primarily within the α1 helix and beta sheet floor of the peptide binding cleft. (d) The chemical and spatial composition of the peptide binding cleft creates six binding pockets in HLA-A2, labeled A-F. Pockets A, B, and F are especially prominent and accommodate the amino terminus, the side chain of P2, and the carboxyl-terminal leucine, respectively. (e) The molecular surface of the peptide/MHC complex is dictated by the bound peptide and the conformation of the MHC heavy chain. Peptide surface atoms are shaded black. Elipses represent the binding regions of TCR domains that make contact with the MHC heavy chain based on crystal structures of pMHC-TCR complexes with the Vα binding on the α2 domain and the Vβ binding more diffusely on the α1 domain. Figures were generated using PyMOL (DeLano, 2002).

peptide binding cleft (Figure 1c). This allows the MHC to bind peptides with a diverse set of identities.

Examination of peptide/MHC structures reveal that not all peptide side chains are solvent exposed for TCR recognition. Some of these side chains bind in pockets, termed specificity pockets, down in the peptide-binding cleft of the MHC (Figure 1d). Pocket A is composed of conserved residues that act as hydrogen bond acceptors for the amino terminus of the peptide backbone. The entrance to the F pocket provides conserved hydrogen bond donors for the negatively charged carboxyl terminus of the peptide (Matsumura et al., 1992). Pockets B-E and the base of pocket F are formed by a small set of conserved residues in conjunction with the polymorphic residues in the MHC. These pockets are used to bind a variety of peptide side chains depending on the identity of the MHC molecule and the peptide.

1.2.2 Properties of Peptides

Peptides bound in class I MHC are typically eight to ten residues in length. This strict requirement in length led to early predictions of class I peptides bulging in order to fit into the binding pocket of the class I MHC molecule (Maryanski et al., 1990), which

has been confirmed by a number of peptide-MHC complex crystal structures (Collins et al., 1995; Fremont et al., 1992; Garrett et al., 1989; Guo et al., 1992; Kjer-Nielsen et al., 2002; Madden et al., 1991; Meijers et al., 2005; Saper et al., 1991; Zhang et al., 1992; Zhao et al., 1999). All peptides have a hydrophobic carboxyl-terminal end, with a predominance of leucine, isoleucine, or valine. Each allelic peptide tends to have an additional anchor residue besides the one found at the carboxyl terminus (Falk et al., 1991). As a result of their specificity pockets, different MHC proteins bind different subsets of peptides. The specificity pockets of HLA-A2 are shown in Figure 1e. Importantly, as it relates to the data presented in this body of work, in addition to primary anchors of position 2 (P2) and P9, positions 1, 3, and 7 have been identified as secondary anchors, as they bind into the specificity pockets A, C, and E, respectively. Leucine or Methionine is preferred at P2 and a large bulky aromatic at P3 (Ruppert et al., 1993). This propensity for particular amino acids at particular positions allows one to predict the

Table 1. Peptide Binding Motifs of Common MHC Alleles

	Position								
Allele	1	2	3	4	5	6	7	8/9/10	**Reference**
HLA-A1	-	T,S	D,E	-	-	-	-	Y	(Kubo et al., 1994)
HLA-A2	-	L,M	-	-	-	-	-	V,L	(Falk et al., 1991)
HLA-A3	-	V,L,M	-	-	-	-	-	K	(Kubo et al., 1994)
HLA-A11	-	T,V	-	-	-	-	-	K	(Kubo et al., 1994; Zhang et al., 1993)
HLA-A24	-	Y	-	-	-	-	-	F,L	(Kubo et al., 1994)
HLA-B27	-	R	-	-	-	-	-	K	(Jardetzky et al., 1991)
H-2K^{d}	-	Y	-	-	-	-	-	L,I	(Falk et al., 1991)
H-2D^{b}	-	-	-	-	N	-	-	M,I	(Falk et al., 1991)
H-2K^{b}	-	-	-	-	F,Y	-	-	L	(Falk et al., 1991)
H-2L^{d}	-	P	-	-	-	-	-	L,F,M	(Corr et al., 1992)
H-2D^{d}	-	G	P	-	-	-	-	L,I,F	(Corr et al., 1993)

types of peptides that may bind to a particular MHC. Table 1 lists a representative set of peptide-binding motifs. A complete listing up thru 1994 was compiled by Rammensee et al. (Rammensee et al., 1995).

1.2.3 Peptide-MHC Binding Affinity

Peptides bind to class I MHC molecules with moderate to high affinity (K_d around 10^{-8} to 10^{-7} M (Binz et al., 2003; Cerundolo et al., 1991)), and have extremely slow off-rates (tens to hundreds of hours at 37 ^{o}C (Bjorkman et al., 1987; Buus et al., 1986; Cerundolo et al., 1991)). However, this system cannot be described as a simple equilibrium. The pMHC structure suggests that a conformational change would be required to bind or release peptide, which has been confirmed experimentally (Elliott et al., 1992; Neefjes et al., 1993a).

Peptides play an important structural role in the class I MHC molecule. They are essential in stabilizing the heavy chain during assembly of the MHC molecule in the endoplasmic reticulum (Townsend et al., 1990; Townsend et al., 1989). In their absence class I MHC molecules can form, but are unstable at physiological temperatures (Ljunggren et al., 1990). Generally, peptides that confer the greatest stability also have the highest affinity. The fact that peptide-free MHC is extremely unstable and rapidly denatures is also a reason that it is not proper to discuss peptide binding to class I MHC as a standard equilibrium system. If the system were in simple equilibrium, LeChatelier's principle would govern. Scheme 1 shows that peptide bound complex (pMHC) would be rapidly depleted due to the loss of peptide-free MHC to denaturation and free peptide to dilution.

Scheme 1

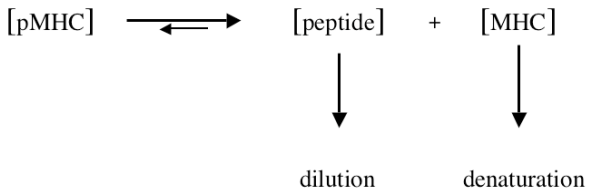

1.2.4 Peptide Processing

MHC-associated peptides are generated by cleavage of cellular proteins by the proteasome and other peptidases (Paradela et al., 2000; Serwold and Shastri, 1999). These peptides are derived from proteins that are degraded at the end of their useful lifespan as part of normal protein turnover. Consistent with this thinking, the ubiquitin-dependent proteolytic pathway plays a major role in the production of peptides for class I MHC restricted presentation (Michalek et al., 1993). A key factor in selection of a peptide for MHC presentation is the peptide's ability to be liberated from its precursor by proteolysis (Deng et al., 1997). The peptide sequence must possess protease-recognition sites flanking its amino and carboxyl termini (Del Val et al., 1991; Eggers et al., 1995; Eisenlohr et al., 1992), and must lack internal cleavage sites in order to be processed successfully (Niedermann et al., 1995; Ossendorp et al., 1996).

The proteasome is a multicatalytic proteinase complex consisting of five known proteolytic components that hydrolyze peptide bonds on the carboxyl side of basic, acidic, aromatic, branched chain, and small amino acids. The proteasome contains only endoprotease activity, yielding peptides of discrete length and not single amino acids (Dick et al., 1991). In a pathogen-infected cell, peptide generation is increased and the peptide sequences generated are different due to the expression of an altered proteasome, the immunoproteasome. The immunoproteasome contains some of the constitutively

expressed subunits of the proteasome, as well as unique subunits, termed low molecular weight proteins (LMPs). The LMP molecules are up-regulated by IFNγ during infection (Barton et al., 2002). Incorporation of LMP2 reduces cleavage following acidic residues and increases cleavage after basic residues without affecting hydrophobic activity**.** LMP7 incorporation specifically increases cleavage after hydrophobic and basic residues without affecting acidic proteolysis (Gaczynska et al., 1994; Groettrup et al., 1995).

The proteasome and immunoproteasome generate peptide lengths with a range of 3-22 amino acids and less then 15% of those peptides are 8 or 9 residues in length (Kisselev et al., 1999). Some peptides are further trimmed by aminopeptidases in the cytoplasm (Reits et al., 2003). However, a great deal of amino-terminal trimming takes place in the endoplasmic reticulum (ER). The primary aminopeptidase in the ER seems to be the ER aminopeptidase associated with antigen processing (ERAAP), or ERAP1, which is upregulated by IFNγ (Saric et al., 2002; Serwold et al., 2002). ERAP1, unlike other aminopeptidases, seems to limit trimming to create peptides of no less than eight residues in length.

1.2.5 Peptide Transport into the Endoplasmic Reticulum

The loading of peptide onto folded class I MHC molecules occurs in the ER (Townsend et al., 1989). Therefore, peptides generated in the cytosol via the constitutive proteasome, immunoproteasome, or other cytosolic proteases must be translocated into the ER for loading into a class I MHC molecule. The most prevalent pathway is via the heterodimeric transporter associated with antigen presentation (TAP).

TAP1 and TAP2, encoded within the *MHC* locus, are members of the ATP-binding cassette (ABC) family of membrane transporters (Deverson et al., 1990; Monaco

et al., 1990; Spies et al., 1990; Trowsdale et al., 1990). The TAP heterodimer spans the ER membrane allowing for movement of peptides from the cytoplasm to the lumen of the ER (Kleijmeer et al., 1992). Like other ABC transporters, transport of peptides across the ER membrane via TAP requires ATP and/or possibly GTP (Androlewicz et al., 1993; Neefjes et al., 1993b; Saveanu et al., 2001; Shepherd et al., 1993; van Endert, 1999). Hydrolysis of the bound nucleotides by both TAP1 and 2 induces a conformational change in the transmembrane domains, which results in the transport of peptide across the membrane (Alberts et al., 2001; Gorbulev et al., 2001; Karttunen et al., 2001; Saveanu et al., 2001).

TAP does not transport every peptide with the same efficiency. The selectivity of TAP is dependent on the sequence and length of peptide, not just overall charge or hydrophobicity (Androlewicz et al., 1993; Neefjes et al., 1993b; Shepherd et al., 1993). The ideal length of peptides binding to TAP is 8-11 residues, which is also to the ideal length for binding to class I MHC molecules, and seems to be the most important factor in transport. After length, the greatest determinant for TAP selectivity is the carboxyl-terminal residue. Peptides containing a basic or hydrophobic residues at the carboxyl terminus are translocated most effectively (Androlewicz and Cresswell, 1994; Momburg et al., 1994; Uebel et al., 1997).

1.2.6 Class I MHC Peptide Loading

TAP facilitates loading of peptides directly onto class I MHC molecules by its association in the ER lumen with a large complex of proteins, termed the peptide loading complex (PLC), which includes: nascently-formed class I MHC (with β_2m) (Ortmann et

al., 1994; Suh et al., 1994), tapasin, calreticulin, and ERp57 (Reits et al., 2000). Each of these peptide loading molecules are discussed briefly below.

While not directly part of peptide loading, calnexin is a chaperone found in the ER that promotes the correct folding of glycosylated proteins including class I MHC heavy chain (Hammond et al., 1994; Hebert et al., 1996; Nauseef et al., 1995; Peterson et al., 1995; Wada et al., 1995; Zhang et al., 1995). Tapasin is a 48 kDa type I transmembrane glycoprotein encoded within the *MHCI* locus, which is essential for peptide loading of class I MHC molecules. Cells that lack expression of tapasin have no detectable class I molecules, calreticulin, or ERp57 associated with TAP (Grandea et al., 1998; Li et al., 1999; Li et al., 1997; Ortmann et al., 1997; Sadasivan et al., 1996). ERp57 is responsible for facilitating disulfide bond formation in the α2 and α3 domains of the class I MHC heavy chain (Farmery et al., 2000; Lindquist et al., 1998). After being recruited by calnexin to the class I heavy chain, ERp57 remains as part of the PLC until peptide is loaded (Lindquist et al., 2001). Calreticulin, a 46 kDa soluble protein found in the ER, displays high sequence homology to the lumenal domain of calnexin (Michalak et al., 1992) and functions to keep the class I heavy chain-β_2m complex in a peptide receptive state (Culina et al., 2004).

1.3 The T cell Receptor

1.3.1 T cell Receptor Structure

The T cell receptor (TCR) was hypothesized to be structurally similar to an arm of an antibody based on sequence similarity (Claverie et al., 1989; Davis and Bjorkman, 1988). This was found to be the case in 1996 when the first two TCR structures were

Table 2. Determined Structures of TCR-pMHC

TCR	Vα	Vβ	Bound pMHC(s)	PDB	Reference
MHC Class I Restricted TCR					
A6	TRAV12-2*02	TRBV6-5*01	tax/A2	1AO7	(Garboczi et al., 1996)
			tax(P6A)/A2	1QRN	(Ding et al., 1999)
			tax(V7R)/A2	1QSE	(Ding et al., 1999)
			HLA-A2-tax(Y8A)	1QSF	(Ding et al., 1999)
			tax(hapten)/A2	2GJ6	(Gagnon et al., 2006)
B7	TRAV29/DV5*01	TRBV6-5*01	tax/A2	1BD2	(Ding et al., 1998)
1G4	TRAV21*01	TRBV6-5*01	1G4 alone	2BNU	(Chen et al., 2005)
			NY-ESO-1(9C)/A2	2BNR	(Chen et al., 2005)
			NY-ESO-1(9V)/A2	2BNQ	(Chen et al., 2005)
JM22	TRAV27*01	TRBV19*01	flu/A2	1OGA	(Stewart-Jones et al., 2003)
			JM22 alone	2VLM	(Ishizuka et al., 2008)
			flu/A2	2VLJ	(Ishizuka et al., 2008)
SB27	TRAV19*01	TRBV6-1*01	LPEP/B35	2AK4	(Tynan et al., 2005)
LC13	TRAV26-2*01	TRBV7-8*01	EBV/B8	1MI5	(Kjer-Nielsen et al., 2003)
ELS4	TRAV1-2*01	TRBV10-3*01	ELS4 alone	2NW2	(Tynan et al., 2007)
			EBV/B35	2NX5	(Tynan et al., 2007)
BM3.3	TRAV16D/DV11*01	TRBV1*01	pBM1/K^b	1FO0	(Reiser et al., 2000)
			VSV8/K^b	1NAM	(Reiser et al., 2003)
			pBM8/K^{bm8}	2OL3	(Mazza et al., 2007)
KB5-C20	TRAV14-1*01	TRBV1*01	pKB1/K^b	1KJ2	(Reiser et al., 2002)
			Fab	1KB5	(Housset et al., 1997)
AHIII12.2	TRAV12D-2*01	TRBV13-3*01	p1049/A2	1LP9	(Buslepp et al., 2003b)
			p1049/A2(T163A)	2UWE	(Miller et al., 2007)
			p1049/A2(W167A)	2JCC	(Miller et al., 2007)
			p1049/A2(K66A)	2J8U	(Miller et al., 2007)
N15	TRAV12D-1*01	TRBV12-1*01	VSV8/K^b	N/A	(Teng et al., 1998)
			H57 Fab	1FND	(Wang et al., 1998)
2C	TRAV9-4*01	TRBV13-2*01	2C alone	1TCR	(Garcia et al., 1996)
			dEV8/K^b	2CKB	(Garcia et al., 1998)
			SIYR/K^b	1G6R	(Degano et al., 2000)
			dEV8/K^{bm3}	1MWA	(Luz et al., 2002)
2C(m6)			QL9/L^d	2E7L	(Colf et al., 2007)
			QL9/L^d	2OI9	(Colf et al., 2007)

(Table 2 continued)

MHC Class II Restricted TCR					
HA1.7	TRAV8-4*05	TRBV28*01	HA/DR1	1FYT	(Hennecke et al., 2000)
			HA/DR4	1J8H	(Hennecke and Wiley, 2002)
Ob.1A12	TRAV17*01	TRBV20*01	MBP/DR2	1YMM	(Hahn et al., 2005)
3A6	TRAV9-2*01	TRBV5-1*01	MBP/DR2a	1ZGL	(Li et al., 2005)
E8	TRAV22*01	TRBV6-6*01	E8 alone	2IAL	(Deng et al., 2007)
			TPI/DR1	2IAN	(Deng et al., 2007)
			TPI-mut/DR1	2IAM	(Deng et al., 2007)
D10	TRAV14D-2*01	TRBV13-2*01	CA/A^k	1D9K	(Reinherz et al., 1999)
			D10 alone (NMR)	1BWM	(Hare et al., 1999)
172.1	TRAV14-3*01	TRBV13-2*01	MBP/A^u	1U3H	(Maynard et al., 2005)
1.D9.B2	TRAV14-3*01	TRBV13-2*01	MBP/A^u	2P1Y	(McBeth et al., 2008)
B3K506			3K/A^b	3C5Z	(Dai et al., 2008)
2W20			3K/A^b	3C6O	(Dai et al., 2008)
YAe62			3K/A^b	3C6L	(Dai et al., 2008)

determined (Garboczi et al., 1996; Garcia et al., 1996). Twelve years later, a total of 23 unique class I or class II MHC restricted αβTCR have been studied structurally. These TCR along with their respective co-crystal pMHC targets are listed in Table 2. The TCR is a membrane bound heterodimeric molecule of approximately 60 kDa, which is comprised of an alpha and beta chain, and less frequently a gamma and delta chain. Each chain contains a variable and constant immunoglobulin domain, a trans-membrane segment, and a short cytoplasmic tail. The constant and variable domains each fold into

immunoglobulin (Ig) domains, composed entirely of β-sheets (Figure 2b). Similar to an antibody-epitope interaction, the TCR contacts its ligand, pMHC, using the membrane distal variable domains; more specifically using the complementarity determining region (CDR) loops within the variable domains. Generation of these CDR loops will be covered in greater detail in section 1.3.2. The TCR molecule and its interaction with pMHC is diagramed in Figure 2.

1.3.2 T cell Receptor Generation and T cell Maturation

T cell precursors are generated in the bone marrow and then migrate to the thymus for maturation (hence the name T cell). It is in the thymus that the T cell receptor (TCR) is expressed. Each T cell is clonotypic, meaning it expresses only one TCR. Each unique TCR variable domain is generated through a recombination of three gene segments, the variable (V), diversity (D) (only in β-chain), and joining (J) segments, termed V(D)J recombination (Schatz and Spanopoulou, 2005; Spicuglia et al., 2006). The CDR1 and CDR2 loops are germ-line encoded within the variable gene segment. The diversity seen in the CDR1 and CDR2 loops is derived from the large number of Vα and Vβ TCR genes. The gene for each CDR3 loop is unique and is located where the V, D, and J segments are joined. V(D)J recombination utilizes non-homologous end-joining, which is an imperfect process, often adding or deleting nucleotide bases in the process (Schatz and Spanopoulou, 2005; Spicuglia et al., 2006). The process of V(D)J recombination in T cells can theoretically produce approximately 10^{15} unique TCR variable domains (Davis et al., 1998). However, this number of T cells is pared down through the thymic selection leaving an estimated 10^{8} different TCR.

Thymic selection, thymic education, or T cell maturation are all names for the action of selecting T cells that can recognize antigen (Starr et al., 2003; von Boehmer et al., 2003). The procedure has two distinct processes: positive and negative selection. In positive selection the newly formed TCR must recognize self-peptide in the context of self-MHC presented on the surface of thymic epithelial cells. This is essential because the TCR must be able to recognize the peptide/MHC complex once outside the thymus. The T cell must receive a signal from the TCR that it identifies self-pMHC, or it will die

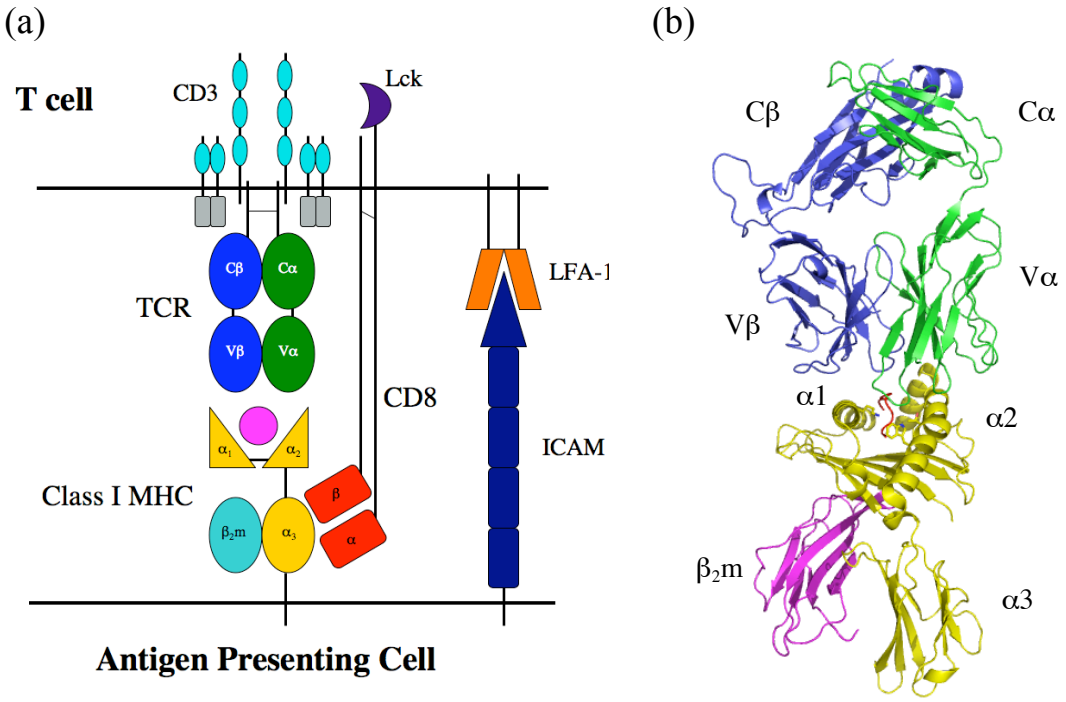

Figure 2. TCR-pMHC interaction is the keystone of the immunological synapse. (a) Diagram of interface between CTL and antigen presenting cell. While discrimination between self and non-self peptides is determined TCR-pMHC interaction, T cell activation requires the recruitment of other molecules to the synapse. ITAMs on the CD3 complex molecules are phosphorylated by Lck, which is recruited along with CD8. Coreceptor CD8 and adhesion molecules LFA-1 and ICAM increase the avidity of the interaction between the cells. (b) Ribbon diagram of AHIII TCR bound to p1049/A2 (1LP9). CDR loops of the Vα and Vβ domains contact the peptide (red) and the α1 and α2 domains of the class I MHC.

by neglect. This is also where the CD4 or CD8 coreceptor lineage commitment of a T cell is determined as the coreceptors are involved in the TCR signaling into the cell (Germain, 2002; He and Kappes, 2006). In negative selection, if TCR recognizes self-pMHC too strongly, the T cell is deleted through apoptosis (Starr et al., 2003; von Boehmer et al., 2003). Negative selection prevents self-reactive T cells from escaping the thymus, which could lead to potential autoimmune disorders.

1.4 Molecular Recognition of pMHC by the T cell Receptor

While the overall three-dimensional structure of the TCR resembles the epitope binding arm of an antibody (Fab), the key difference between them is the ligands to which they bind. Antibodies can recognize a broad spectrum of linear and non-linear epitopes, but TCR only recognize self or foreign peptides presented in the context of the MHC molecule. TCR binds to the molecular surface that is formed by a combination of atoms from the peptide and the class I MHC molecule, with the TCR α chain docking over the $\alpha 2$ α helix and the TCR β chain docking on the $\alpha 1$ α helix (Figures 1e and 2). Recognition of pMHC by the TCR heterodimer is accomplished using the three CDR loops from each chain of the TCR. While recognition of the pMHC is carried out using all the CDR loops of each chain, generally the CDR3 makes more contacts with the bound peptide and the CDR1 and CDR2 loops contact the $\alpha 1$ and $\alpha 2$ α helices of the MHC (Rudolph et al., 2006). Consequently, the TCR has the ability to recognize both the MHC and the peptide, allowing recognition of multiple peptides presented by one or more MHC molecules. This ability, along with the diversity of CDR loop combinations produced by V(D)J recombination (section 1.3.2), provides the power of the adaptive immune response. This diversity of recognition, or the ability of a TCR to recognize

multiple pMHC ligands, is termed polyspecificity (Wucherpfennig et al., 2007). Polyspecificity can be broken into parts: syngeneic, allogeneic, xenogeneic and cross-reactivity. Basically, syngeneic refers to TCR recognition of a self-MHC, allogeneic is recognition of genetically different MHC molecules within the same species, and xenogeneic is TCR recognition of MHC from different species. Understanding and controlling allogeneic and xenogeneic responses is key to controlling organ transplant rejection. Cross-reactivity is a general term that has been used to describe the ability of multiple pMHC to initiate a T cell response. This is the basis of CTL response to antigenic peptide. Early explanations of polyspecificity involved the model of molecular mimicry; or the idea that the molecular surfaces of the different pMHC that one TCR recognized would be almost identical regardless of sequence. However, this has been shown not to be the case (Colf et al., 2007; Zhao et al., 1999). Each pMHC has a unique surface and the TCR accommodates this in different manners.

Compared to antibody-antigen interactions, the TCR binds pMHC with relatively low affinity (K_d = 1-100 μM) and fast off-rates. However, this low affinity interaction is surprisingly selective. To illustrate, a vesicular stomatitis virus (VSV) peptide (RGYVYQGL) presented in the context of mouse MHC K^b elicits a T cell response with clones of predominantly Vβ13. A variant peptide E6 (RGYVYEGL) abrogates the response of Vβ13 expressing T cells. The structures of these two peptides in K^b have been determined and the only difference is the side chain of position 6 (Q→E) (Thomson et al., 2001).

Mutations in both the sequence of the peptide or the MHC molecule can have significant effects on recognition. Often molecular recognition of the pMHC by the TCR

is dissected into peptide recognition and MHC recognition. However, one cannot dissociate the two. Peptide side chains bound into their complementary specificity pockets in the MHC can also influence the reactivity of cytotoxic T lymphocytes (Buxton et al., 1992; Matsui et al., 1993; Rohren et al., 1993; Santos-Aguado et al., 1989; Villadangos et al., 1992; Winter et al., 1991), even turning them from agonist to antagonist by mutating one residue (Dong et al., 1996). Presumably, these mutations cause a slight conformational change in the peptide or in the MHC, altering the molecular surface of the pMHC complex, and hence, recognition by TCR. This argument is especially lucid when considering that the buried surface area of the pMHC is generally greater than 900 $Å^2$, while the peptide is buried so deeply in the groove that only 100-300 $Å^2$ is exposed outside the MHC to the TCR (Fremont et al., 1992).

Understanding the paradox of TCR-pMHC recognition being promiscuous, or polyspecific, but yet highly specific at the same time has been the great challenge for structural immunologists. Interestingly, there are no significant differences in the way that TCR binds to syngeneic, allogeneic, or xenogeneic pMHC based on the determined co-crystal structures (Table 2).

1.4.1 Induced Fit or Pre-Existing Equilibrium

Induced fit is a general biophysical mechanism that describes plasticity in the binding site allowing for an initial weak association, following by an induced conformational change in the binding site, leading toward tight association in the active state (Goh et al., 2004). This has been applied to TCR-pMHC binding. After analyzing the association rate constants (k_{on}) measured between the 2B4 TCR and class II MCC/I-E^k mutants, Wu *et al*. proposed a two-step binding mechanism (Wu et al., 2002). In this

model the CDR1 and CDR2 loops of the TCR first bind to the MHC prior to a binding transition state, followed by an induced fit of the CDR3 loops onto the peptide as the transition state moves to the bound state. The two-step binding model has been challenged by data from other laboratories. Davis-Harrison *et al*. have recently shown that the CDR3 loops of both A6 and B7 TCR do contribute to the initial formation of the TCR-pMHC complex when binding Tax/HLA-A2 (Davis-Harrison et al., 2007). Lee *et al*. propose a variation of induced-fit involving a conformational change in the peptide following the TCR-pMHC transition state based on their thermodynamic data (Lee et al., 2004). The recently determined structures of the ELS4 TCR in non-ligand form and in complex with EPLP/HLA-B*3501 show limited movement of the CDR3α loop, as well as a large conformational change in the peptide upon binding (Tynan et al., 2007), similar to what had been seen by Lee *et al*. (Lee et al., 2004). In contrast to the 2C (Degano et al., 2000; Garcia et al., 1998) and KB5-C20 TCR (Reiser et al., 2002) structural studies, where large conformational changes were limited to the CDR3 loops, upon binding its pMHC ligand the LC13 TCR undergoes dramatic changes in not just its CDR3s, but also the CDR1 and CDR2 alpha loops (Kjer-Nielsen et al., 2003). Additionally, the CDR1α loop is critical in the LC13 system for peptide specificity, while the CDR3α loop interacts principally with the MHC. Energetic studies of the LC13 TCR system, which demonstrate the CDR3 loops are key in initial pMHC recognition while the CDR1 and CDR2 loops only help stabilize the TCR-pMHC interaction, are also inconsistent with the two-step binding mechanism (Borg et al., 2005). Crystal structures of the BM3.3 TCR bound to the H-2K^b MHC presenting two different peptides show that the CDR1 and CDR2 loops are flexible and make unique contacts with each pMHC surface, suggesting

that the cross-reactivity seen with TCR for various pMHC is not due to changes seen in the CDR3 loops alone (Reiser et al., 2003). These examples suggest that the two-step model, dissecting TCR-MHC and TCR-peptide binding, is not general to TCR-pMHC binding. The two-step model may better describe TCR binding to class II pMHC, where the peptide is buried deeper in the groove.

Moreover, perhaps an induced fit model does not best describe TCR-pMHC binding. The pre-existing equilibrium model theorizes that the protein binding site exists in a number of conformations, and that binding will occur once the ligand encounters the appropriate conformation (Goh et al., 2004). A pre-existing equilibrium model still reconciles with the slower on-rates determined by surface plasmon resonance for many TCR binding to pMHC variants. The TCR conformation necessary to bind a particular pMHC may be sparse in the overall population, taking longer for these TCR to find the pMHC and bind. It has been suggested that TCR-pMHC binding may utilize pre-existing equilibrium and induced fit to allow both cross-reactivity and high specificity, respectively (Gakamsky et al., 2004). Further supporting this idea, James *et al*. recently determined structures of two pre-existing conformations of the same antibody, as well as structures of each conformation bound to their respective antigens (James et al., 2003).

Aside from the conformations of the CDR loops themselves the juxtaposition of the TRC α and β chains may play a role in pMHC recognition, especially when it comes to polyspecificity. Analysis of the different TCR structures bound to their cognate pMHC has found that interdomain angles (between Vα and Vβ) vary among the different TCR. Even more interesting, they were varied between structures of the same TCR bound to different pMHC ligands (McBeth et al., 2008).

1.4.2 The Thermodynamics of TCR-pMHC Recognition

Isothermal titration calorimetry (ITC) provides a direct measure of enthalpy (ΔH) and is hence considered the most reliable determination of thermodynamic parameters. However, ITC has been rarely utilized for TCR-pMHC studies because of large amounts of protein required for the experiment. More often, surface plasmon resonance (SPR) has been used to examine the thermodynamics of binding of many TCR to pMHC. SPR can provide an indirect estimation of enthalpy based on the van't Hoff equation using the affinity determined at various temperatures. The caveats of van't Hoff analysis have recently been discussed, including proton linkage (Armstrong et al., 2008) and the sensitivity of the analysis to errors in temperature or determined K_d (Zhukov and Karlsson, 2007). Whether using ITC or SPR, early thermodynamic experiments suggested that TCR-pMHC interactions seem to be dominated by large enthalpic contributions and with unfavorable entropy (Anikeeva et al., 2003; Boniface et al., 1999; Garcia et al., 2001; Krogsgaard et al., 2003; Lee et al., 2004; Willcox et al., 1999). These results were satisfying considering polar interactions should provide the specificity seen with TCR-pMHC recognition, compared to relying on non-polar, or van der Waals contacts. In addition, entropically unfavorable binding seems to correlate well with the idea that flexible CDR loops are being constricted upon TCR-pMHC binding. However, more recent thermodynamic data of L13-FLR/B8 (Ely et al., 2006), A6-Tax/A2 (Davis-Harrison et al., 2005), 2C-QL9/L^d (Colf et al., 2007), and our AHIII-p1049/A2 presented in Chapter 2 (Miller et al., 2007) all show entropically favorable associations, or even completely entropically driven in the case of the A6 TCR (Davis-Harrison et al., 2005).

These data demonstrate that entropically unfavorable binding is not a signature of TCR-pMHC recognition. Furthermore, it has been shown that the same TCR can bind different ligands using varied thermodynamic mechanisms. Examples include the A6 and B7 TCRs recognizing tax/A2 (Davis-Harrison et al., 2005), the 172.10 and 1934.4 TCRs binding the MBP peptide in the context of class II MHC I-A^u (Garcia et al., 2001), and the 2C TCR recognition of two different MHC, H-$2L^d$ and H-$2K^b$ (Colf et al., 2007; Krogsgaard et al., 2003).

Individual contributions to changes in binding entropy (ΔS) include changes in solvation, loss in translational and rotational degrees of freedom, and protein backbone and side chain conformational changes. While a method exists to dissect these contributions from the overall DS (Spolar and Record, 1994), and has been employed on at least one TCR system to estimate conformational change in CDR loops upon TCR-pMHC binding (Boniface et al., 1999), the accuracy of these calculated contributions is questionable. A better thermodynamic parameter for estimating conformational changes is the heat capacity change (ΔC_p). A number of TCR-pMHC binding analyses have included ΔC_p value in their analyses. In general reported heat capacity changes for TCR-pMHC binding have been large and negative (-400 to -800 cal/K/mol). Since ΔC_p is strongly influenced by changes in solvation, it is widely accepted in the field that these large negative values suggest that conformational changes are altering the solvent exposed surface area upon binding. However, ΔC_p measurements are not error free, including the fact that most for TCR-pMHC have been determined using SPR with van't Hoff analysis (Armstrong et al., 2008; Zhukov and Karlsson, 2007). Additionally, while a negative change in heat capacity suggests conformational change in a solvent exposed

surface upon binding, it can not tell you if that change is occurring in the TCR, the peptide, the MHC, or some distal surface of the proteins. Therefore, the best investigation of conformation change in TCR or pMHC should include thermodynamic and structural analysis.

1.5 T cell activation

1.5.1 T cell signaling

Full T cell activation requires the presence of two sets of signals. The first is provided through the TCR upon engagement of an antigenic pMHC, the second is derived from co-stimulatory molecules. The best-characterized co-stimulatory molecules are CD28 and LFA-1, which bind B7 and ICAM-1, respectively, on the surface of the antigen presenting cell (APC) (Schwartz, 2003). Co-stimulation acts to increase the magnitude and/or duration of the TCR signal and is necessary for optimal IL-2 production and proliferation. More importantly, the first signal originating from the TCR-pMHC interaction ensures the specificity of the T cell response, and is hence, the focus of this work.

The short cytoplasmic tail of the αβTCR is unable to propogate any signal inside the T cell upon TCR-pMHC binding. Hence, the TCR relies on other cytotoxic T cell surface molecules for signaling, primarily the CD3 complex and the CD8 coreceptor (Figure 2a). The CD3 complex is composed of γ, δ, ε, and ζ chains, which co-localize with the TCR on the surface of the CTL. The cytoplasmic tails of all CD3 chains contain Immunological Tyrosine-based Activation Motifs (ITAMs), which are phosphorylated first by the Src family tyrosine kinase $p56^{lck}$ (Lck), followed by Syk family kinase Zap70

(van Oers, 1999). Phosphorylation of the CD3 ITAMs initiates downstream signaling pathways that lead to T cell activation: T cell proliferation and cytokine secretion.

The heterodimeric CD8 coreceptor serves two known roles in the immunological synapse. First, like the TCR, the two Ig domain "heads" of the αβCD8 bind to MHC, but in a peptide independent manner on the α3 domain (Figure 2a). This increases the avidity of the TCR-pMHC interaction, making it more stable (Luescher et al., 1995). Second, the cytoplasmic tail of the CD8α chain recruits Lck (Shaw et al., 1990; Turner et al., 1990). This is the primary means of how Lck is brought into the immunological synapse where it can then phosphoryate the CD3 ITAMs. In addition to binding the MHC, the glycolsylated CD8 β chain has been shown to interact with the TCR α chain (Backstrom et al., 1996; Naeher et al., 2002; Ulivieri et al., 2001; Werlen et al., 2000), providing a mechanism of CD8-TCR association and co-localization. Of course complicating the issue, CD8-independent CTL responses have been documented for many T cell systems (Anel et al., 1997; Buslepp et al., 2003a; Cho et al., 2001; Curnow et al., 1994; Potter et al., 1989; Riddle et al., 2008). The HLA-Aw68 MHC (Aw68) contains a naturally occurring mutation, which reduces CD8-MHC binding (Gao et al., 1997; Hutchinson et al., 2003), resulting in CD8-independent Aw68 restricted CTL activation (Cerundolo et al., 1991). It is unclear how the Lck is able to phosphorylate ITAMs in these CD8-independent systems. One hypothesis is that CD8 still co-localizes with the TCR, bringing along with it Lck, but because the TCR-pMHC has a high enough affinity that CD8 is not required to bind the MHC to increase the avidity (Buslepp et al., 2003a). For T cells that are $CD8^{-/-}$, suggestions include: that Lck is palmitylated and

already membrane associated, it is free and available in high enough concentrations in the cell, that other tyrosine kinases operate in the absence of Lck (Riddle et al., 2008).

While the interaction between one TCR and one pMHC may last on the order of a second or less, full T cell activation requires a sustained TCR-pMHC interaction on the order of hours. This long interaction between the T cell and the APC is accomplished through a supramolecular organization of the various molecules in the immunological synapse, termed supramolecular activation cluster (SMAC) (Bromley et al., 2001; Grakoui et al., 1999; Monks et al., 1998). The SMAC is basically a "bull's eye-like" capping of TCR-pMHC complexes and co-stimulatory molecules, LFA-1 and CD28 with their respective APC ligands. Initial immunological synapse formation is initiated by TCR-pMHC ligation, and subsequent ITAM phosphorylation, results in Ca^{2+} flux, generation of inositol phospholipids, and arrest of T cell migration within approximately 30 sec., followed by co-stimulatory signals. Initially SMAC organization has co-stimulatory molecule LFA-1 in the center of the bull's eye and TCR around the periphery. Between 5 minutes and 60 minutes the molecules reorganize and the TCR creates the bull's eye and the co-stimulatory molecules surround them. The density of TCR-pMHC molecules in SMAC reaches approximately 200 molecules per μm^2 after 10 minutes and maintains that density for more than 30 minutes (Grakoui et al., 1999).

1.5.2 Levels of T cell Activation: Agonist, Partial Agonist, and Antagonist

TCR triggering of T cell activation cannot be described as a binary system, i.e. on or off. Instead, qualitatively different T cell signaling can lead to a range of responses from maximal activation to desensitization (reviewed in (Bongrand and Malissen, 1998; Uhlin et al., 2006)). The cognate pMHC ligand of a TCR that leads to a full response is

generally referred to as an agonist. Agonists elicit the full range of T cell responses, including cell proliferation, cytokine secretion, expression of activation markers, and cytotoxicity (for CTLs). Variants of the cognate pMHC, often called altered peptide ligands (APLs), can result in various responses. Partial agonists result in some, but not all, of these responses. Null agonists elicit no response. Other ligands, called antagonists, not only elicit no response, but actually seem to block T cell responses to agonist ligands, sometimes even resulting in T cell anergy (Sloan-Lancaster et al., 1993). Importantly, these antagonist peptides must be co-presented with agonists on the same antigen presenting cell (APC) to mediate their suppressive effects.

The diverse range of T cell activation is critical not only for CTL cytoxicity, but also early during thymic selection (described in section 1.3.2) and later for survival in the secondary lymphoid organs. Circulating mature T cells interact with self-pMHC after leaving the thymus. These weak interactions do not activate the cell, but send small signals keeping them alive and ready to respond when necessary (Krogsgaard and Davis, 2005; Stefanova et al., 2002).

Antagonistic peptides do not follow a simple competitive model, occupying the TCR-pMHC binding and dampening T cell signaling in a dose dependent manner. Rather, the qualitative differences manifested above are the result of alternate patterns of phosphorylation in the signaling pathway for T cell activation. Pull down experiments have shown that agonistic peptides result in full phosphorylation of Lck, ZAP-70, CD3ε, and both p21-CD3ζ and p23-CD3ζ chains, where as null or antagonistic peptides resulted in phosphorylation of only p21-CD3ζ and not p23-CD3ζ, CD3ε, or ZAP-70 (reviewed in (Madrenas and Germain, 1996)). Importantly, this qualitative difference in

phosphorylation cannot be reproduced by just stimulating T cells with lower concentrations of weak or full agonists (Reis e Sousa et al., 1996). It is theorized that this pattern is the result of incomplete activation, i.e. lack of the second activation signal from co-stimulatory receptors, primarily CD28 and LFA-1 (Schwartz, 2003). Partial agonists and antagonists also affect the downstream patterns of Ca^{2+} flux compared to full agonists (Chen et al., 1998). The formation of the supramolecular activation complex (SMAC), described above in 1.5.1, is also detrimentally affected by antagonist peptides, disabling MHC clustering and the signal to stop cell motility (Sumen et al., 2004).

The most extreme effect of antagonism is T cell anergy, where the cell becomes functionally inactive following encounter with antagonist pMHC (reviewed in (Schwartz, 2003)). Anergic T cells have a similar phosphorylation pattern described above for antagonists. Clonal anergy of CTLs often manifests itself in a somewhat normal secretion of IFNγ, but drastically reduced levels of IL-2 and an arrest in cell growth. These cells can sometimes be rescued from anergy with the addition of high levels of IL-2 (Schwartz, 2003).

The study of agonist, partial agonist, and antagonist peptides provides a means of deciphering the mechanisms of T cell activation. Better understanding of these activation phenomena could also lead to be treatment of certain diseases. Antagonist peptides have been encountered in viral infections and may aid in immune evasion. Mutations in HIV, Hepatitis B and C, and LCMV have been reported to produce antagonistic peptides; and even self-peptides presented by MHC have been shown to enhance or suppress immune response to certain antigens (Vukmanovic et al., 2003). Naturally processed antagonist peptides during a Listeria infection in mice were shown to suppress activation of naïve T

cells by agonist peptide, suppress memory response upon challenge, and alter the hierarchy of immunodominance (Lau et al., 2005). These results suggest the need to study possible antagonistics associated with vaccine development. A clearer understanding of T cell antagonism could potentially allow for the use of antagonistic peptides as therapeutics; potentially down-regulating a cytotoxic T cell response in autoimmune disorders or transplantation (Garcia-Peydro et al., 2000).

1.5.3 Models of T cell activation

The qualitatively different signals described above lead to a range of T cell responses, which stem from quantitative differences for TCR-pMHC molecular recognition. However, it is still unclear how that quantitative difference is determined by the TCR. As it has been discussed above in section 1.4, the structural and thermodynamic mechanisms of TCR-pMHC molecular recognition vary greatly. It seems that each TCR finds a unique way in which to bind its respective pMHC targets.

As the first TCR-pMHC co-crystal structures were determined (Garboczi et al., 1996; Garcia et al., 1996) structural immunologists hypothesized that T cell activation would be mediated through some allosteric mechanism involving the TCR. More specifically, upon binding an antigenic pMHC complex, the structure of the TCR would change and be distinct from the structure of the TCR bound to a self-pMHC, translating some quantitative difference into the T cell propagating the appropriate signal. This was soon shown not to be the case when Ding *et al.* found that the structure of the A6 TCR in complex with four different pMHC ligands including an agonist, antagonist, and two weak antagonists was virtually unchanged between them (Ding et al., 1999). This is true of many other TCR-pMHC structures determined since (Table 2). The only other

structural hypothesis regarding T cell activation suggests that a small movement in a loop of the TCR Cα domain upon binding agonist pMHC allows for an interaction with CD3ε (Kjer-Nielsen et al., 2003); however, this has not been corroborated by any other TCR-pMHC structure. If a conformational change in the TCR structure does not relay the pMHC readout into the cell then some other biophysical mechanism must.

A few biophysical models exist to explain differences in TCR triggering and downstream T cell outcome. The kinetic model proposes that the level of T cell activation is dependent on the dissociation rate of the TCR-pMHC interaction; slower off-rate equals greater signal. Due to the two sets of signals required for full T cell activation (discussed above in section 1.5.1) the kinetic model proposes that the TCR-pMHC must be engaged long enough for both the first TCR initiated signal and the co-stimulatory signal to occur (McKeithan, 1995; Rabinowitz et al., 1996). This correlation has been supported by a number of experimental observations (Kersh et al., 1998; Lyons et al., 1996; Matsui et al., 1994; Rosette et al., 2001). A more recent refinement of this basic off-rate model combines off-rate with a measure of conformational change upon binding (ΔCp) to predict T cell stimulation (Krogsgaard et al., 2003).

Another popular model is the affinity model, which states that T cell activation relates to the concentration or number of pMHC ligands engaged. The affinity model is also supported by an abundance of experimental data, which all show a correlation between determined TCR-pMHC affinities and activation (Alam et al., 1996; Baker et al., 2000; Buslepp et al., 2001; Garcia et al., 2001; Holler and Kranz, 2003; Miller et al., 2007; Schodin et al., 1996; Sykulev et al., 1994; Sykulev et al., 1998; Tian et al., 2007). The A6 T cell response to the pMHC structures referred to previously, that showed no

TCR conformational change (Ding et al., 1999), were ultimately shown to correlate with TCR-pMHC affinity (Baker et al., 2000). Another case supporting a correlation with affinity involves activation of the P14 T cell. Recently, two independent laboratories have determined the affinity to be consistent with other agonist pMHC interactions, but the shortest half-life of any other agonist TCR-pMHC interaction (k_{off} >1 s^{-1}) (Boulter et al., 2007; Tian et al., 2007).

The serial triggering model attempts to explain the paradox of high specificity with a low affinity interaction. It does not compete with kinetic or affinity models, but rather incorporates them both. Following ITAM phosphorylation the TCR-CD3 complex is downregulated, or internalized, in the T cell. Lanzavecchia and colleagues measured this internalization following stimulation by agonist pMHC (Valitutti et al., 1995). They determined that a single pMHC complex could serially trigger ~200 TCR, due to the fast off-rate of TCR-pMHC binding. They also showed a correlated between IFNγ production and the number of TCRs downregulated. Partial agonists were shown to downregulate fewer TCR, suggesting that there exists an optimum affinity and off-rate (or dwell time) that allows TCR triggering and pMHC complex recycling. Without a full TCR trigger, antagonists would actually inhibit downregulation of TCR. This model is able to account for the fact that antigenic peptides are presented in low-copy number compared to self-peptide. Because of the fast serial triggering a small number of antigenic pMHC can trigger T cell activation. Finally this model suggests that there is a threshold of "triggered" TCRs needed in order to fully activate the cell (Lanzavecchia et al., 1999; Valitutti et al., 1995).

The segregation model is the final model. The bound TCR-pMHC and their accessory molecules create an immunological synapse of ~14 nm in distance between the cells. The ectodomains of receptor protein tyrosine phosphatases known to inhibit TCR triggering, including CD45, are larger than 14 nm. The segregation model suggests that large inhibitory molecules are segregated in a size-dependent manner from the immunological synapse, allowing for phosphorylation of the CD3 ITAMS (Choudhuri et al., 2005; van der Merwe and Davis, 2003).

1.6 The AHIII12.2 T cell

Many of the experiments performed within this body of work were done using the AHIII12.2 (AHIII) T cell system. AHII is a murine T cell clone that was generated by injecting human lymphoblasts into a B6 (H-2b) mouse (Bernhard et al., 1987; Herman et al., 1983; Hogan et al., 1989). The AHIII T cell is very interesting in that it recognizes a xenogenic human class I MHC, HLA-A2.1 (A2), when presenting the peptide p1049 (ALFGFFPVL) (Henderson et al., 1993). It was later discovered that AHIII also recognizes class I H-2D^b (D^b) in complex with the synthetic peptides p1027 (FAPGVFPYM) and p1058 (FAPGFFPYL) and related variants (Loftus et al., 1997). That study included a careful analysis of p1049 in A2 and p1058 in D^b, which concluded that the AHIII TCR must engage the surfaces of p1049/A2 and p1058/D^b in a different manner due to the results of alanine scanning of the peptide. Substitutions at P3 and P5 were deleterious in p1049, while P5 and P8 were more important to p1058 (Loftus et al., 1997). They hypothesized that these were critical residues involved with TCR contacts. We now know that in the case of AHIII-p1049/A2 that the Phe at P5 is a critical contact, and Trp at P3 does not contact the TCR, but rather is a secondary anchor residue for the

peptide binding to A2 (Buslepp et al., 2003b). So, p1058/D^b and p1049/A2 both produce an agonistic response in AHIII. Interestingly, it was found that when p1058 is bound and presented by A2 it becomes antagonistic. Experiments using fluorescently labeled p1058/A2 tetramer also suggested that the AHIII TCR bound p1058/A2 with lower affinity than p1049/A2 (Buslepp et al., 2001). However, this affinity has never been directly measured.

1.7 References

Alam S. M., Travers P. J., Wung J. L., Nasholds W., Redpath S., Jameson S. C. and Gascoigne N. R. (1996) T-cell-receptor affinity and thymocyte positive selection. *Nature* 381, 616-20.

Alberts P., Daumke O., Deverson E. V., Howard J. C. and Knittler M. R. (2001) Distinct functional properties of the TAP subunits coordinate the nucleotide-dependent transport cycle. *Curr Biol* 11, 242-51.

Androlewicz M. J., Anderson K. S. and Cresswell P. (1993) Evidence that transporters associated with antigen processing translocate a major histocompatibility complex class I-binding peptide into the endoplasmic reticulum in an ATP-dependent manner. *Proc Natl Acad Sci U S A* 90, 9130-4.

Androlewicz M. J. and Cresswell P. (1994) Human transporters associated with antigen processing possess a promiscuous peptide-binding site. *Immunity* 1, 7-14.

Anel A., Martinez-Lorenzo M. J., Schmitt-Verhulst A. M. and Boyer C. (1997) Influence on CD8 of TCR/CD3-generated signals in CTL clones and CTL precursor cells. *J Immunol* 158, 19-28.

Anikeeva N., Lebedeva T., Krogsgaard M., Tetin S. Y., Martinez-Hackert E., Kalams S. A., Davis M. M. and Sykulev Y. (2003) Distinct molecular mechanisms account for the specificity of two different T-cell receptors. *Biochemistry* 42, 4709-16.

Armstrong K. M., Insaidoo F. K. and Baker B. M. (2008) Thermodynamics of T-cell receptor-peptide/MHC interactions: progress and opportunities. *J Mol Recognit* 21, 275-287.

Backstrom B. T., Milia E., Peter A., Jaureguiberry B., Baldari C. T. and Palmer E. (1996) A motif within the T cell receptor alpha chain constant region connecting peptide domain controls antigen responsiveness. *Immunity* 5, 437-47.

Baker B. M., Gagnon S. J., Biddison W. E. and Wiley D. C. (2000) Conversion of a T cell antagonist into an agonist by repairing a defect in the TCR/peptide/MHC interface: implications for TCR signaling. *Immunity* 13, 475-84.

Barton L. F., Cruz M., Rangwala R., Deepe G. S., Jr. and Monaco J. J. (2002) Regulation of immunoproteasome subunit expression in vivo following pathogenic fungal infection. *J Immunol* 169, 3046-52.

Bernhard E. J., Le A. X., Yannelli J. R., Holterman M. J., Hogan K. T., Parham P. and Engelhard V. H. (1987) The ability of cytotoxic T cells to recognize HLA-A2.1 or HLA-B7 antigens expressed on murine cells correlates with their epitope specificity. *J Immunol* 139, 3614-21.

Binz A. K., Rodriguez R. C., Biddison W. E. and Baker B. M. (2003) Thermodynamic and kinetic analysis of a peptide-class I MHC interaction highlights the noncovalent nature and conformational dynamics of the class I heterotrimer. *Biochemistry* 42, 4954-61.

Bjorkman P. J., Saper M. A., Samraoui B., Bennett W. S., Strominger J. L. and Wiley D. C. (1987) The foreign antigen binding site and T cell recognition regions of class I histocompatibility antigens. *Nature* 329, 512-8.

Bongrand P. and Malissen B. (1998) Quantitative aspects of T-cell recognition: from within the antigen-presenting cell to within the T cell. *Bioessays* 20, 412-22.

Boniface J. J., Reich Z., Lyons D. S. and Davis M. M. (1999) Thermodynamics of T cell receptor binding to peptide-MHC: evidence for a general mechanism of molecular scanning. *Proc Natl Acad Sci U S A* 96, 11446-51.

Borg N. A., Ely L. K., Beddoe T., Macdonald W. A., Reid H. H., Clements C. S., Purcell A. W., Kjer-Nielsen L., Miles J. J., Burrows S. R., McCluskey J. and Rossjohn J. (2005) The CDR3 regions of an immunodominant T cell receptor dictate the 'energetic landscape' of peptide-MHC recognition. *Nat Immunol* 6, 171-80.

Boulter J. M., Schmitz N., Sewell A. K., Godkin A. J., Bachmann M. F. and Gallimore A. M. (2007) Potent T cell agonism mediated by a very rapid TCR/pMHC interaction. *Eur J Immunol* 37, 798-806.

Bromley S. K., Burack W. R., Johnson K. G., Somersalo K., Sims T. N., Sumen C., Davis M. M., Shaw A. S., Allen P. M. and Dustin M. L. (2001) The immunological synapse. *Annu Rev Immunol* 19, 375-96.

Buslepp J., Kerry S. E., Loftus D., Frelinger J. A., Appella E. and Collins E. J. (2003a) High affinity xenoreactive TCR:MHC interaction recruits CD8 in absence of binding to MHC. *J Immunol* 170, 373-83.

Buslepp J., Wang H., Biddison W. E., Appella E. and Collins E. J. (2003b) A correlation between TCR Valpha docking on MHC and CD8 dependence: implications for T cell selection. *Immunity* 19, 595-606.

Buslepp J., Zhao R., Donnini D., Loftus D., Saad M., Appella E. and Collins E. J. (2001) T cell activity correlates with oligomeric peptide-major histocompatibility complex binding on T cell surface. *J Biol Chem* 276, 47320-8.

Buus S., Colon S., Smith C., Freed J. H., Miles C. and Grey H. M. (1986) Interaction between a "processed" ovalbumin peptide and Ia molecules. *Proc Natl Acad Sci U S A* 83, 3968-71.

Buxton S. E., Benjamin R. J., Clayberger C., Parham P. and Krensky A. M. (1992) Anchoring pockets in human histocompatibility complex leukocyte antigen (HLA) class I molecules: analysis of the conserved B ("45") pocket of HLA-B27. *J Exp Med* 175, 809-20.

Cerundolo V., Elliott T., Elvin J., Bastin J., Rammensee H. G. and Townsend A. (1991) The binding affinity and dissociation rates of peptides for class I major histocompatibility complex molecules. *Eur J Immunol* 21, 2069-75.

Chen J. L., Stewart-Jones G., Bossi G., Lissin N. M., Wooldridge L., Choi E. M., Held G., Dunbar P. R., Esnouf R. M., Sami M., Boulter J. M., Rizkallah P., Renner C., Sewell A., van der Merwe P. A., Jakobsen B. K., Griffiths G., Jones E. Y. and Cerundolo V. (2005) Structural and kinetic basis for heightened immunogenicity of T cell vaccines. *J Exp Med* 201, 1243-55.

Chen Y. Z., Lai Z. F., Nishi K. and Nishimura Y. (1998) Modulation of calcium responses by altered peptide ligands in a human T cell clone. *Eur J Immunol* 28, 3929-39.

Cho B. K., Lian K. C., Lee P., Brunmark A., McKinley C., Chen J., Kranz D. M. and Eisen H. N. (2001) Differences in antigen recognition and cytolytic activity of CD8(+) and CD8(-) T cells that express the same antigen-specific receptor. *Proc Natl Acad Sci U S A* 98, 1723-7.

Choudhuri K., Wiseman D., Brown M. H., Gould K. and van der Merwe P. A. (2005) T-cell receptor triggering is critically dependent on the dimensions of its peptide-MHC ligand. *Nature* 436, 578-82.

Claverie J. M., Prochnicka-Chalufour A. and Bougueleret L. (1989) Implications of a Fab-like structure for the T-cell receptor. *Immunol Today* 10, 10-4.

Colf L. A., Bankovich A. J., Hanick N. A., Bowerman N. A., Jones L. L., Kranz D. M. and Garcia K. C. (2007) How a single T cell receptor recognizes both self and foreign MHC. *Cell* 129, 135-46.

Collins E. J., Garboczi D. N., Karpusas M. N. and Wiley D. C. (1995) The three-dimensional structure of a class I major histocompatibility complex molecule missing the alpha 3 domain of the heavy chain. *Proc Natl Acad Sci U S A* 92, 1218-21.

Corr M., Boyd L. F., Frankel S. R., Kozlowski S., Padlan E. A. and Margulies D. H. (1992) Endogenous peptides of a soluble major histocompatibility complex class I molecule, H-2Lds: sequence motif, quantitative binding, and molecular modeling of the complex. *J Exp Med* 176, 1681-92.

Corr M., Boyd L. F., Padlan E. A. and Margulies D. H. (1993) H-2Dd exploits a four residue peptide binding motif. *J Exp Med* 178, 1877-92.

Culina S., Lauvau G., Gubler B. and van Endert P. M. (2004) Calreticulin promotes folding of functional human leukocyte antigen class I molecules in vitro. *J Biol Chem* 279, 54210-5.

Curnow S. J., Guimezanes A. and Schmitt-Verhulst A. M. (1994) CD8 requirements for negative selection events are directly related to the TCR-antigen interaction. *Thymus* 22, 255-65.

Dai S., Huseby E. S., Rubtsova K., Scott-Browne J., Crawford F., Macdonald W. A., Marrack P. and Kappler J. W. (2008) Crossreactive T Cells spotlight the germline rules for alphabeta T cell-receptor interactions with MHC molecules. *Immunity* 28, 324-34.

Davis M. M. and Bjorkman P. J. (1988) T-cell antigen receptor genes and T-cell recognition. *Nature* 334, 395-402.

Davis M. M., Boniface J. J., Reich Z., Lyons D., Hampl J., Arden B. and Chien Y. (1998) Ligand recognition by alpha beta T cell receptors. *Annu Rev Immunol* 16, 523-44.

Davis-Harrison R. L., Armstrong K. M. and Baker B. M. (2005) Two different T cell receptors use different thermodynamic strategies to recognize the same peptide/MHC ligand. *J Mol Biol* 346, 533-50.

Davis-Harrison R. L., Insaidoo F. K. and Baker B. M. (2007) T Cell Receptor Binding Transition States and Recognition of Peptide/MHC. *Biochemistry* 46, 1840-50.

Degano M., Garcia K. C., Apostolopoulos V., Rudolph M. G., Teyton L. and Wilson I. A. (2000) A functional hot spot for antigen recognition in a superagonist TCR/MHC complex. *Immunity* 12, 251-61.

Del Val M., Schlicht H. J., Ruppert T., Reddehase M. J. and Koszinowski U. H. (1991) Efficient processing of an antigenic sequence for presentation by MHC class I molecules depends on its neighboring residues in the protein. *Cell* 66, 1145-53.

DeLano W. L. (2002) The PyMOL Molecular Graphics System. DeLano Scientific, San Carlos, CA, USA.

Deng L., Langley R. J., Brown P. H., Xu G., Teng L., Wang Q., Gonzales M. I., Callender G. G., Nishimura M. I., Topalian S. L. and Mariuzza R. A. (2007) Structural basis for the recognition of mutant self by a tumor-specific, MHC class II-restricted T cell receptor. *Nat Immunol* 8, 398-408.

Deng Y., Yewdell J. W., Eisenlohr L. C. and Bennink J. R. (1997) MHC affinity, peptide liberation, T cell repertoire, and immunodominance all contribute to the paucity

of MHC class I-restricted peptides recognized by antiviral CTL. *J Immunol* 158, 1507-15.

Deverson E. V., Gow I. R., Coadwell W. J., Monaco J. J., Butcher G. W. and Howard J. C. (1990) MHC class II region encoding proteins related to the multidrug resistance family of transmembrane transporters. *Nature* 348, 738-41.

Dick L. R., Moomaw C. R., DeMartino G. N. and Slaughter C. A. (1991) Degradation of oxidized insulin B chain by the multiproteinase complex macropain (proteasome). *Biochemistry* 30, 2725-34.

Ding Y. H., Baker B. M., Garboczi D. N., Biddison W. E. and Wiley D. C. (1999) Four A6-TCR/peptide/HLA-A2 structures that generate very different T cell signals are nearly identical. *Immunity* 11, 45-56.

Ding Y. H., Smith K. J., Garboczi D. N., Utz U., Biddison W. E. and Wiley D. C. (1998) Two human T cell receptors bind in a similar diagonal mode to the HLA-A2/Tax peptide complex using different TCR amino acids. *Immunity* 8, 403-11.

Dong T., Boyd D., Rosenberg W., Alp N., Takiguchi M., McMichael A. and Rowland-Jones S. (1996) An HLA-B35-restricted epitope modified at an anchor residue results in an antagonist peptide. *Eur J Immunol* 26, 335-9.

Eggers M., Boes-Fabian B., Ruppert T., Kloetzel P. M. and Koszinowski U. H. (1995) The cleavage preference of the proteasome governs the yield of antigenic peptides. *J Exp Med* 182, 1865-70.

Eisenlohr L. C., Yewdell J. W. and Bennink J. R. (1992) Flanking sequences influence the presentation of an endogenously synthesized peptide to cytotoxic T lymphocytes. *J Exp Med* 175, 481-7.

Elliott T., Elvin J., Cerundolo V., Allen H. and Townsend A. (1992) Structural requirements for the peptide-induced conformational change of free major histocompatibility complex class I heavy chains. *Eur J Immunol* 22, 2085-91.

Ely L. K., Beddoe T., Clements C. S., Matthews J. M., Purcell A. W., Kjer-Nielsen L., McCluskey J. and Rossjohn J. (2006) Disparate thermodynamics governing T cell receptor-MHC-I interactions implicate extrinsic factors in guiding MHC restriction. *Proc Natl Acad Sci U S A* 103, 6641-6.

Falk K., Rotzschke O., Stevanovic S., Jung G. and Rammensee H. G. (1991) Allele-specific motifs revealed by sequencing of self-peptides eluted from MHC molecules. *Nature* 351, 290-6.

Farmery M. R., Allen S., Allen A. J. and Bulleid N. J. (2000) The role of ERp57 in disulfide bond formation during the assembly of major histocompatibility

complex class I in a synchronized semipermeabilized cell translation system. *J Biol Chem* 275, 14933-8.

Fremont D. H., Matsumura M., Stura E. A., Peterson P. A. and Wilson I. A. (1992) Crystal structures of two viral peptides in complex with murine MHC class I H-2Kb. *Science* 257, 919-27.

Gaczynska M., Rock K. L., Spies T. and Goldberg A. L. (1994) Peptidase activities of proteasomes are differentially regulated by the major histocompatibility complex-encoded genes for LMP2 and LMP7. *Proc Natl Acad Sci U S A* 91, 9213-7.

Gagnon S. J., Borbulevych O. Y., Davis-Harrison R. L., Turner R. V., Damirjian M., Wojnarowicz A., Biddison W. E. and Baker B. M. (2006) T cell receptor recognition via cooperative conformational plasticity. *J Mol Biol* 363, 228-43.

Gakamsky D. M., Luescher I. F. and Pecht I. (2004) T cell receptor-ligand interactions: a conformational preequilibrium or an induced fit. *Proc Natl Acad Sci U S A* 101, 9063-6.

Gao G. F., Tormo J., Gerth U. C., Wyer J. R., McMichael A. J., Stuart D. I., Bell J. I., Jones E. Y. and Jakobsen B. K. (1997) Crystal structure of the complex between human CD8alpha(alpha) and HLA-A2. *Nature* 387, 630-4.

Garboczi D. N., Ghosh P., Utz U., Fan Q. R., Biddison W. E. and Wiley D. C. (1996) Structure of the complex between human T-cell receptor, viral peptide and HLA-A2. *Nature* 384, 134-41.

Garcia K. C., Degano M., Pease L. R., Huang M., Peterson P. A., Teyton L. and Wilson I. A. (1998) Structural basis of plasticity in T cell receptor recognition of a self peptide-MHC antigen. *Science* 279, 1166-72.

Garcia K. C., Degano M., Stanfield R. L., Brunmark A., Jackson M. R., Peterson P. A., Teyton L. and Wilson I. A. (1996) An alphabeta T cell receptor structure at 2.5 A and its orientation in the TCR-MHC complex. *Science* 274, 209-19.

Garcia K. C., Radu C. G., Ho J., Ober R. J. and Ward E. S. (2001) Kinetics and thermodynamics of T cell receptor- autoantigen interactions in murine experimental autoimmune encephalomyelitis. *Proc Natl Acad Sci U S A* 98, 6818-23.

Garcia-Peydro M., Paradela A., Albar J. P. and Castro J. A. (2000) Antagonism of direct alloreactivity of an HLA-B27-specific CTL clone by altered peptide ligands of its natural epitope. *J Immunol* 165, 5680-5.

Garrett T. P., Saper M. A., Bjorkman P. J., Strominger J. L. and Wiley D. C. (1989) Specificity pockets for the side chains of peptide antigens in HLA-Aw68. *Nature* 342, 692-6.

Germain R. N. (2002) T-cell development and the CD4-CD8 lineage decision. *Nat Rev Immunol* 2, 309-22.

Goh C. S., Milburn D. and Gerstein M. (2004) Conformational changes associated with protein-protein interactions. *Curr Opin Struct Biol* 14, 104-9.

Gorbulev S., Abele R. and Tampe R. (2001) Allosteric crosstalk between peptide-binding, transport, and ATP hydrolysis of the ABC transporter TAP. *Proc Natl Acad Sci U S A* 98, 3732-7.

Grakoui A., Bromley S. K., Sumen C., Davis M. M., Shaw A. S., Allen P. M. and Dustin M. L. (1999) The immunological synapse: a molecular machine controlling T cell activation. *Science* 285, 221-7.

Grandea A. G., 3rd, Comber P. G., Wenderfer S. E., Schoenhals G., Fruh K., Monaco J. J. and Spies T. (1998) Sequence, linkage to H2-K, and function of mouse tapasin in MHC class I assembly. *Immunogenetics* 48, 260-5.

Groettrup M., Ruppert T., Kuehn L., Seeger M., Standera S., Koszinowski U. and Kloetzel P. M. (1995) The interferon-gamma-inducible 11 S regulator (PA28) and the LMP2/LMP7 subunits govern the peptide production by the 20 S proteasome in vitro. *J Biol Chem* 270, 23808-15.

Guo H. C., Jardetzky T. S., Garrett T. P., Lane W. S., Strominger J. L. and Wiley D. C. (1992) Different length peptides bind to HLA-Aw68 similarly at their ends but bulge out in the middle. *Nature* 360, 364-6.

Hahn M., Nicholson M. J., Pyrdol J. and Wucherpfennig K. W. (2005) Unconventional topology of self peptide-major histocompatibility complex binding by a human autoimmune T cell receptor. *Nat Immunol* 6, 490-6.

Hammond C., Braakman I. and Helenius A. (1994) Role of N-linked oligosaccharide recognition, glucose trimming, and calnexin in glycoprotein folding and quality control. *Proc Natl Acad Sci U S A* 91, 913-7.

Hare B. J., Wyss D. F., Osburne M. S., Kern P. S., Reinherz E. L. and Wagner G. (1999) Structure, specificity and CDR mobility of a class II restricted single-chain T-cell receptor. *Nat Struct Biol* 6, 574-81.

He X. and Kappes D. J. (2006) CD4/CD8 lineage commitment: light at the end of the tunnel? *Curr Opin Immunol* 18, 135-42.

Hebert D. N., Foellmer B. and Helenius A. (1996) Calnexin and calreticulin promote folding, delay oligomerization and suppress degradation of influenza hemagglutinin in microsomes. *Embo J* 15, 2961-8.

Henderson R. A., Cox A. L., Sakaguchi K., Appella E., Shabanowitz J., Hunt D. F. and Engelhard V. H. (1993) Direct identification of an endogenous peptide recognized by multiple HLA-A2.1-specific cytotoxic T cells. *Proc Natl Acad Sci U S A* 90, 10275-9.

Hennecke J., Carfi A. and Wiley D. C. (2000) Structure of a covalently stabilized complex of a human alphabeta T-cell receptor, influenza HA peptide and MHC class II molecule, HLA-DR1. *EMBO J* 19, 5611-24.

Hennecke J. and Wiley D. C. (2002) Structure of a complex of the human alpha/beta T cell receptor (TCR) HA1.7, influenza hemagglutinin peptide, and major histocompatibility complex class II molecule, HLA-DR4 (DRA*0101 and DRB1*0401): insight into TCR cross-restriction and alloreactivity. *J Exp Med* 195, 571-81.

Herman A., Parham P., Weissman S. M. and Engelhard V. H. (1983) Recognition by xenogeneic cytotoxic T lymphocytes of cells expressing HLA-A2 or HLA-B7 after DNA-mediated gene transfer. *Proc Natl Acad Sci U S A* 80, 5056-60.

Hogan K. T., Clayberger C., Bernhard E. J., Walk S. F., Ridge J. P., Parham P., Krensky A. M. and Engelhard V. H. (1989) A panel of unique HLA-A2 mutant molecules define epitopes recognized by HLA-A2-specific antibodies and cytotoxic T lymphocytes. *J Immunol* 142, 2097-104.

Holler P. D. and Kranz D. M. (2003) Quantitative analysis of the contribution of TCR/pepMHC affinity and CD8 to T cell activation. *Immunity* 18, 255-64.

Housset D., Mazza G., Gregoire C., Piras C., Malissen B. and Fontecilla-Camps J. C. (1997) The three-dimensional structure of a T-cell antigen receptor V alpha V beta heterodimer reveals a novel arrangement of the V beta domain. *Embo J* 16, 4205-16.

Hutchinson S. L., Wooldridge L., Tafuro S., Laugel B., Glick M., Boulter J. M., Jakobsen B. K., Price D. A. and Sewell A. K. (2003) The CD8 T cell coreceptor exhibits disproportionate biological activity at extremely low binding affinities. *J Biol Chem* 278, 24285-93.

Ishizuka J., Stewart-Jones G. B., van der Merwe A., Bell J. I., McMichael A. J. and Jones E. Y. (2008) The structural dynamics and energetics of an immunodominant T cell receptor are programmed by its Vbeta domain. *Immunity* 28, 171-82.

James L. C., Roversi P. and Tawfik D. S. (2003) Antibody multispecificity mediated by conformational diversity. *Science* 299, 1362-7.

Jardetzky T. S., Lane W. S., Robinson R. A., Madden D. R. and Wiley D. C. (1991) Identification of self peptides bound to purified HLA-B27. *Nature* 353, 326-9.

Karttunen J. T., Lehner P. J., Gupta S. S., Hewitt E. W. and Cresswell P. (2001) Distinct functions and cooperative interaction of the subunits of the transporter associated with antigen processing (TAP). *Proc Natl Acad Sci U S A* 98, 7431-6.

Kersh G. J., Kersh E. N., Fremont D. H. and Allen P. M. (1998) High- and low-potency ligands with similar affinities for the TCR: the importance of kinetics in TCR signaling. *Immunity* 9, 817-26.

Kieper W. C. and Jameson S. C. (1999) Homeostatic expansion and phenotypic conversion of naive T cells in response to self peptide/MHC ligands. *Proc Natl Acad Sci U S A* 96, 13306-11.

Kisselev A. F., Akopian T. N., Woo K. M. and Goldberg A. L. o. (1999) The sizes of peptides generated from protein by mammalian 26 and 20 S proteasomes. Implications for understanding the degradative mechanism and antigen presentation. *J Biol Chem* 274, 3363-71.

Kjer-Nielsen L., Clements C. S., Brooks A. G., Purcell A. W., Fontes M. R., McCluskey J. and Rossjohn J. (2002) The structure of HLA-B8 complexed to an immunodominant viral determinant: peptide-induced conformational changes and a mode of MHC class I dimerization. *J Immunol* 169, 5153-60.

Kjer-Nielsen L., Clements C. S., Purcell A. W., Brooks A. G., Whisstock J. C., Burrows S. R., McCluskey J. and Rossjohn J. (2003) A structural basis for the selection of dominant alphabeta T cell receptors in antiviral immunity. *Immunity* 18, 53-64.

Kleijmeer M. J., Kelly A., Geuze H. J., Slot J. W., Townsend A. and Trowsdale J. (1992) Location of MHC-encoded transporters in the endoplasmic reticulum and cis-Golgi. *Nature* 357, 342-4.

Krogsgaard M. and Davis M. M. (2005) How T cells 'see' antigen. *Nat Immunol* 6, 239-45.

Krogsgaard M., Prado N., Adams E. J., He X. L., Chow D. C., Wilson D. B., Garcia K. C. and Davis M. M. (2003) Evidence that structural rearrangements and/or flexibility during TCR binding can contribute to T cell activation. *Mol Cell* 12, 1367-78.

Kubo R. T., Sette A., Grey H. M., Appella E., Sakaguchi K., Zhu N. Z., Arnott D., Sherman N., Shabanowitz J., Michel H. and et al. (1994) Definition of specific peptide motifs for four major HLA-A alleles. *J Immunol* 152, 3913-24.

Lanzavecchia A., Lezzi G. and Viola A. (1999) From TCR engagement to T cell activation: a kinetic view of T cell behavior. *Cell* 96, 1-4.

Lau L. L., Jiang J. and Shen H. (2005) In vivo modulation of T cell responses and protective immunity by TCR antagonism during infection. *J Immunol* 174, 7970-6.

Lee J. K., Stewart-Jones G., Dong T., Harlos K., Di Gleria K., Dorrell L., Douek D. C., van der Merwe P. A., Jones E. Y. and McMichael A. J. (2004) T cell cross-reactivity and conformational changes during TCR engagement. *J Exp Med* 200, 1455-66.

Li S., Paulsson K. M., Sjogren H. O. and Wang P. (1999) Peptide-bound major histocompatibility complex class I molecules associate with tapasin before dissociation from transporter associated with antigen processing. *J Biol Chem* 274, 8649-54.

Li S., Sjogren H. O., Hellman U., Pettersson R. F. and Wang P. (1997) Cloning and functional characterization of a subunit of the transporter associated with antigen processing. *Proc Natl Acad Sci U S A* 94, 8708-13.

Li Y., Huang Y., Lue J., Quandt J. A., Martin R. and Mariuzza R. A. (2005) Structure of a human autoimmune TCR bound to a myelin basic protein self-peptide and a multiple sclerosis-associated MHC class II molecule. *EMBO J* 24, 2968-79.

Lindquist J. A., Hammerling G. J. and Trowsdale J. (2001) ER60/ERp57 forms disulfide-bonded intermediates with MHC class I heavy chain. *Faseb J* 15, 1448-50.

Lindquist J. A., Jensen O. N., Mann M. and Hammerling G. J. (1998) ER-60, a chaperone with thiol-dependent reductase activity involved in MHC class I assembly. *Embo J* 17, 2186-95.

Ljunggren H. G., Stam N. J., Ohlen C., Neefjes J. J., Hoglund P., Heemels M. T., Bastin J., Schumacher T. N., Townsend A., Karre K. and et al. (1990) Empty MHC class I molecules come out in the cold. *Nature* 346, 476-80.

Loftus D. J., Chen Y., Covell D. G., Engelhard V. H. and Appella E. (1997) Differential contact of disparate class I/peptide complexes as the basis for epitope cross-recognition by a single T cell receptor. *J Immunol* 158, 3651-8.

Luescher I. F., Vivier E., Layer A., Mahiou J., Godeau F., Malissen B. and Romero P. (1995) CD8 modulation of T-cell antigen receptor-ligand interactions on living cytotoxic T lymphocytes. *Nature* 373, 353-6.

Luz J. G., Huang M., Garcia K. C., Rudolph M. G., Apostolopoulos V., Teyton L. and Wilson I. A. (2002) Structural comparison of allogeneic and syngeneic T cell receptor-peptide-major histocompatibility complex complexes: a buried alloreactive mutation subtly alters peptide presentation substantially increasing V(beta) Interactions. *J Exp Med* 195, 1175-86.

Lyons D. S., Lieberman S. A., Hampl J., Boniface J. J., Chien Y., Berg L. J. and Davis M. M. (1996) A TCR binds to antagonist ligands with lower affinities and faster dissociation rates than to agonists. *Immunity* 5, 53-61.

Madden D. R., Gorga J. C., Strominger J. L. and Wiley D. C. (1991) The structure of HLA-B27 reveals nonamer self-peptides bound in an extended conformation. *Nature* 353, 321-5.

Madrenas J. and Germain R. N. (1996) Variant TCR ligands: new insights into the molecular basis of antigen-dependent signal transduction and T-cell activation. *Semin Immunol* 8, 83-101.

Maryanski J. L., Verdini A. S., Weber P. C., Salemme F. R. and Corradin G. (1990) Competitor analogs for defined T cell antigens: peptides incorporating a putative binding motif and polyproline or polyglycine spacers. *Cell* 60, 63-72.

Matsui K., Boniface J. J., Steffner P., Reay P. A. and Davis M. M. (1994) Kinetics of T-cell receptor binding to peptide/I-Ek complexes: correlation of the dissociation rate with T-cell responsiveness. *Proc Natl Acad Sci U S A* 91, 12862-6.

Matsui M., Hioe C. E. and Frelinger J. A. (1993) Roles of the six peptide-binding pockets of the HLA-A2 molecule in allorecognition by human cytotoxic T-cell clones. *Proc Natl Acad Sci U S A* 90, 674-8.

Matsumura M., Fremont D. H., Peterson P. A. and Wilson I. A. (1992) Emerging principles for the recognition of peptide antigens by MHC class I molecules. *Science* 257, 927-34.

Maynard J., Petersson K., Wilson D. H., Adams E. J., Blondelle S. E., Boulanger M. J., Wilson D. B. and Garcia K. C. (2005) Structure of an autoimmune T cell receptor complexed with class II peptide-MHC: insights into MHC bias and antigen specificity. *Immunity* 22, 81-92.

Mazza C., Auphan-Anezin N., Gregoire C., Guimezanes A., Kellenberger C., Roussel A., Kearney A., van der Merwe P. A., Schmitt-Verhulst A. M. and Malissen B.

(2007) How much can a T-cell antigen receptor adapt to structurally distinct antigenic peptides? *EMBO J* 26, 1972-83.

McBeth C., Seamons A., Pizarro J. C., Fleishman S. J., Baker D., Kortemme T., Goverman J. M. and Strong R. K. (2008) A new twist in TCR diversity revealed by a forbidden alphabeta TCR. *J Mol Biol* 375, 1306-19.

McKeithan T. W. (1995) Kinetic proofreading in T-cell receptor signal transduction. *Proc Natl Acad Sci U S A* 92, 5042-6.

Meijers R., Lai C. C., Yang Y., Liu J. H., Zhong W., Wang J. H. and Reinherz E. L. (2005) Crystal structures of murine MHC Class I H-2 D(b) and K(b) molecules in complex with CTL epitopes from influenza A virus: implications for TCR repertoire selection and immunodominance. *J Mol Biol* 345, 1099-110.

Michalak M., Milner R. E., Burns K. and Opas M. (1992) Calreticulin. *Biochem J* 285 (Pt 3), 681-92.

Michalek M. T., Grant E. P., Gramm C., Goldberg A. L. and Rock K. L. (1993) A role for the ubiquitin-dependent proteolytic pathway in MHC class I-restricted antigen presentation. *Nature* 363, 552-4.

Miller P. J., Pazy Y., Conti B., Riddle D., Appella E. and Collins E. J. (2007) Single MHC mutation eliminates enthalpy associated with T cell receptor binding. *J Mol Biol* 373, 315-27.

Momburg F., Roelse J., Howard J. C., Butcher G. W., Hammerling G. J. and Neefjes J. J. (1994) Selectivity of MHC-encoded peptide transporters from human, mouse and rat. *Nature* 367, 648-51.

Monaco J. J., Cho S. and Attaya M. (1990) Transport protein genes in the murine MHC: possible implications for antigen processing. *Science* 250, 1723-6.

Monks C. R., Freiberg B. A., Kupfer H., Sciaky N. and Kupfer A. (1998) Three-dimensional segregation of supramolecular activation clusters in T cells. *Nature* 395, 82-6.

Naeher D., Luescher I. F. and Palmer E. (2002) A role for the alpha-chain connecting peptide motif in mediating TCR-CD8 cooperation. *J Immunol* 169, 2964-70.

Nauseef W. M., McCormick S. J. and Clark R. A. (1995) Calreticulin functions as a molecular chaperone in the biosynthesis of myeloperoxidase. *J Biol Chem* 270, 4741-7.

Neefjes J. J., Dierx J. and Ploegh H. L. (1993a) The effect of anchor residue modifications on the stability of major histocompatibility complex class I-peptide interactions. *Eur J Immunol* 23, 840-5.

Neefjes J. J., Momburg F. and Hammerling G. J. (1993b) Selective and ATP-dependent translocation of peptides by the MHC-encoded transporter. *Science* 261, 769-71.

Niedermann G., Butz S., Ihlenfeldt H. G., Grimm R., Lucchiari M., Hoschutzky H., Jung G., Maier B. and Eichmann K. (1995) Contribution of proteasome-mediated proteolysis to the hierarchy of epitopes presented by major histocompatibility complex class I molecules. *Immunity* 2, 289-99.

Ortmann B., Androlewicz M. J. and Cresswell P. (1994) MHC class I/beta 2-microglobulin complexes associate with TAP transporters before peptide binding. *Nature* 368, 864-7.

Ortmann B., Copeman J., Lehner P. J., Sadasivan B., Herberg J. A., Grandea A. G., Riddell S. R., Tampe R., Spies T., Trowsdale J. and Cresswell P. (1997) A critical role for tapasin in the assembly and function of multimeric MHC class I-TAP complexes. *Science* 277, 1306-9.

Ossendorp F., Eggers M., Neisig A., Ruppert T., Groettrup M., Sijts A., Mengede E., Kloetzel P. M., Neefjes J., Koszinowski U. and Melief C. (1996) A single residue exchange within a viral CTL epitope alters proteasome-mediated degradation resulting in lack of antigen presentation. *Immunity* 5, 115-24.

Paradela A., Alvarez I., Garcia-Peydro M., Sesma L., Ramos M., Vazquez J. and Lopez De Castro J. A. (2000) Limited diversity of peptides related to an alloreactive T cell epitope in the HLA-B27-bound peptide repertoire results from restrictions at multiple steps along the processing-loading pathway. *J Immunol* 164, 329-37.

Parham P., Adams E. J. and Arnett K. L. (1995) The origins of HLA-A,B,C polymorphism. *Immunol Rev* 143, 141-80.

Peterson J. R., Ora A., Van P. N. and Helenius A. (1995) Transient, lectin-like association of calreticulin with folding intermediates of cellular and viral glycoproteins. *Mol Biol Cell* 6, 1173-84.

Potter T. A., Rajan T. V., Dick R. F., 2nd and Bluestone J. A. (1989) Substitution at residue 227 of H-2 class I molecules abrogates recognition by CD8-dependent, but not CD8-independent, cytotoxic T lymphocytes. *Nature* 337, 73-5.

Rabinowitz J. D., Beeson C., Lyons D. S., Davis M. M. and McConnell H. M. (1996) Kinetic discrimination in T-cell activation. *Proc Natl Acad Sci U S A* 93, 1401-5.

Rammensee H. G., Friede T. and Stevanoviic S. (1995) MHC ligands and peptide motifs: first listing. *Immunogenetics* 41, 178-228.

Reinherz E. L., Tan K., Tang L., Kern P., Liu J., Xiong Y., Hussey R. E., Smolyar A., Hare B., Zhang R., Joachimiak A., Chang H. C., Wagner G. and Wang J. (1999) The crystal structure of a T cell receptor in complex with peptide and MHC class II. *Science* 286, 1913-21.

Reis e Sousa C., Levine E. H. and Germain R. N. (1996) Partial signaling by CD8+ T cells in response to antagonist ligands. *J Exp Med* 184, 149-57.

Reiser J. B., Darnault C., Gregoire C., Mosser T., Mazza G., Kearney A., van der Merwe P. A., Fontecilla-Camps J. C., Housset D. and Malissen B. (2003) CDR3 loop flexibility contributes to the degeneracy of TCR recognition. *Nat Immunol* 4, 241-7.

Reiser J. B., Darnault C., Guimezanes A., Gregoire C., Mosser T., Schmitt-Verhulst A. M., Fontecilla-Camps J. C., Malissen B., Housset D. and Mazza G. (2000) Crystal structure of a T cell receptor bound to an allogeneic MHC molecule. *Nat Immunol* 1, 291-7.

Reiser J. B., Gregoire C., Darnault C., Mosser T., Guimezanes A., Schmitt-Verhulst A. M., Fontecilla-Camps J. C., Mazza G., Malissen B. and Housset D. (2002) A T cell receptor CDR3beta loop undergoes conformational changes of unprecedented magnitude upon binding to a peptide/MHC class I complex. *Immunity* 16, 345-54.

Reits E., Griekspoor A., Neijssen J., Groothuis T., Jalink K., van Veelen P., Janssen H., Calafat J., Drijfhout J. W. and Neefjes J. (2003) Peptide diffusion, protection, and degradation in nuclear and cytoplasmic compartments before antigen presentation by MHC class I. *Immunity* 18, 97-108.

Reits E. A., Vos J. C., Gromme M. and Neefjes J. (2000) The major substrates for TAP in vivo are derived from newly synthesized proteins. *Nature* 404, 774-8.

Riddle D. S., Miller P. J., Vincent B. G., Kepler T. B., Maile R., Frelinger J. A. and Collins E. J. (2008) Rescue of cytotoxic function in the CD8alpha knockout mouse by removal of MHC class II. *Eur J Immunol* 38, 1511-21.

Rohren E. M., Pease L. R., Ploegh H. L. and Schumacher T. N. (1993) Polymorphisms in pockets of major histocompatibility complex class I molecules influence peptide preference. *J Exp Med* 177, 1713-21.

Rosette C., Werlen G., Daniels M. A., Holman P. O., Alam S. M., Travers P. J., Gascoigne N. R., Palmer E. and Jameson S. C. (2001) The impact of duration versus extent of TCR occupancy on T cell activation: a revision of the kinetic proofreading model. *Immunity* 15, 59-70.

Rudolph M. G., Stanfield R. L. and Wilson I. A. (2006) How TCRs bind MHCs, peptides, and coreceptors. *Annu Rev Immunol* 24, 419-66.

Ruppert J., Sidney J., Celis E., Kubo R. T., Grey H. M. and Sette A. (1993) Prominent role of secondary anchor residues in peptide binding to HLA-A2.1 molecules. *Cell* 74, 929-37.

Sadasivan B., Lehner P. J., Ortmann B., Spies T. and Cresswell P. (1996) Roles for calreticulin and a novel glycoprotein, tapasin, in the interaction of MHC class I molecules with TAP. *Immunity* 5, 103-14.

Santos-Aguado J., Crimmins M. A., Mentzer S. J., Burakoff S. J. and Strominger J. L. (1989) Alloreactivity studied with mutants of HLA-A2. *Proc Natl Acad Sci U S A* 86, 8936-40.

Saper M. A., Bjorkman P. J. and Wiley D. C. (1991) Refined structure of the human histocompatibility antigen HLA-A2 at 2.6 A resolution. *J Mol Biol* 219, 277-319.

Saric T., Chang S. C., Hattori A., York I. A., Markant S., Rock K. L., Tsujimoto M. and Goldberg A. L. (2002) An IFN-gamma-induced aminopeptidase in the ER, ERAP1, trims precursors to MHC class I-presented peptides. *Nat Immunol* 3, 1169-76.

Saveanu L., Daniel S. and van Endert P. M. (2001) Distinct functions of the ATP binding cassettes of transporters associated with antigen processing: a mutational analysis of Walker A and B sequences. *J Biol Chem* 276, 22107-13.

Schatz D. G. and Spanopoulou E. (2005) Biochemistry of V(D)J recombination. *Curr Top Microbiol Immunol* 290, 49-85.

Schodin B. A., Tsomides T. J. and Kranz D. M. (1996) Correlation between the number of T cell receptors required for T cell activation and TCR-ligand affinity. *Immunity* 5, 137-46.

Schwartz R. H. (2003) T cell anergy. *Annu Rev Immunol* 21, 305-34.

Serwold T., Gonzalez F., Kim J., Jacob R. and Shastri N. (2002) ERAAP customizes peptides for MHC class I molecules in the endoplasmic reticulum. *Nature* 419, 480-3.

Serwold T. and Shastri N. (1999) Specific proteolytic cleavages limit the diversity of the pool of peptides available to MHC class I molecules in living cells. *J Immunol* 162, 4712-9.

Shaw A. S., Chalupny J., Whitney J. A., Hammond C., Amrein K. E., Kavathas P., Sefton B. M. and Rose J. K. (1990) Short related sequences in the cytoplasmic domains of CD4 and CD8 mediate binding to the amino-terminal domain of the p56lck tyrosine protein kinase. *Mol Cell Biol* 10, 1853-62.

Shepherd J. C., Schumacher T. N., Ashton-Rickardt P. G., Imaeda S., Ploegh H. L., Janeway C. A., Jr. and Tonegawa S. (1993) TAP1-dependent peptide translocation in vitro is ATP dependent and peptide selective. *Cell* 74, 577-84.

Sloan-Lancaster J., Evavold B. D. and Allen P. M. (1993) Induction of T-cell anergy by altered T-cell-receptor ligand on live antigen-presenting cells. *Nature* 363, 156-9.

Spicuglia S., Franchini D. M. and Ferrier P. (2006) Regulation of V(D)J recombination. *Curr Opin Immunol* 18, 158-63.

Spies T., Bresnahan M., Bahram S., Arnold D., Blanck G., Mellins E., Pious D. and DeMars R. (1990) A gene in the human major histocompatibility complex class II region controlling the class I antigen presentation pathway. *Nature* 348, 744-7.

Spolar R. S. and Record M. T., Jr. (1994) Coupling of local folding to site-specific binding of proteins to DNA. *Science* 263, 777-84.

Starr T. K., Jameson S. C. and Hogquist K. A. (2003) Positive and negative selection of T cells. *Annu Rev Immunol* 21, 139-76.

Stefanova I., Dorfman J. R. and Germain R. N. (2002) Self-recognition promotes the foreign antigen sensitivity of naive T lymphocytes. *Nature* 420, 429-34.

Stewart-Jones G. B., McMichael A. J., Bell J. I., Stuart D. I. and Jones E. Y. (2003) A structural basis for immunodominant human T cell receptor recognition. *Nat Immunol* 4, 657-63.

Suh W. K., Cohen-Doyle M. F., Fruh K., Wang K., Peterson P. A. and Williams D. B. (1994) Interaction of MHC class I molecules with the transporter associated with antigen processing. *Science* 264, 1322-6.

Sumen C., Dustin M. L. and Davis M. M. (2004) T cell receptor antagonism interferes with MHC clustering and integrin patterning during immunological synapse formation. *J Cell Biol* 166, 579-90.

Sykulev Y., Brunmark A., Jackson M., Cohen R. J., Peterson P. A. and Eisen H. N. (1994) Kinetics and affinity of reactions between an antigen-specific T cell receptor and peptide-MHC complexes. *Immunity* 1, 15-22.

Sykulev Y., Vugmeyster Y., Brunmark A., Ploegh H. L. and Eisen H. N. (1998) Peptide antagonism and T cell receptor interactions with peptide-MHC complexes. *Immunity* 9, 475-83.

Teng M. K., Smolyar A., Tse A. G., Liu J. H., Liu J., Hussey R. E., Nathenson S. G., Chang H. C., Reinherz E. L. and Wang J. H. (1998) Identification of a common docking topology with substantial variation among different TCR-peptide-MHC complexes. *Curr Biol* 8, 409-12.

Thomson C. T., Kalergis A. M., Sacchettini J. C. and Nathenson S. G. (2001) A structural difference limited to one residue of the antigenic peptide can profoundly alter the biological outcome of the TCR-peptide/MHC class I interaction. *J Immunol* 166, 3994-7.

Tian S., Maile R., Collins E. J. and Frelinger J. A. (2007) CD8+ T cell activation is governed by TCR-peptide/MHC affinity, not dissociation rate. *J Immunol* 179, 2952-60.

Townsend A., Elliott T., Cerundolo V., Foster L., Barber B. and Tse A. (1990) Assembly of MHC class I molecules analyzed in vitro. *Cell* 62, 285-95.

Townsend A., Ohlen C., Bastin J., Ljunggren H. G., Foster L. and Karre K. (1989) Association of class I major histocompatibility heavy and light chains induced by viral peptides. *Nature* 340, 443-8.

Trowsdale J., Hanson I., Mockridge I., Beck S., Townsend A. and Kelly A. (1990) Sequences encoded in the class II region of the MHC related to the 'ABC' superfamily of transporters. *Nature* 348, 741-4.

Turner J. M., Brodsky M. H., Irving B. A., Levin S. D., Perlmutter R. M. and Littman D. R. (1990) Interaction of the unique N-terminal region of tyrosine kinase p56lck with cytoplasmic domains of CD4 and CD8 is mediated by cysteine motifs. *Cell* 60, 755-65.

Tynan F. E., Burrows S. R., Buckle A. M., Clements C. S., Borg N. A., Miles J. J., Beddoe T., Whisstock J. C., Wilce M. C., Silins S. L., Burrows J. M., Kjer-Nielsen L., Kostenko L., Purcell A. W., McCluskey J. and Rossjohn J. (2005) T cell receptor recognition of a 'super-bulged' major histocompatibility complex class I-bound peptide. *Nat Immunol* 6, 1114-22.

Tynan F. E., Reid H. H., Kjer-Nielsen L., Miles J. J., Wilce M. C., Kostenko L., Borg N. A., Williamson N. A., Beddoe T., Purcell A. W., Burrows S. R., McCluskey J. and Rossjohn J. (2007) A T cell receptor flattens a bulged antigenic peptide presented by a major histocompatibility complex class I molecule. *Nat Immunol* 8, 268-76.

Uebel S., Kraas W., Kienle S., Wiesmuller K. H., Jung G. and Tampe R. (1997) Recognition principle of the TAP transporter disclosed by combinatorial peptide libraries. *Proc Natl Acad Sci U S A* 94, 8976-81.

Uhlin M., Masucci M. and Levitsky V. (2006) Is the activity of partially agonistic MHC:peptide ligands dependent on the quality of immunological help? *Scand J Immunol* 64, 581-7.

Ulivieri C., Peter A., Orsini E., Palmer E. and Baldari C. T. (2001) Defective signaling to Fyn by a T cell antigen receptor lacking the alpha -chain connecting peptide motif. *J Biol Chem* 276, 3574-80.

Valitutti S., Muller S., Cella M., Padovan E. and Lanzavecchia A. (1995) Serial triggering of many T-cell receptors by a few peptide-MHC complexes. *Nature* 375, 148-51.

van der Merwe P. A. and Davis S. J. (2003) Molecular interactions mediating T cell antigen recognition. *Annu Rev Immunol* 21, 659-84.

van Endert P. M. (1999) Role of nucleotides and peptide substrate for stability and functional state of the human ABC family transporters associated with antigen processing. *J Biol Chem* 274, 14632-8.

van Oers N. S. (1999) T cell receptor-mediated signs and signals governing T cell development. *Semin Immunol* 11, 227-37.

Villadangos J. A., Galocha B., Lopez D., Calvo V. and Lopez de Castro J. A. (1992) Role of binding pockets for amino-terminal peptide residues in HLA-B27 allorecognition. *J Immunol* 149, 505-10.

von Boehmer H., Aifantis I., Gounari F., Azogui O., Haughn L., Apostolou I., Jaeckel E., Grassi F. and Klein L. (2003) Thymic selection revisited: how essential is it? *Immunol Rev* 191, 62-78.

Vukmanovic S., Neubert T. A. and Santori F. R. (2003) Could TCR antagonism explain associations between MHC genes and disease? *Trends Mol Med* 9, 139-46.

Wada I., Imai S., Kai M., Sakane F. and Kanoh H. (1995) Chaperone function of calreticulin when expressed in the endoplasmic reticulum as the membrane-anchored and soluble forms. *J Biol Chem* 270, 20298-304.

Wang J., Lim K., Smolyar A., Teng M., Liu J., Tse A. G., Liu J., Hussey R. E., Chishti Y., Thomson C. T., Sweet R. M., Nathenson S. G., Chang H. C., Sacchettini J. C. and Reinherz E. L. (1998) Atomic structure of an alphabeta T cell receptor (TCR) heterodimer in complex with an anti-TCR fab fragment derived from a mitogenic antibody. *Embo J* 17, 10-26.

Werlen G., Hausmann B. and Palmer E. (2000) A motif in the alphabeta T-cell receptor controls positive selection by modulating ERK activity. *Nature* 406, 422-6.

Willcox B. E., Gao G. F., Wyer J. R., Ladbury J. E., Bell J. I., Jakobsen B. K. and van der Merwe P. A. (1999) TCR binding to peptide-MHC stabilizes a flexible recognition interface. *Immunity* 10, 357-65.

Winter C. C., Carreno B. M., Turner R. V., Koenig S. and Biddison W. E. (1991) The 45 pocket of HLA-A2.1 plays a role in presentation of influenza virus matrix peptide and alloantigens. *J Immunol* 146, 3508-12.

Wu L. C., Tuot D. S., Lyons D. S., Garcia K. C. and Davis M. M. (2002) Two-step binding mechanism for T-cell receptor recognition of peptide MHC. *Nature* 418, 552-6.

Wucherpfennig K. W., Allen P. M., Celada F., Cohen I. R., De Boer R., Garcia K. C., Goldstein B., Greenspan R., Hafler D., Hodgkin P., Huseby E. S., Krakauer D. C., Nemazee D., Perelson A. S., Pinilla C., Strong R. K. and Sercarz E. E. (2007) Polyspecificity of T cell and B cell receptor recognition. *Semin Immunol* 19, 216-24.

Zhang Q., Tector M. and Salter R. D. (1995) Calnexin recognizes carbohydrate and protein determinants of class I major histocompatibility complex molecules. *J Biol Chem* 270, 3944-8.

Zhang Q. J., Gavioli R., Klein G. and Masucci M. G. (1993) An HLA-A11-specific motif in nonamer peptides derived from viral and cellular proteins. *Proc Natl Acad Sci U S A* 90, 2217-21.

Zhang W., Young A. C., Imarai M., Nathenson S. G. and Sacchettini J. C. (1992) Crystal structure of the major histocompatibility complex class I H-2Kb molecule containing a single viral peptide: implications for peptide binding and T-cell receptor recognition. *Proc Natl Acad Sci U S A* 89, 8403-7.

Zhao R., Loftus D. J., Appella E. and Collins E. J. (1999) Structural evidence of T cell xeno-reactivity in the absence of molecular mimicry. *J Exp Med* 189, 359-70.

Zhukov A. and Karlsson R. (2007) Statistical aspects of van't Hoff analysis: a simulation study. *J Mol Recognit* 20, 379-85.

CHAPTER 2

Single MHC Mutation Eliminates Enthalpy Associated with T Cell Receptor Binding

Reprinted from *Journal of Molecular Biology*, Volume 373, Peter J. Miller, Yael Pazy, Brian Conti, David Riddle, Ettore Appella, and Edward J. Collins, Single MHC Mutation Eliminates Enthalpy Associated with T Cell Receptor Binding, pages 315-27, Copyright 2007, with permission from Elsevier.

2.1 ABSTRACT

The keystone of the adaptive immune response is T cell receptor (TCR) recognition of peptide presented by Major Histocompatibility Complex (pMHC) molecules. The co-crystal structure of AHIII TCR bound to the MHC, HLA-A2, showed a large interface with an atypical binding orientation. MHC mutations in the interface of the proteins were tested for changes in TCR recognition. From the range of responses observed, three representative HLA-A2 mutants, T163A, W167A, and K66A, was selected for further study. Binding constants and co-crystal structures of the AHIII TCR and the three mutants were determined. K66 in HLA-A2 makes contacts with both peptide and TCR and previously has been identified as a critical residue for recognition by numerous TCR. The K66A mutation resulted in the lowest AHIII T cell response and the lowest binding affinity, which suggests T cell response may correlate with affinity. Importantly, the K66A mutation does not affect the conformation of the peptide. The change in affinity appears to be due to a loss in hydrogen bonds in the interface as a result of a conformational change in the TCR complementarity-determining region 3 (CDR3)

loop. Isothermal titration calorimetry confirmed the loss of hydrogen bonding by a large loss in enthalpy. Our findings are inconsistent with the notion that the CDR1 and CDR2 loops of the TCR are responsible for MHC restriction, while the CDR3 loops interact solely with the peptide. Instead, we present here a MHC mutation that does not change the conformation of the peptide, yet results in an altered conformation of a CDR3.

2.2 INTRODUCTION

T cells are an integral part of the adaptive immune system's ability to recognize virtually any pathogen that might attack the host. A critical step required for T cell activation is the recognition of peptides derived from these pathogens when presented by the Major Histocompatibility Complex protein (MHC). Recognition of foreign peptide bound to MHC is achieved through the clonotypic T cell receptor (TCR). Upon TCR recognition of a peptide bound to MHC (pMHC) sets of T cells either kill the cell presenting the foreign peptide (cytotoxic T cells) or produce cytokines to "help" B cells and other T cells (helper T cells). The pathogens are subsequently eliminated from the host by a combination of killing infected cells to remove reservoirs of replicating pathogen, and antibody-mediated neutralization of the pathogen outside of the cell. Although TCR binding to pMHC is paramount for T cell activation, there are still many unanswered questions regarding how TCR-pMHC interactions dictate T cell response.

Recognition of pMHC by the TCR heterodimer is accomplished using the three complementarity determining region (CDR) loops from each chain. The CDR1 and CDR2 loops are germ-line encoded within the variable gene segment of each TCRα and TCRβ chain. The CDR3 loop of each chain is unique and arises through V(D)J

recombination (Schatz and Spanopoulou, 2005; Spicuglia et al., 2006). While recognition of the pMHC is carried out using all the CDR loops of each chain, generally the CDR3 makes more contacts with the bound peptide than CDR1 and CDR2 (Rudolph et al., 2006).

Engagement of TCR with pMHC may result in a variety of reactions from the T cell, and the mechanisms that generate these different responses are not understood (Rudolph et al., 2006). The structures of TCR bound to partial agonist or antagonist pMHC complexes do not show changes in the TCR domains (Degano et al., 2000; Ding et al., 1999) that would suggest a way for the TCR to propagate a qualitatively different signal to the T cell through the plasma membrane. It is generally accepted that there is great plasticity in the interaction between TCR and pMHC. However, as seen in a variety of TCR-pMHC co-crystal structures the degree and location of this plasticity is not generalizable. For example, the co-crystal structures of 2C-dEV8/K^b (Garcia et al., 1998), 2C-SIYR/K^b (Degano et al., 2000), and KB5-C20-pKB1/K^b (Reiser et al., 2002) when compared to crystal structures of those TCRs alone show great flexibility in the CDR3 loops of the TCR. The LC13 (Kjer-Nielsen et al., 2003) and BM3.3 (Reiser et al., 2003) TCRs undergo changes in not just their CDR3s, but also their CDR1 and CDR2 loops. Conversely, the A6-Tax/A2 (Garboczi et al., 1996) and ELS4-EPLP/B*3501 (Tynan et al., 2007) co-crystal structures exhibit conformational changes in the peptides upon TCR-pMHC binding. Finally, the crystal structures of the 1G4 TCR alone and complexed with its pMHC ligands show no significant changes in either the TCR or the pMHC (Chen et al., 2005).

Similarly, there appear to be no general thermodynamic rules that describe TCR binding to pMHC. Although surface plasmon resonance (SPR) has been used for more than a decade to examine binding of TCR to pMHC, it measures kinetic constants between TCR and pMHC and binding via Scatchard Analysis or mathematically using the kinetic constants. Isothermal titration calorimetry (ITC) provides a direct measure of ΔH and is hence considered a more reliable determination of thermodynamic parameters. ITC has been rarely utilized for TCR-pMHC studies because of the much larger amounts of protein required for the studies. Early experiments suggested that TCR-pMHC interactions seem to be governed by large enthalpically favorable and entropically unfavorable thermodynamics (Garcia et al., 2001; Krogsgaard et al., 2003; Lee et al., 2004; Willcox et al., 1999). However, more recent thermodynamic data of L13-FLR/B8 (Ely et al., 2006), A6-Tax/A2 (Davis-Harrison et al., 2005), and 2C-QL9/L^d (Colf et al., 2007) all show entropically favorable associations.

The human MHC, HLA-A2, is the most frequent MHC found in Caucasians and African Americans (Ellis et al., 2000). A large panel of A2 mutants were created and tested against a panel of T cells. Most interesting from that study, the K66A mutant was found to adversely affect recognition of 98% of the T cells examined (Baker et al., 2001). K66 has been shown to be a critical residue in TCR recognition of A2, regardless of the peptide presented (Baker et al., 2001; Baxter et al., 2004; Gagnon et al., 2005; Wang et al., 2002), resulting in K66 to be labeled a potential "hot spot" for TCR recognition of A2. Importantly, even though K66 interacts with the peptide, the structure of Tax/A2(K66A) shows that the K66A mutation does not alter the structure of A2 or the

conformation of the Tax peptide (Gagnon et al., 2005). However, the effect of the K66A mutation on the cognate TCR has never been determined structurally.

AHIII12.2 (AHIII) is a murine T cell clone that recognizes human HLA-A2.1 (Engelhard and Benjamin, 1982) when peptide 1049 (ALWGFFPVL) is presented (Henderson et al., 1993). Reactivity towards p1049/A2 does not require binding of the TCR co-receptor CD8, (Buslepp et al., 2003a) which allows for the study of TCR-pMHC interactions without the additional complexity of the third protein. We have previously described the crystal structure of the AHIII TCR complexed with p1049/A2 (Buslepp et al., 2003b). From the AHIII-p1049/A2 co-crystal structure, we identified a number of A2 surface residues that may be responsible for binding the AHIII TCR. These residues were mutated in A2 and the changes in T cell cytolytic activity were examined as a function of the mutation. Three mutants were then selected for kinetic, thermodynamic, and structural studies. Most importantly, the K66A mutation causes substantial changes to cytotoxicity and the affinity. This change in affinity appears to be due to a large reduction in hydrogen bonding that is a result of a large conformational change in the CDR3 loop. This loss of hydrogen bonding is reflected in the almost complete loss of enthalpy in the binding reaction.

2.3 RESULTS

2.3.1 AHIII T Cell Reactivity

Based on the co-crystal structure of AHIII bound to p1049/A2 (Buslepp et al., 2003b), thirteen HLA-A2 mutations were selected to probe the interface. The ability of AHIII T cells to lyse target cells expressing this panel of A2 variants was assessed by

loading the target cells with radioactive chromium (^{51}Cr), incubating the T cells with the target cells for four hours and then measuring the radioactivity released to the media. Measured lysis was normalized to AHIII lysis of wild-type A2 expressing cells in each experiment. A spectrum of responses to the mutations was seen (Figure 1). Some of the mutants showed little affect on reactivity (E166A and T163A). On the other end of the spectrum the K66A mutation almost completely abolished the response. In addition to the K66 "hot spot" in A2 (Baker et al., 2001; Baxter et al., 2004; Gagnon et al., 2005; Wang et al., 2002), it has been suggested that positions 65, 69, and 155 could be critical to MHC-restriction due to the high frequency with which they are seen contacting TCRs

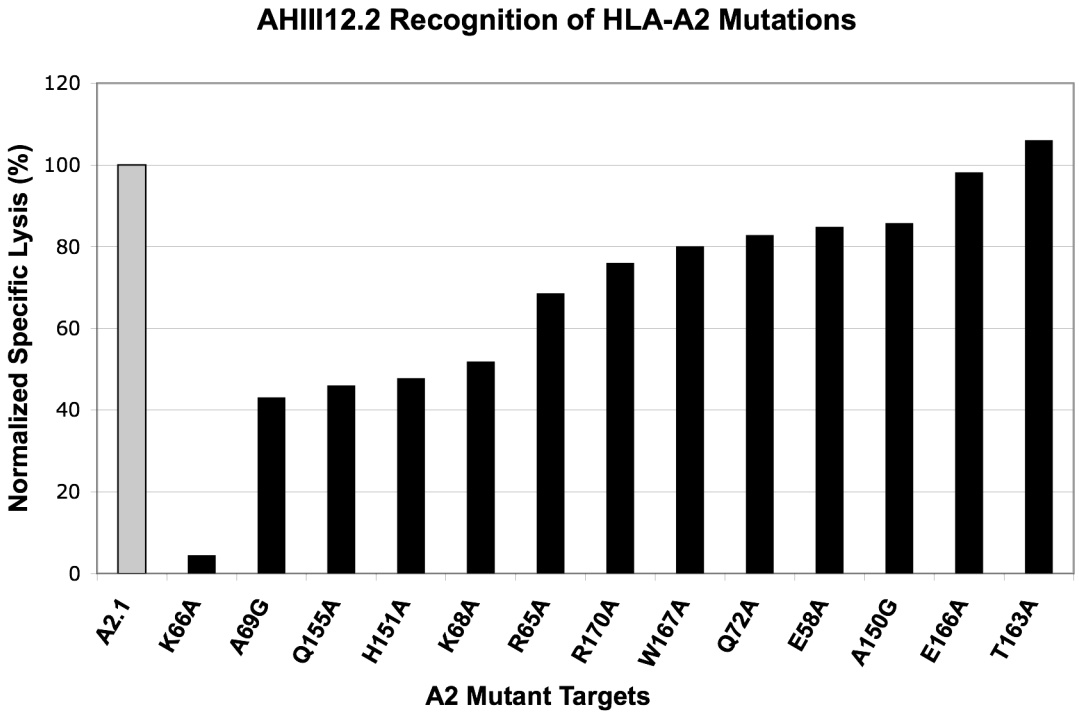

Figure 1. CTL Killing as a Function of Substitutions in the p1049/A2 Complex. Cytotoxic lysis assays (^{51}Cr release assays) were performed with AHIII T cells against cells expressing mutant A2 complexes. Data was normalized such that lytic activity against native HLA-A2 is 100%.

in determined TCR-pMHC structures (Clements et al., 2006; Rudolph et al., 2006; Tynan et al., 2005). Consistent with those data, mutations at positions 65, 69, and 155 all had deleterious effects on AHIII cytotoxicity.

Three A2 variants that represent the range of T cell reactivity were chosen for further study: T163A (high), W167A (medium), and K66A (low). Mutant proteins were expressed recombinantly as inclusion bodies in *E. coli* and refolded *in vitro* with p1049

Table 1. Equilibrium and kinetic binding parameters for AHIII TCR binding p1049/A2 mutants.

pMHC Complex	K_d Equilibrium (μM)	K_d Kinetic (μM)	k_{on} ($x10^4$ $M^{-1}s^{-1}$)	k_{off} (s^{-1})
p1049/A2	9.3	8.7	3.1	0.27
p1049/A2(T163A)	4.7	4.6	3.3	0.16
p1049/A2(W167A)	15.4	14.8	4.1	0.63
p1049/A2(K66A)	31.8	34.0	0.47	0.15

Parameters were obtained by fitting data with Scrubber 2.0 and CLAMP. Kinetic dissociation constants (K_d) were obtained from kinetic data using the determined k_{on} and k_{off} values. Equilibrium dissociation constants were obtained separately by fitting maximum binding responses for various concentrations of pMHC using Scrubber.

peptide. Binding to the recombinant AHIII TCR was measured using surface plasmon resonance (SPR). Binding curves for these three complexes in addition to wild-type A2 are shown in Figure 2. The mutations in the MHC cause significant changes to the affinity for AHIII TCR (Table 1) with K_d values ranging from 4.7 μM (p1049/A2(T163A)) to 31.8 μM (p1049/A2(K66A)). The kinetics were also dramatically affected. The dissociation rates (k_{off}) were both faster and slower than wild-type p1049/A2 (0.27 s^{-1}). Interestingly, even though the affinity of AHIII for p1049/A2(K66A) is significantly lower than for wild-type A2, the dissociation rate is significantly slower (Figure 2 and Table 1). Association rates (k_{on}) were generally less affected by the substitutions, except for p1049/A2(K66A) (4.7 X 10^3 $M^{-1}s^{-1}$), which has a much slower on-rate compared to wild-type A2 (3.1 X 10^4 $M^{-1}s^{-1}$).

2.3.2 Structural Analysis of A2 Variants

The physical manifestation of the differences found in T cell recognition and binding was examined using x-ray crystallography. The three mutants described above (A2(K66A) A2(T163A) and A2(W167A)) were co-crystallized with AHIII TCR. The locations of the mutations in the interface between the AHIII TCR and p1049/A2 are shown in Figure 3. Based on previous work, (Ding et al., 1999) it seemed unlikely that these relatively small alterations would cause large changes in the overall structures of the TCR or pMHC, or the docking orientation of the TCR. Therefore, we hypothesized that the substitutions resulted in local alterations in the MHC or peptide, changing hydrogen bonds or van der Waals contacts present in our previously determined AHIII-p1049/A2 structure (Buslepp et al., 2003b). Crystallographic

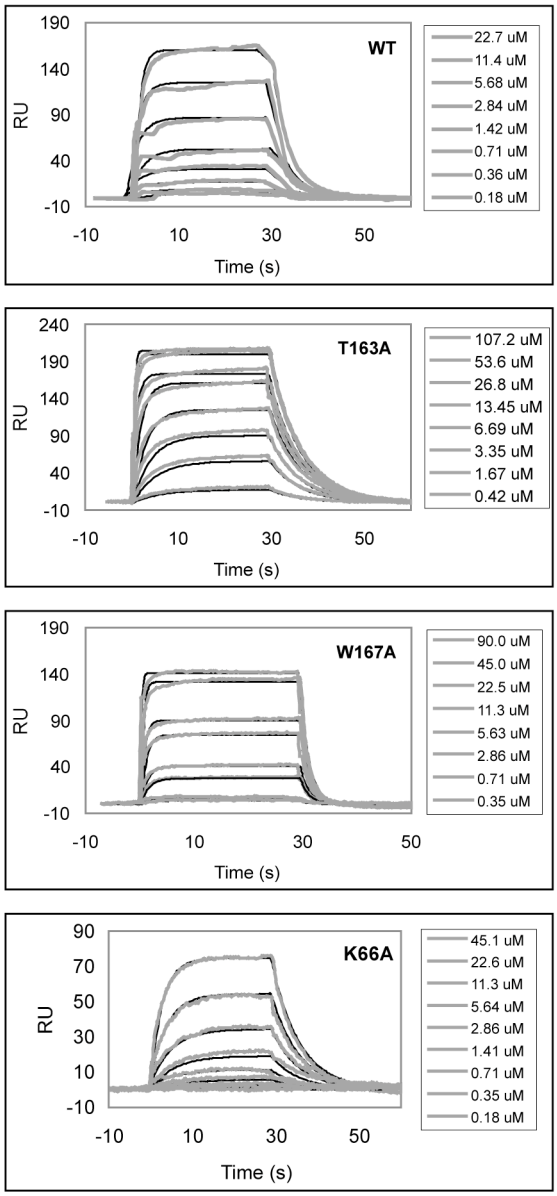

Figure 2. AHIII TCR binding to p1049/A2 variants as measured by SPR. Kinetic data between AHIII TCR and wild-type p1049/A2 as well as p1049/A2 mutants at various pMHC concentrations were obtained using SPR and globally fit to a reversible bimolecular reaction using Clamp (Myszka and Morton, 1998). Model binding curves are drawn in black. Curve fits are drawn in grey.

data were collected from three single co-crystals comprised of AHIII TCR complexed with p1049/A2(T163A), p1049/A2(W167A), or p1049/A2(K66A), to a resolution of 2.4 Å, 2.5 Å, and 2.88 Å, respectively. All the crystals were nearly isomorphous with AHIII-p1049/A2 (Buslepp et al., 2003b). Data collection and refinement statistics can be found in Table 2.

As might be expected because of the similar level of T cell activity, no gross structural changes were observed in the structure of p1049/A2(T163A) bound to AHIII

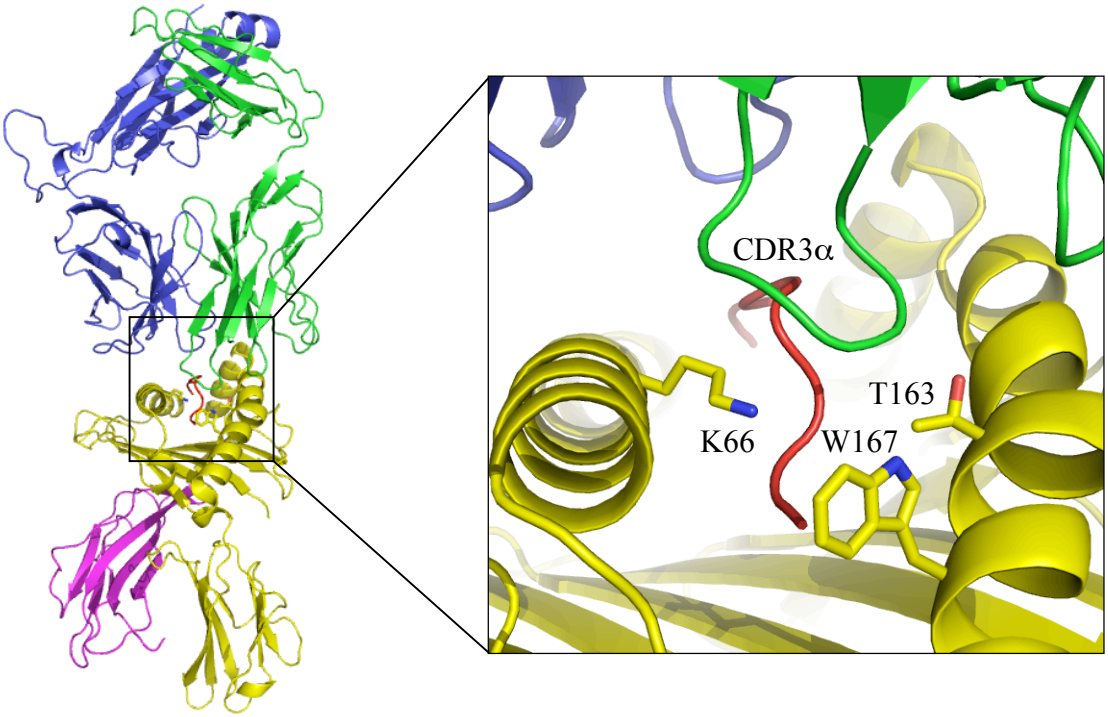

Figure 3. Structure of AHIII TCR bound to p1049/A2. The AHIII TCR alpha (green) and beta (blue) chains, interact with the p1049/A2 surface via CDR loops. HLA-A2, consisting of a heavy chain (yellow) and β_2m (magenta), present the peptide, p1049 (red). (Inset) The surface of the p1049/A2 is contacted by the CDR loops of the AHIII TCR. Residues that have been mutated to alanine for structural experiments (T163, W167, K66) are shown. Figure generated using PDB coordinates 1LP9 and PyMol (Delano, 2002).

TCR (Figure 4a). For all three structures superimposition was performed using the "align" feature in PyMol (Delano, 2002), restraining the alignment to the α-carbons of

Table 2. Data Statistics

	AHIII-p1049/A2(T163A)	AHIII-p1049/A2(W167A)	AHIII-p1049/A2(K66A)
Data Collection			
Space Group	$P2_1$	$P2_1$	$P2_1$
Cell Dimensions	a=93.49 Å, b=84.18 Å, c=121.77 Å, β=92.05°	a=94.28 Å, b=84.35 Å, c=122.47 Å, β=92.53°	a=93.42 Å, b=83.89 Å, c=122.27 Å, β=92.21°
Molecules/AU	2	2	2
Resolution	50.0 - 2.10 Å	50.0 - 2.5 Å	50.0 - 2.88 Å
R_{merge}(%)[a,b]	5.9 (46.7)	6.6 (31.8)	7.8 (42.1)
$\langle I/\sigma \rangle$[c]	11.4 (1.6)	18.0 (1.8)	11.2 (1.3)
Unique Reflections	76,682	61,781	40,707
Avg. Redundancy	2.7 (1.7)	4 (2.5)	3.4 (2.3)
Completeness (%)	70.0 (24.7)	92.8 (67.8)	95.7 (69.0)
Solvent Content (%)	41.5	40.7	44.1
Refinement			
Resolution Range	30.0 - 2.4 Å	30.0 - 2.5 Å	30.0 - 2.88 Å
Number of Reflections	59,694	58,660	38,683
R_{fac}[d]	24.0	25.3	26.8
R_{free}	28.9	29.9	29.3
Number of non-H atoms	13,160	12,995	12,956
Number of waters modeled	267	52	0
<Rs fit>[e]	93%	93%	90%
Coordinate error[f, (Murshudov et al., 1997; Reed, 1996)]	0.25	0.32	0.46
Deviations from ideality			
Bond lengths	0.006 Å	0.006 Å	0.005 Å
Bond angles	1.040°	1.192°	0.750°
<Temperature Factor>			
Overall	37.6	49.7	47.2
TCR	37.8	49.6	47.5
MHC	37.6	50.1	47.1
Peptide	34.7	48.6	37.5
Ramachandran			
Most favored	1305 (91.4%)	1291 (90.7%)	1287 (90.4%)
Additional allowed	121 (8.5%)	131 (9.2%)	134 (9.4%)
Generously allowed	0	0	0
Disallowed	2 (0.1%)	2 (0.1%)	2 (0.1%)
PDB Entry	2UWE	2JCC	2J8U

the TCR-pMHC interface (TCR Vα, Vβ; and MHC α1, α2 and peptide). The AHIII-p1049/A2(T163A) complex superimposed onto AHIII-p1049/A2 with an RMSD of 0.20 $Å^2$. Difference electron density ($Fobs_{wild\text{-}type}$ - $Fobs_{mutant}$) maps show a large negative electron density peak in the position of the mutated residue that demonstrates the quality of the data and confirms the location of the mutation (Figure 4a). One change in the TCR was observed. The side chain of serine 99 in the TCR CDR3α has rotated into the cavity where the MHC threonine side chain is found in the wild-type structure. Interestingly, the electron density maps show the location of the serine without ambiguity, but there are no contacts visible for the serine side chain. This side chain orientation is not the most preferred rotamer (Lovell et al., 2003); that preferred conformation is found in the wild-type structure. Therefore, it may be that this position is taken to reduce undesired energetic contributions to the binding such as the fixation of solvent or the production of a cavity in the interface.

In addition to its importance to this study concerning T cell reactivity, the A2(W167A) complex was also interesting because W167 forms a boundary of the peptide-binding cleft (Figure 3) and helps form the conserved pocket that binds the amino terminus of the peptide (Madden, 1995). This tryptophan is highly conserved in not only HLA-A2 subtypes (96%), but across all human class I MHC molecules (88.5%) (Robinson et al., 2003). Mutating tryptophan to alanine results in the loss of a hydrogen bond between the Trp indol nitrogen to the Tyr28 hydroxyl on the TCR CDR2 (Figure 4b). Aside from the loss of the W167-Y28 hydrogen bond, the structure of AHIII bound

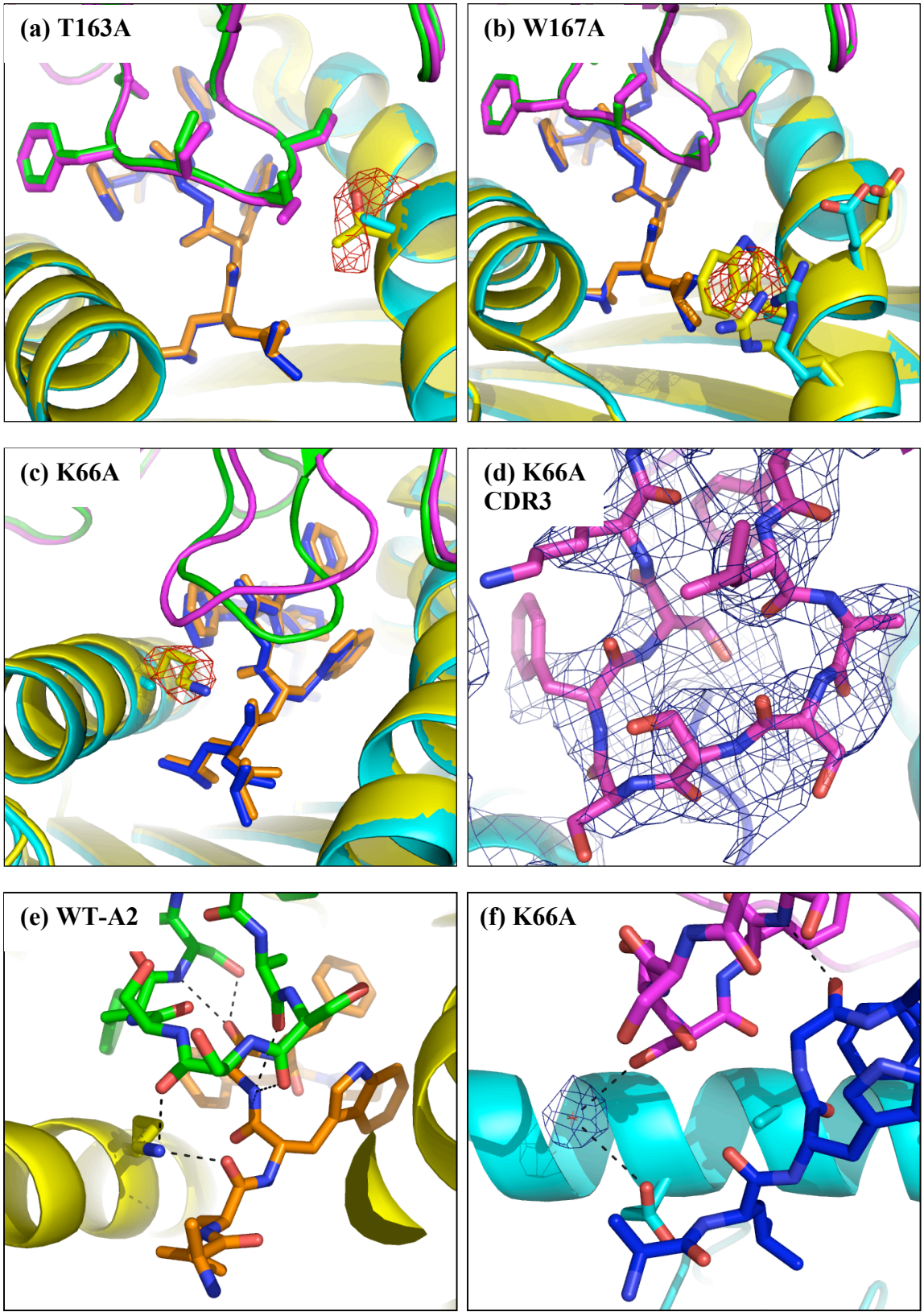
(a) T163A
(b) W167A
(c) K66A
(d) K66A
CDR3
(e) WT-A2
(f) K66A

Figure 4. Mutation of Lys66 to alanine results in large change in CDR3α loop. (a) Complex of AHIII TCR bound to p1049/A2(T163A) superimposed onto wild-type structure of AHIII-A2. Mutant A2 (cyan) and peptide (blue) show little difference from wild-type A2 (yellow) and peptide (orange). Conformations of TCR CDR2 and CDR3 loops and side chains are no different between mutant (magenta) and wild-type (green) structures (coloring scheme same for all panels). (b) Complex of AHIII TCR bound to p1049/A2(W167A) also shows no change in TCR structure and only minor alterations in local MHC side chains. (c) Superimposition with of AHIII TCR bound to p1049/A2(K66A) onto wild-type shows a major rearrangement of the AHIII CDR3α loop, while the structure of pMHC remains unchanged. (a, b, c) Mutations at T163A, W167A, and K66A are confirmed by difference electron density ($Fobs_{wild\text{-}type}$ - $Fobs_{mutant}$) contoured at -3σ surrounding the side chains. (d) 2Fobs-Fcalc density map (blue), contoured at 1 σ, confirms placement of final modeled CDR3α loop at 2.88 Å. (e) Five hydrogen bond interactions occur between AHIII TCR CDR3α and wild-type p1049/A2. As shown above some or all of these bonds may be broken due to loop movement. (f) The 2Fobs-Fcalc electron density suggests the presence of a water molecule in the AHIII-p1049/A2(K66A) structure, which would allow for a water-mediated hydrogen bond between Glu63 of A2 and Ser100 on CDR3α of AHIII (water shown for illustration, but not included in PDB). The only other possible hydrogen bond to CDR3α is from the Ser102 nitrogen to the Gly4 oxygen of the peptide. Figures generated using PyMol (Delano, 2002).

to p1049/A2(W167A) shows no significant changes in the peptide amino terminus, the CDR2α or CDR3α of the AHIII TCR, or the MHC itself. The mutant complex alpha carbons have an RMSD of 0.27 $Å^2$ when superimposed onto the wild-type atoms. The difference electron density ($Fobs_{wild\text{-}type}$ - $Fobs_{mutant}$) map once again shows a large negative peak in the position of the mutated residue demonstrating the quality of the data and confirming the loss of the Trp side chain. Two side chains in A2 near the site of mutation do change conformation, but these differences do not alter binding to the TCR. The amino terminus of the peptide is still coordinated by hydrogen bonds to three tyrosine hydroxyl groups Tyr7, Tyr 159, and Tyr171 of the MHC, as in wild-type p1049/A2. The AHIII-p1049/A2(W167A) structure shows weak positive difference density in the location where the nitrogen of the indole ring of wild-type Trp167 would be (data not shown). This suggests that there may be a weakly associated water molecule replacing the amine, which could hydrogen bond to the hydroxyl group on Tyr28 of CDR2α.

The structure of AHIII bound to p1049/A2(K66A) is critical to this study because of the significantly different binding constants of A2(K66A) (Table 1). Additionally, K66 on the α1 α helix of HLA-A2 has been identified as a "hot spot" for TCR recognition of HLA-A2 in a number of studies (Baker et al., 2001; Baxter et al., 2004; Gagnon et al., 2005; Wang et al., 2002). Structures of A6-Tax/A2 (Ding et al., 1998; Garboczi et al., 1996) and AHIII-p1049/A2 (Buslepp et al., 2003b) also show that K66 is rare in that it makes critical contacts with both the TCR and the peptide. K66A mutants have increased peptide dissociation rates; yet this is not likely to be responsible for the decrease in T cell function because T cell clones have also been identified that do not have altered recognition to the K66A mutation (Baker et al., 2001; Baxter et al., 2004). Furthermore, the K66A mutation does not alter the MHC structure or the conformation of the Tax peptide in Tax/A2(K66A) (Gagnon et al., 2005). So, if increased peptide dissociation from A2(K66A) mutants does not influence T cell activation, and the pMHC molecular surface is not altered by the mutation, the next logical hypothesis would be that the K66A variation results in a change in the TCR that negatively affects T cell function.

The co-crystal structure of AHIII-p1049/A2(K66A) determined to 2.88 Å resolution shows an altered conformation of the CDR3α of the AHIII TCR (Figure 4c). The AHIII-p1049/A2(K66A) structure superimposes onto AHIII bound to wild-type A2 with an RMSD of 0.37 $Å^2$. The $2F_o$-F_c electron density maps show the new conformation of the loop (Figure 4d) and this location is confirmed by omit maps. The conformational change in CDR3α is that the loop appears to fill the void left by the removal of the Lys66 side chain. The Cα atoms of the loop move, on average, 2.0 Å with Ala97 moving over

4.0 Å (Table 3). This altered conformation of the loop likely disrupts the hydrogen bonding contacts found in the native structure (Buslepp et al., 2003b) between the

Table 3. CDR3α Movement

Residue	Distance (Å)
Leu96	1.0
Ala97	4.2
Ser98	2.6
Ser99	3.0
Ser100	2.6
Phe101	0.3
Ser102	1.7
Lys103	0.7
Mean	2.0

Distances limited to 2 significant figures due to low resolution of AHIII-p1049/A2(K66A).

CDR3α and wild-type p1049/A2 (Figure 4e). In a manner similar to the Tax/A2(K66A) structure (Gagnon et al., 2005), the K66A mutation does not change MHC or peptide conformation in this AHIII-p1049/A2(K66A) structure. The CDR3 loop change also negatively affects the surface complementarity (SC). The SC value for the wild-type AHIII-p1049/A2 structure is 0.71 and drops to 0.55 for AHIII-p1049/A2(K66A).

The Tax/A2(K66A) structure showed a water molecule replacing the Lys66 side chain, mediating hydrogen bonds between Glu63 of A2 and the Tax peptide (Gagnon et al., 2005). There is no electron density that would suggest a water replaces the Lys66 side chain in our AHIII-p1049/A2(K66A) structure. It appears that the new conformation of the CDR3α loop pushes further into the peptide binding cleft along the MHC α1 α helix where the Lys66 side chain would have been, displacing any water that might have filled the void before TCR binding. The number of reflections associated with the 2.88 Å resolution data can not support the modeling of water molecules in the structure of AHIII-p1049/A2(K66A). However, there is a small volume in the $2F_o$-F_c electron

density map that suggests that there may be a weakly associated water molecule that would hydrogen bond with Glu63 of A2 and Ser100 on CDR3α of AHIII (Figure 4f). The only other plausible hydrogen bond between the AHIII CDR3α to p1049/A2(K66A) is from the Ser102 nitrogen to the Gly4 oxygen of the peptide (2.88 Å) (Figure 4f). In summary, there is a large alteration in the AHIII CDR3α loop when bound to p1049/A2(K66A) as compared to the wild-type complex and this alteration appears to dramatically change the number of hydrogen bonds in the complex.

2.3.3 Calorimetric measurement of AHIII TCR and HLA-A2 binding

The altered hydrogen bonding pattern proposed here based on the crystal structure of AHIII-p1049/A2(K66A) suggests that there should be a large change in the enthalpy of binding. To examine this directly, the heat of binding was measured using isothermal titration calorimetry (ITC). Our data show that the wild-type complex binding has a relatively small enthalpic component (-3.9 kcal/mol) and that the binding is more entropically driven (Table 4 and Figure 5a). As predicted, this small enthalpic contribution to binding is almost completely eliminated by mutation of K66 to alanine. This change is manifest clearly during the experiments because the K66A mutation changes the reaction from exothermic to endothermic (Figure 5b). The enthalpy of binding (ΔH) goes from -3.9 kcal/mol for AHIII-p1049/A2 to almost zero (-0.6 kcal/mol) for AHIII-p1049/A2(K66A). The free energy of binding (ΔG) measured for the two complexes is in agreement with those determined for other TCR-pMHC (Table 4). The thermodynamic changes for AHIII-p1049/A2(K66A) correspond to a ΔΔG of only 1.4

kcal/mol, which highlights the tight range between activating and non-activating signals for TCR.

Table 4. Thermodynamic Parameters of TCR-pMHC Binding as Measured by ITC

Complex	ΔH (kcal/mol)	TΔS (kcal/mol)	ΔG (kcal/mol)	K_d (μM)	Reference
AHIII-p1049/A2	-3.9 [a]	4.4	-8.3	1 ± 5	
AHIII-p1049/A2(K66A)	-0.6 [b]	6.3	-6.9	7 ± 20	
A6-Tax/A2	5.7	13.6	-7.9	2.2	(Davis-Harrison et al., 2005)
JM22-flu/A2	-19.7	-12.6 [c]	-7.1 [c]	6.6 [c]	(Willcox et al., 1999)
2C-dEV8/K^b	-22.7	-16.2	-6.3	84	(Ely et al., 2006)
2C-QL9/L^d	-4.19	3.4	-7.6	2	(Colf et al., 2007)
LC13-FLR/B8	-3.6	3.4	-7.0	8.1 ± 2.7	(Ely et al., 2006)
2B4-MCC/IE^k	-14.8	-8.2	-6.7	12.6 ± 7	(Krogs. et al., 2003)
2B4-K5/IE^k	-13.5	-6.4	-7.2	6.2 ± 0.2	(Krogs. et al., 2003)

(a) error < 5%; (b) error < 20%; (c) van't Hoff calculation

2.4 DISCUSSION

The initial goal of this study was to determine how structural alterations in the TCR are responsible for the spectrum of T cell cytolysis by AHIII T cells. Mutations in HLA-A2 were made and changes in cytolysis examined as a function of the mutation. Recombinant protein for three A2 variants was produced and binding constants were determined by surface plasmon resonance (SPR). Surprisingly, A2(K66A) showed very different kinetic constants as compared to the wild-type complex. Structural studies showed that most hydrogen bonds involving the CDR3α loop in the complex were lost upon mutation. Isothermal titration calorimetry (ITC) confirmed a greatly decreased enthalpy of binding associated with the conformational change of the loop.

Based on the AHIII-p1049/A2 co-crystal structure previously determined (Buslepp et al., 2003b), A2 residues that were predicted to be involved in binding the

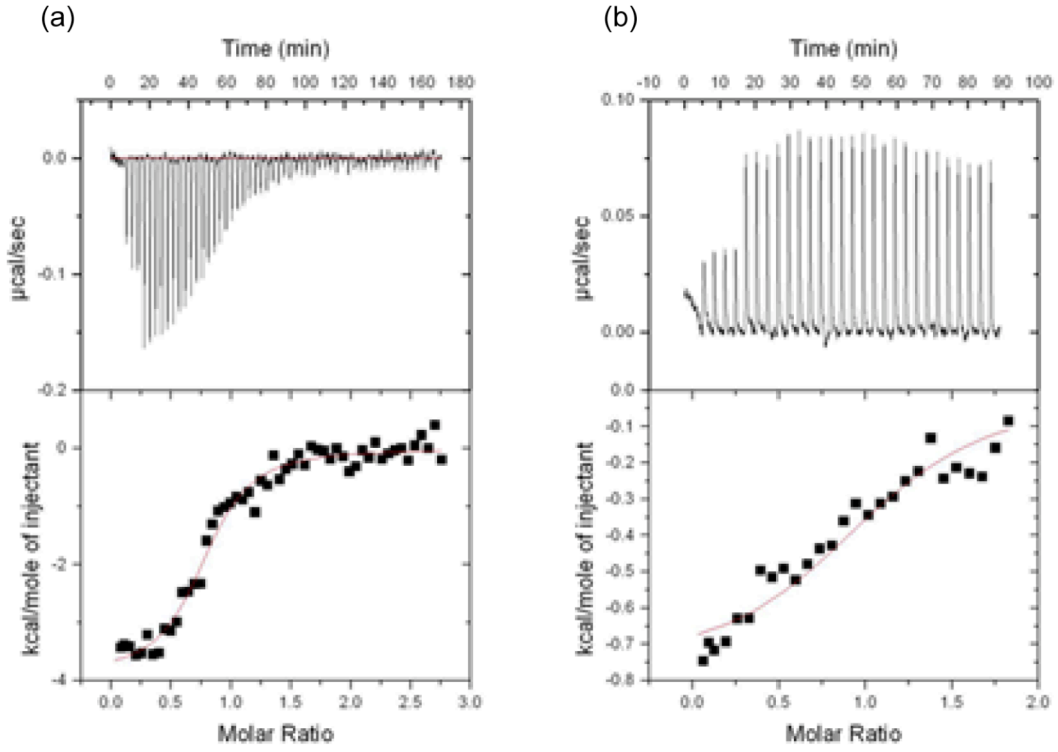

Figure 5. K66A mutation in p1049/A2 dramatically decreases the enthalpy of binding. The binding enthalpy of AHIII TCR was measured directly with ITC for both wild-type p1049/A2, and p1049/A2(K66A). (a) Power versus molar ratio plot for titration of 234 μM p1049/A2 into 19 μM of AHIII TCR (upper panel) and plot of integrated heat versus molar ratio after baseline correction (lower panel). The baseline was generated by averaging heat measured for last 10 injections. (b) Plot of power versus molar ratio for titration of 394 μM p1049/A2(K66A) into 40 μM of AHIII TCR (upper panel) and integrated heat versus molar ratio after baseline correction (lower panel). The baseline derived from titrating p1049/A2(K66A) into buffer alone. All experiments performed at 25 °C. The fitted curves are from the model for single-site binding provided in Microcal Origin Software. Thermodynamic parameters determined are presented in Table 4.

AHIIII TCR were mutated. The AHIII T cells reacted with a full spectrum of outcomes from very low cytotoxicity to slightly improved cytotoxicity as a result of changing residues in the interface between the proteins. Residues at positions 66 (Baker et al., 2001; Baxter et al., 2004; Gagnon et al., 2005; Wang et al., 2002) and 65, 69, and 155 (Clements et al., 2006; Rudolph et al., 2006; Tynan et al., 2005) have all been previously identified as critical contacts in a number of TCR-pMHC systems. Mutations

at all of these four of these positions in A2 resulted in a reduction of AHIII T cell cytotoxicity of 30% to almost 100%. Clearly, these residues are critical for AHIII TCR binding. As an important control, it has been shown previously that peptide binding does not change significantly for the mutations studied except K66A (it has a faster peptide off-rate) (Baxter et al., 2004). However, this faster peptide off-rate cannot account for the changes in activity because T cells can be found that are not affected by the K66A mutation (Baker et al., 2001; Baxter et al., 2004). This implies that significant peptide bound to MHC remains on the cell surface even with the K66A mutation. In addition, the expression levels of the various mutants studied here were confirmed to be similar by flow cytometry (data not shown). Therefore, any observed changes in reactivity, binding, or structure should be due to changes in how the complexes interact. A more thorough study of how those mutations resulted in a change of function was then initiated.

A sub-set of the MHC mutants that represent dramatically reduced to full reactivity (K66A, W167A, and T163A, respectively) were chosen to study the physical manifestation of the differences. TCR-pMHC binding studies were performed using SPR. While all mutants showed some degree of change from wild-type A2, the K66A mutation resulted in remarkably slower on and off-rates than the wild-type complex. The three mutant complexes were then co-crystallized with AHIII TCR. The structures were determined and compared to the wild-type co-crystal structure. Similar to the results seen for the altered peptide ligands for the Tax/A2 specific TCR (Ding et al., 1999), there were no gross differences in any of the structures examined. Significantly, there were no changes in domain packing of the TCR that would suggest a mode to transmit information through the domains to the interior of the cell to confer different activities, as

previously suggested (Krogsgaard et al., 2003). There is always the possibility that the domain movements are dynamic and/or weakly manifested and are overcome here by crystal packing forces that would make it impossible to view using protein crystallography. Similarly, it has been suggested that upon TCR-pMHC interaction, a conformational change in the AB loop of the TCR Cα domain is required for signaling into the cell (Kjer-Nielsen et al., 2003). Although the position of the AB loop for the non-liganded AHIII TCR is unknown, the loop in the AHIII TCR bound to all p1049/A2, even p1049/A2(K66A), is identical, and is the same conformation as seen in the liganded LC13 TCR (Kjer-Nielsen et al., 2003). Importantly, the AB loop in the AHIII structures are not involved in any crystal contacts. These data imply that the AB loop has no impact on the level of cytotoxicity seen in the AHIII system.

There are no definitive structural explanations for the "improved" AHIII T cell reactivity for the A2(T163A) mutant. With threonine being conserved in 98% of all known HLA-A2 subtypes (Robinson et al., 2003), we had expected a greater impact mutating it to alanine. If anything, the rotation of the TCR CDR3α Ser99 into the cavity formed by the removal of the MHC threonine side chain would be expected to contribute negatively to the binding due to the less favorable rotamer that is chosen. There are no hydrogen bonding partners near the new position of the serine hydroxyl. There is no significant increase in the complementarity in the fit between the complexes. The complementarity of fit of AHIII to p1049/A2(T163A) is 0.72 versus 0.71 for the wild-type structure. We conclude that the most likely explanation for the slightly increased binding affinity is that there is a set of very subtle changes that increase the complementarity of fit.

The A2(W167A) mutation results in a 20% loss in lysis by the AHIII T cells. There are no significant structural changes other than the loss of the W167-Y28 hydrogen bond. Loss of the W167 indole also affects surface complementarity between AHIII-p1049/A2(W167A) (SC = 0.68) compared to AHIII-p1049/A2 (SC = 0.71). Therefore, the dramatic loss of affinity to the AHIII TCR is likely a result of the lost hydrogen bond and the concomitant loss of complementarity (ie van der Waals contacts). The fact that the absence of the indole group from the end of the peptide binding cleft in the AHIII-p1049/A2(W167A) structure did not significantly alter the conformation of the bound peptide is surprising. Tryptophan is present at position 167 in 96% of all known HLA-A2 subtypes and 88.5% conserved in all human class I MHC molecules (Robinson et al., 2003). It begs the question, why is this amino acid so highly conserved? Unfortunately, the data provided in the AHIII-p1049/A2(W167A) structure are unable to address this.

Of all the mutants tested, the K66A mutation caused the largest decrease in AHIII cytolysis. The slow on-rate seen for AHIII-p1049/A2(K66A) and significant energy barriers measured for other TCR-pMHC (Davis-Harrison et al., 2007; Wu et al., 1996) imply that there are structural changes associated with binding, and in fact, a large change was seen in the CDR3α loop of the AHIII TCR. This suggests that binding requires a conformational change in the TCR, but when exactly does this occur? Does the AHIII TCR make initial contact with p1049/A2(K66A) and then the CDR3α loop moves (induced-fit) or does p1049/A2(K66A) associate with a minority member of the population of the AHIII TCRs in solution (pre-existing equilibrium). The induced-fit or two-step model (Wu et al., 2002) has been a popular means of describing TCR-pMHC interaction. However, the validity of the two-step model has been questioned by both

thermodynamic (Davis-Harrison et al., 2007) and structural (Chen et al., 2005; Kjer-Nielsen et al., 2003; Reiser et al., 2003) data. We propose that a pre-existing equilibrium model better describes TCR-pMHC association. The idea that CDR loops exist in alternative pre-existing conformations in solution has been shown in antibody crystal structures (James et al., 2003). Knowing the structural similarities between antibodies and TCR, it is easy to imagine this binding mechanism to exist for TCR and pMHC. The total number of possible conformations that the CDR loops can adopt is finite and limited by the conserved framework regions of the TCR and/or antibody structure (Al-Lazikani et al., 1997; Chothia et al., 1992; Chothia et al., 1989; Morea et al., 1998). The residues that constitute the loop will maintain phi and psi angles that allow for the lowest potential energy. Loops in higher potential energy conformations would be found less often in the population (minority member). Therefore, the pMHC surface that allows the TCR to have the greatest number of its CDR loops in conformations with the lowest energy would provide the most stable interaction, a higher affinity, and subsequent greater activation of the T cell. The structural and thermodynamic data presented here for AHIII TCR-p1049/A2(K66A) demonstrates this relationship between energetics and activation. When the CDR3α loop is required to take a conformation with higher energy, the interactions between TCR and pMHC suffer, and T cell activation is adversely affected. As there is not currently a structure of the AHIII TCR alone, we cannot be sure where the CDR3α loop lies when it is free in solution. However, the on-rate of AHIII-p1049/A2(K66A) being an order of magnitude slower than wild-type AHII-p1049/A2 binding, suggests the loop to undergo greater change in order to bind p1049/A2(K66A) than wild-type p1049/A2. We propose the TCR conformations seen in our AHIII-

p1049/A2(K66A) complex are minor in the population, so the longer k_{on} is a reflection of the unfavorable equilibrium of the pMHC binding that minority member.

The AHIII-p1049/A2(K66A) structure also suggested most of the hydrogen bonds found between AHIII CDR3α and wild-type p1049/A2 are not present in the mutant structure. The conformational change in CDR3α potentially leaves only the Ser102 to Gly4 hydrogen bond. This suggested that the enthalpy of binding is greatly diminished. The ITC data complement the structural data, as it shows there is a significant loss in binding enthalpy. Due to the small amount of heat absorbed upon AHIII-p1049/A2(K66A) binding, the titration curve generated is not satisfactory to allow for confident analysis of the entropy in the system. However, the endothermic binding combined with the loss of enthalpy suggests that the binding of AHIII TCR to p1049/A2(K66A) is nearly entirely entropically driven. For TCR-pMHC complexes where heats of binding have been measured directly (and inferred from van't Hoff calculations), the enthalpic and entropic contributions are different for each TCR-pMHC system without any unifying thermodynamic properties. Originally it was thought that TCR-pMHC interactions were governed by enthalpically favorable and entropically unfavorable thermodynamics features (Krogsgaard et al., 2003; Lee et al., 2004; Willcox et al., 1999); however, AHIII-p1049/A2 joins LC13-FLR/B8 (Ely et al., 2006), A6-Tax/A2 (Davis-Harrison et al., 2005), and 2C-QL9/L^d (Colf et al., 2007) as TCR-pMHC systems that rely on entropically favorable binding.

One of the difficulties associated with studying diverse receptor systems such as TCR recognition of pMHC is that it is difficult to extract general rules about the system. However, in the context of what has been done with other TCR-pMHC, there are some

general features that we can present from these data. Previous structural studies have highlighted TCR recognition of altered peptide ligands (Chen et al., 2005; Ding et al., 1999), different peptides presented by the same MHC (Degano et al., 2000; Garcia et al., 1998; Reiser et al., 2003; Reiser et al., 2000), or the effects of mutation in the TCR to binding (Borg et al., 2005), but not the structural effects of MHC mutation on TCR-pMHC binding. The effects of mutations in the MHC through biological readout, co-crystal structures, and thermodynamics suggest a correlation between T cell response and affinity. As many as 32 hydrogen bonds determine specificity in BM3.3-pBM1/K^b (Reiser et al., 2000), but only 21 in AHIII-p1049/A2 (Buslepp et al., 2003b) and approximately 15 in the AHIII-p1049/A2(K66A) complex. The recently determined structure of 2C-QL9/L^d (Colf et al., 2007) reveals an interface with less than 10 hydrogen bonds and entropically favorable binding. What does this say about specificity? If there are no hydrogen bonds determining specificity, the only way the TCR can be sure to only recognize the foreign complex must be complementarity of fit. Not surprisingly perhaps, AHIII-p1049/A2 (Buslepp et al., 2003b) and 2C-QL9/L^d (Colf et al., 2007) have the greatest complementarity of fit of all TCR-pMHC structures determined to date. In addition to other published results, our data suggest that the thermodynamics for each TCR-pMHC interaction is unique. The large range of thermodynamic constants reveals that there are many ways to get to T cell activation. This all suggests that the pathways to activation are not important, just the end point.

Most importantly, the AHIII-p1049/A2(K66A) structure provides evidence that a variation in the MHC and not the peptide can directly affect a CDR3 loop. The idea of CDR1 and CDR2 recognition of MHC followed by CDR3 binding to peptide works for a

select few TCR, but not for most. In the case of K66, Lys is not conserved across all MHC (93% of HLA-A2 subtypes, but only 42.5% conserved in HLA-A overall, and only 1.5% of HLA-B molecules (Robinson et al., 2003)). Therefore, the presence of this charge is not required, but can be thought of as another piece of the antigen surface. TCR recognition of the pMHC surface cannot be divorced into separate binding events of peptide and MHC.

2.5 MATERIALS AND METHODS

2.5.1 Cell Lines and Expression Plasmids

The HLA-A2 mutants transfected into Hmy2.C1R cells have been described previously (Wang et al., 2002). All cell lines showed cell surface expression of HLA-A2 at similar levels as wild-type HLA-A2 as detected by the HLA-A2-specific Ab BB7.2 (Brodsky et al., 1979).

2.5.2 Protein Production and Purification

Soluble AHIII12.2 TCR was produced as previously described (Buslepp et al., 2003b). Briefly, the ectodomains of AHIII TCR α and β chains were expressed as inclusion bodies in *E. coli*. Purified inclusion bodies, previously dissolved in 8M urea, were rapidly injected into a folding buffer optimized for the AHIII TCR at a concentration of 50 μg/ml. After incubation for 36 hours at 10 °C and extensive dialysis the native TCR was purified and concentrated by DE52 anion exchange (Whatman, Florham Park, NJ)) followed by gel filtration chromatography (Phenomenex, Torrance, CA) on HPLC. The purified AHIII TCR was concentrated to 10 mg/ml and stored at -80 °C. Soluble AHIII TCR was tested for proper folding and activity through an ELISA

using HLA-A2 tetramer. Typical yield for each 1 L refold is about 3-5 mg of active TCR.

Similarly, soluble HLA-A2 variants were produced as inclusion bodies in *E. coli* and refolded in vitro (Garboczi et al., 1992). Peptide p1049 (ALWGFFPVL), presented by A2, was synthesized by the UNC Peptide Synthesis Facility (Chapel Hill, NC). Briefly, peptide, β_2m, and heavy chain were injected in that order into a folding buffer optimized for refolding class I MHC at a concentration of 50 μg/ml. After incubation for 24-36 hours at 10 °C the folded pMHC was concentrated in an Amicon ultrafiltration cell (Millipore, Billerica, MA) and purified using gel filtration chromatography (Phenomenex) on HPLC. The purified wild-type and A2 variants were concentrated to 10 mg/ml and stored at -80°C. Typical yield for each 1 L refold is about 5 mg of pMHC.

2.5.3 Cytotoxicity Assay

Cytotoxicity was assayed using a standard 4 hour ^{51}Cr release assay as described previously (Loftus et al., 1997). Briefly, between 5.0×10^3 and 5.0×10^4 AHIII 12.2 T cells were incubated with 5000 peptide-pulsed ^{51}Cr-labeled A2 mutant-transfected cells. Since p1049 is a human self-antigen, the transfectants were recognized without the addition of p1049 to the cells. Additional p1049 did not increase cytotoxicity (data not shown).

2.5.4 Surface Plasmon Resonance Experiments

Five-thousand resonance units (RUs) of H57-597 (capturing molecule, anti-TCR Cβ Ab) were covalently bound to a Biacore CM5 sensor chip (Uppsala, Sweden) using standard amine coupling. Soluble AHIII12.2 TCR (ligand) was then added to the Ab at a concentration of 50-100 nM to generate 300–400 RU of bound TCR. Soluble class I

MHC (analyte) was injected onto the surface at a flow rate of 100 µl/min in a 30-s pulse. TCR and MHC were removed from the surface with 0.1 M Glycine, 0.5 M NaCl, pH 2.5, and the procedure was repeated until at least three curves were obtained for the different concentrations of analyte. Curves obtained at each concentration were subtracted from a reference surface that contained Ab alone without TCR or using recombinant P14 TCR as a negative control. Data were processed using Scrubber (BioLogic Software, Campbell, Australia) and CLAMP (Myszka and Morton, 1998). The suitability of the fit was measured based on χ^2 values and the appearance of residuals. In all cases, χ^2 was below 1, residuals were small and random, and the experimental curves visually matched the predicted curves.

2.5.5 Protein Crystallization and Structure Determination

The crystallization conditions for the co-crystal complexes were similar to those optimized for AHIII TCR with wild-type A2 (Buslepp et al., 2003b). Briefly, crystals are grown by hanging drop, vapor diffusion, using AHIII TCR and A2 variants mixed at equal ratios at a concentration of 10 mg/ml. Drops contain 1 µl of protein mixed with 1 µl of a well solution containing Hepes, pH 7.5-8.0, 1 M NaCl, and 14%-18% PEG 8000. Small crystals formed within 3 days along with precipitate in drops. Crystal size was improved by macro-seeding into identical conditions. Crystals were transferred to mother liquor containing 25% glycerol as cryoprotectant. Crystallographic data were collected at Southeast Regional Collaborative Access Team (SER-CAT) 22-ID and 22-BM beamlines at the Advanced Photon Source, Argonne National Laboratory (Argonne, IL). Data for AHIII-p1049/A2(T163A) was collected on the 22-BM beamline at 12,398.42 eV for 360° at a distance of 200 mm using 1.0° oscillations. Two datasets for

AHIII-p1049/A2(W167A) were collected on the 22-ID beamline at 12,759.89 eV at a distance of 300 mm using 1.0° oscillations. 180° were collected at an omega angle of 90° and an additional 45° was collected at an omega of 45°. These data sets were indexed separately and then scaled together. Data for AHIII-p1049/A2(K66A) was collected on the 22-ID beamline at 12,759.89 eV for 180° at a distance of 300 mm using 1.0° oscillations. Data for all co-crystal complexes were indexed and scaled with HKL2000 (Otwinowski, 1997). The data for AHIII-p1049/A2(T163A) was originally collected out to 2.1 Å, but it was highly anisotropic. As a result, the statistics in the highest shells were poor, so the data was truncate at 2.4 Å. Molecular replacement solutions were determined using Rigid Body Refinement in Refmac 5.0 (1994) with AHIII-p1049/A2 (1LP9) (Buslepp et al., 2003b) as the search model. Temperature factors were set to 30.0 using Moleman (Kleywegt, 1992-2004). Positional refinement using noncrystallographic symmetry restraints for the first few cycles and TLS refinement (Winn et al., 2001) in Refmac 5.0 was performed iteratively with manual intervention with O (Jones et al., 1991). When the statistics did not improve over two subsequent rounds of refinement and the Rfree was below 30%, waters were added using Arp within Refmac 5.0 to AHIII-p1049/A2(T163A) and AHIII-p1049/A2(W167A) models. All waters were examined to confirm the presence of hydrogen bond donors or acceptors at reasonable geometries. For the AHIII-p1049/A2(K66A) model, an omit map of the CDR3α loop was generated to verify the conformational change. The refinement statistics for the final models are presented in Table 2. Surface complementarity (SC) calculated using Sc (Lawrence and Colman, 1993) in CCP4 (1994).

2.5.6 Isothermal Titration Calorimetry

ITC experiments on AHIII TCR with wild-type p1049/A2 and p1049/A2(K66A) were performed on a Microcal VP-ITC in the UNC Macromolecular Interactions Facility (Chapel Hill, NC). Thermodynamic constants were obtained for AHIII TCR binding wild-type p1049/A2 as well as p1049/A2(K66A) by fitting the calorimetric data using a one-site binding model in Microcal Origin Version 5.0 Software (OriginLab Corporation, Northampton, MA). Soluble AHIII TCR was placed in the mixing chamber. p1049/A2 or p1049/A2(K66A) was titrated into the AHIII TCR solution until binding reached saturation. Titration of wild-type p1049/A2 into AHIII TCR was performed in duplicate, once in Phosphate buffer, pH 7.5, and then in Tris buffer, pH 7.5, to ensure that the determined enthalpy was not affected by ionization enthalpy of the buffer (Baker and Murphy, 1996). Concentrations of AHIII TCR and p1049/A2 were 17 μM and 217 μM, respectively, in Phosphate and 19 μM and 234 μM, respectively in Tris. For wild-type p1049/A2 experiments, a volume of 3 μL was used for the first four injections, and then 5 μL for the remaining titrations. The baseline, generated by averaging the heat measured for the last 10 injections, was subtracted from all peaks. Titration of p1049/A2(K66A) in AHIII TCR was performed in triplicate in Phosphate buffer, pH 7.5. Concentrations of AHIII TCR and p1049/A2(K66A) were 40 μM and 618 μM, 65 μM and 450 μM, and 43 μM and 394 μM, respectively, for the three replicates. For all p1049/A2(K66A) experiments, 5 μL was injected for the first four peaks, increasing to 10 μL for the remainder of the experiment. Because of the relatively small amount of heat released upon AHIII-p1049/A2(K66A) binding, a more accurate baseline was determined by injecting p1049/A2(K66A) into Phosphate buffer to measure heat of dilution. This

reference data set was then subtracted from the experimental data set in Origin Software. All concentrations were determined before the proteins were placed in the microcalorimeter using extinction coefficients. ΔH and ΔS were calculated using the Origin software. Gibbs free energy was calculated as $\Delta G = \Delta H - T\Delta S$, $T = 298$ K.

2.5.7 ACKNOWLEDGEMENTS

We thank William E. Biddison, Ph.D. of the Molecular Immunology Section of the National Institutes of Health, Bethesda, MD for supplying the HLA-A2 variant cells lines for our cytotoxicity assays. Data were collected at Southeast Regional Collaborative Access Team (SER-CAT) 22-ID beamline at the Advanced Photon Source, Argonne National Laboratory. Staff at the beamline are acknowledged for assistance in data collection. Use of the Advanced Photon Source was supported by the U. S. Department of Energy, Office of Science, Office of Basic Energy Sciences, under Contract No. W-31-109-Eng-38. The director of the UNC Macromolecular Interations Facility, Ashutosh Tripathy, Ph.D. is gratefully acknowledged for his assistance with collecting and interpreting ITC data. Members of the Collins and Frelinger labs are acknowledged for helpful discussions.

2.6 References

(1994) The CCP4 suite: programs for protein crystallography. *Acta Crystallogr D Biol Crystallogr* **50**, 760-3.

Al-Lazikani B., Lesk A. M. and Chothia C. (1997) Standard conformations for the canonical structures of immunoglobulins. *J Mol Biol* **273**, 927-48.

Baker B. M. and Murphy K. P. (1996) Evaluation of linked protonation effects in protein binding reactions using isothermal titration calorimetry. *Biophys J* **71**, 2049-55.

Baker B. M., Turner R. V., Gagnon S. J., Wiley D. C. and Biddison W. E. (2001) Identification of a crucial energetic footprint on the alpha1 helix of human histocompatibility leukocyte antigen (HLA)-A2 that provides functional interactions for recognition by tax peptide/HLA-A2-specific T cell receptors. *J Exp Med* **193**, 551-62.

Baxter T. K., Gagnon S. J., Davis-Harrison R. L., Beck J. C., Binz A. K., Turner R. V., Biddison W. E. and Baker B. M. (2004) Strategic mutations in the class I major histocompatibility complex HLA-A2 independently affect both peptide binding and T cell receptor recognition. *J Biol Chem* **279**, 29175-84.

Borg N. A., Ely L. K., Beddoe T., Macdonald W. A., Reid H. H., Clements C. S., Purcell A. W., Kjer-Nielsen L., Miles J. J., Burrows S. R., McCluskey J. and Rossjohn J. (2005) The CDR3 regions of an immunodominant T cell receptor dictate the 'energetic landscape' of peptide-MHC recognition. *Nat Immunol* **6**, 171-80.

Brodsky F. M., Parham P., Barnstable C. J., Crumpton M. J. and Bodmer W. F. (1979) Monoclonal antibodies for analysis of the HLA system. *Immunol Rev* **47**, 3-61.

Buslepp J., Kerry S. E., Loftus D., Frelinger J. A., Appella E. and Collins E. J. (2003a) High affinity xenoreactive TCR:MHC interaction recruits CD8 in absence of binding to MHC. *J Immunol* **170**, 373-83.

Buslepp J., Wang H., Biddison W. E., Appella E. and Collins E. J. (2003b) A correlation between TCR Valpha docking on MHC and CD8 dependence: implications for T cell selection. *Immunity* **19**, 595-606.

Chen J. L., Stewart-Jones G., Bossi G., Lissin N. M., Wooldridge L., Choi E. M., Held G., Dunbar P. R., Esnouf R. M., Sami M., Boulter J. M., Rizkallah P., Renner C., Sewell A., van der Merwe P. A., Jakobsen B. K., Griffiths G., Jones E. Y. and Cerundolo V. (2005) Structural and kinetic basis for heightened immunogenicity of T cell vaccines. *J Exp Med* **201**, 1243-55.

Chothia C., Lesk A. M., Gherardi E., Tomlinson I. M., Walter G., Marks J. D., Llewelyn M. B. and Winter G. (1992) Structural repertoire of the human VH segments. *J Mol Biol* **227**, 799-817.

Chothia C., Lesk A. M., Tramontano A., Levitt M., Smith-Gill S. J., Air G., Sheriff S., Padlan E. A., Davies D., Tulip W. R. and et al. (1989) Conformations of immunoglobulin hypervariable regions. *Nature* **342**, 877-83.

Clements C. S., Dunstone M. A., Macdonald W. A., McCluskey J. and Rossjohn J. (2006) Specificity on a knife-edge: the alphabeta T cell receptor. *Curr Opin Struct Biol* **16**, 787-95.

Colf L. A., Bankovich A. J., Hanick N. A., Bowerman N. A., Jones L. L., Kranz D. M. and Garcia K. C. (2007) How a single T cell receptor recognizes both self and foreign MHC. *Cell* **129**, 135-46.

Davis-Harrison R. L., Armstrong K. M. and Baker B. M. (2005) Two different T cell receptors use different thermodynamic strategies to recognize the same peptide/MHC ligand. *J Mol Biol* **346**, 533-50.

Davis-Harrison R. L., Insaidoo F. K. and Baker B. M. (2007) T Cell Receptor Binding Transition States and Recognition of Peptide/MHC. *Biochemistry* **46**, 1840-50.

Degano M., Garcia K. C., Apostolopoulos V., Rudolph M. G., Teyton L. and Wilson I. A. (2000) A functional hot spot for antigen recognition in a superagonist TCR/MHC complex. *Immunity* **12**, 251-61.

Delano W. L. (2002) The PyMOL Molecular Graphics System DeLano Scientific, San Carlos, CA.

Ding Y. H., Baker B. M., Garboczi D. N., Biddison W. E. and Wiley D. C. (1999) Four A6-TCR/peptide/HLA-A2 structures that generate very different T cell signals are nearly identical. *Immunity* **11**, 45-56.

Ding Y. H., Smith K. J., Garboczi D. N., Utz U., Biddison W. E. and Wiley D. C. (1998) Two human T cell receptors bind in a similar diagonal mode to the HLA-A2/Tax peptide complex using different TCR amino acids. *Immunity* **8**, 403-11.

Ellis J. M., Henson V., Slack R., Ng J., Hartzman R. J. and Katovich Hurley C. (2000) Frequencies of HLA-A2 alleles in five U.S. population groups. Predominance Of A*02011 and identification of HLA-A*0231. *Hum Immunol* **61**, 334-40.

Ely L. K., Beddoe T., Clements C. S., Matthews J. M., Purcell A. W., Kjer-Nielsen L., McCluskey J. and Rossjohn J. (2006) Disparate thermodynamics governing T cell receptor-MHC-I interactions implicate extrinsic factors in guiding MHC restriction. *Proc Natl Acad Sci U S A* **103**, 6641-6.

Engelhard V. H. and Benjamin C. (1982) Isolation and characterization of monoclonal mouse cytotoxic T lymphocytes with specificity for HLA-A,B or -DR alloantigens. *J Immunol* **129**, 2621-9.

Gagnon S. J., Borbulevych O. Y., Davis-Harrison R. L., Baxter T. K., Clemens J. R., Armstrong K. M., Turner R. V., Damirjian M., Biddison W. E. and Baker B. M. (2005) Unraveling a hotspot for TCR recognition on HLA-A2: evidence against the existence of peptide-independent TCR binding determinants. *J Mol Biol* **353**, 556-73.

Garboczi D. N., Ghosh P., Utz U., Fan Q. R., Biddison W. E. and Wiley D. C. (1996) Structure of the complex between human T-cell receptor, viral peptide and HLA-A2. *Nature* **384**, 134-41.

Garboczi D. N., Hung D. T. and Wiley D. C. (1992) HLA-A2-peptide complexes: refolding and crystallization of molecules expressed in Escherichia coli and complexed with single antigenic peptides. *Proc Natl Acad Sci U S A* **89**, 3429-33.

Garcia K. C., Degano M., Pease L. R., Huang M., Peterson P. A., Teyton L. and Wilson I. A. (1998) Structural basis of plasticity in T cell receptor recognition of a self peptide-MHC antigen. *Science* **279**, 1166-72.

Garcia K. C., Radu C. G., Ho J., Ober R. J. and Ward E. S. (2001) Kinetics and thermodynamics of T cell receptor- autoantigen interactions in murine experimental autoimmune encephalomyelitis. *Proc Natl Acad Sci U S A* **98**, 6818-23.

Henderson R. A., Cox A. L., Sakaguchi K., Appella E., Shabanowitz J., Hunt D. F. and Engelhard V. H. (1993) Direct identification of an endogenous peptide recognized by multiple HLA-A2.1-specific cytotoxic T cells. *Proc Natl Acad Sci U S A* **90**, 10275-9.

James L. C., Roversi P. and Tawfik D. S. (2003) Antibody multispecificity mediated by conformational diversity. *Science* **299**, 1362-7.

Jones T. A., Zou J. Y., Cowan S. W. and Kjeldgaard. (1991) Improved methods for building protein models in electron density maps and the location of errors in these models. *Acta Crystallogr A* **47 (Pt 2)**, 110-9.

Kjer-Nielsen L., Clements C. S., Purcell A. W., Brooks A. G., Whisstock J. C., Burrows S. R., McCluskey J. and Rossjohn J. (2003) A structural basis for the selection of dominant alphabeta T cell receptors in antiviral immunity. *Immunity* **18**, 53-64.

Kleywegt G. J. (1992-2004). Uppsala University, Uppsala, Sweden.

Krogsgaard M., Prado N., Adams E. J., He X. L., Chow D. C., Wilson D. B., Garcia K. C. and Davis M. M. (2003) Evidence that structural rearrangements and/or flexibility during TCR binding can contribute to T cell activation. *Mol Cell* **12**, 1367-78.

Lawrence M. C. and Colman P. M. (1993) Shape complementarity at protein/protein interfaces. *J Mol Biol* **234**, 946-50.

Lee J. K., Stewart-Jones G., Dong T., Harlos K., Di Gleria K., Dorrell L., Douek D. C., van der Merwe P. A., Jones E. Y. and McMichael A. J. (2004) T cell cross-reactivity and conformational changes during TCR engagement. *J Exp Med* **200**, 1455-66.

Loftus D. J., Chen Y., Covell D. G., Engelhard V. H. and Appella E. (1997) Differential contact of disparate class I/peptide complexes as the basis for epitope cross-recognition by a single T cell receptor. *J Immunol* **158**, 3651-8.

Lovell S. C., Davis I. W., Arendall W. B., 3rd, de Bakker P. I., Word J. M., Prisant M. G., Richardson J. S. and Richardson D. C. (2003) Structure validation by Calpha geometry: phi,psi and Cbeta deviation. *Proteins* **50**, 437-50.

Madden D. R. (1995) The three-dimensional structure of peptide-MHC complexes. *Annu Rev Immunol* **13**, 587-622.

Morea V., Tramontano A., Rustici M., Chothia C. and Lesk A. M. (1998) Conformations of the third hypervariable region in the VH domain of immunoglobulins. *J Mol Biol* **275**, 269-94.

Murshudov G. N., Vagin A. A. and Dodson E. J. (1997) Refinement of macromolecular structures by the maximum-likelihood method. *Acta Crystallogr D Biol Crystallogr* **53**, 240-55.

Myszka D. G. and Morton T. A. (1998) CLAMP: a biosensor kinetic data analysis program. *Trends Biochem Sci* **23**, 149-50.

Otwinowski Z. a. M., M. (1997) *Processing of X-ray Diffraction Data Collected in Oscillation Mode*. Academic Press, New York.

Reed N. S. P. a. R. J. (1996) Improved Structure Refinement Through Maximum Likelihood. *Acta Crystallogr A* **52**, 659-668.

Reiser J. B., Darnault C., Gregoire C., Mosser T., Mazza G., Kearney A., van der Merwe P. A., Fontecilla-Camps J. C., Housset D. and Malissen B. (2003) CDR3 loop flexibility contributes to the degeneracy of TCR recognition. *Nat Immunol* **4**, 241-7.

Reiser J. B., Darnault C., Guimezanes A., Gregoire C., Mosser T., Schmitt-Verhulst A. M., Fontecilla-Camps J. C., Malissen B., Housset D. and Mazza G. (2000) Crystal structure of a T cell receptor bound to an allogeneic MHC molecule. *Nat Immunol* **1**, 291-7.

Reiser J. B., Gregoire C., Darnault C., Mosser T., Guimezanes A., Schmitt-Verhulst A. M., Fontecilla-Camps J. C., Mazza G., Malissen B. and Housset D. (2002) A T cell receptor CDR3beta loop undergoes conformational changes of unprecedented magnitude upon binding to a peptide/MHC class I complex. *Immunity* **16**, 345-54.

Robinson J., Waller M. J., Parham P., de Groot N., Bontrop R., Kennedy L. J., Stoehr P. and Marsh S. G. (2003) IMGT/HLA and IMGT/MHC: sequence databases for the study of the major histocompatibility complex. *Nucleic Acids Res* **31**, 311-4.

Rudolph M. G., Stanfield R. L. and Wilson I. A. (2006) How TCRs bind MHCs, peptides, and coreceptors. *Annu Rev Immunol* **24**, 419-66.

Schatz D. G. and Spanopoulou E. (2005) Biochemistry of V(D)J recombination. *Curr Top Microbiol Immunol* **290**, 49-85.

Spicuglia S., Franchini D. M. and Ferrier P. (2006) Regulation of V(D)J recombination. *Curr Opin Immunol* **18**, 158-63.

Tynan F. E., Burrows S. R., Buckle A. M., Clements C. S., Borg N. A., Miles J. J., Beddoe T., Whisstock J. C., Wilce M. C., Silins S. L., Burrows J. M., Kjer-Nielsen L., Kostenko L., Purcell A. W., McCluskey J. and Rossjohn J. (2005) T cell receptor recognition of a 'super-bulged' major histocompatibility complex class I-bound peptide. *Nat Immunol* **6**, 1114-22.

Tynan F. E., Reid H. H., Kjer-Nielsen L., Miles J. J., Wilce M. C., Kostenko L., Borg N. A., Williamson N. A., Beddoe T., Purcell A. W., Burrows S. R., McCluskey J. and Rossjohn J. (2007) A T cell receptor flattens a bulged antigenic peptide presented by a major histocompatibility complex class I molecule. *Nat Immunol* **8**, 268-76.

Wang Z., Turner R., Baker B. M. and Biddison W. E. (2002) MHC allele-specific molecular features determine peptide/HLA-A2 conformations that are recognized by HLA-A2-restricted T cell receptors. *J Immunol* **169**, 3146-54.

Willcox B. E., Gao G. F., Wyer J. R., Ladbury J. E., Bell J. I., Jakobsen B. K. and van der Merwe P. A. (1999) TCR binding to peptide-MHC stabilizes a flexible recognition interface. *Immunity* **10**, 357-65.

Winn M. D., Isupov M. N. and Murshudov G. N. (2001) Use of TLS parameters to model anisotropic displacements in macromolecular refinement. *Acta Crystallogr D Biol Crystallogr* **57**, 122-33.

Wu L. C., Tuot D. S., Lyons D. S., Garcia K. C. and Davis M. M. (2002) Two-step binding mechanism for T-cell receptor recognition of peptide MHC. *Nature* **418**, 552-6.

Wu W., Harley P. H., Punt J. A., Sharrow S. O. and Kearse K. P. (1996) Identification of CD8 as a peanut agglutinin (PNA) receptor molecule on immature thymocytes. *J Exp Med* **184**, 759-64.

CHAPTER 3

Biophysical Characterization of AHIII TCR Interaction with Agonist and Antagonist Peptide/MHC Complexes

3.1 ABSTRACT

T cell receptor (TCR) recognition of peptide presented by MHC (pMHC) is the critical first step for T cell activation. T cell activation is not binary, as a full range of T cell responses have been reported, which stem from the discriminatory ability of the TCR to recognize self from non-self pMHC ligands. Altered peptide ligands (APL) can produce this range of responses, including antagonism, whereby the T cell response is actually inhibited by a particular pMHC. It remains unclear through what mechanism this inhibition occurs. The p1058 peptide, when presented by the class I MHC HLA-A2.1 (A2), has been previous recorded as an antagonist peptide for the AHIII12.2 (AHIII) T cell. This p1058 peptide differs from the agonist p1049 peptide by only a few residues. A panel of over 20 variants of these peptides presented in A2 was used in surface plasmon resonance experiments to determine binding constants to the AHIII TCR. The data presented here suggest that the antagonism of p1058 correlates with a very weak binding affinity and this weak binding is due to the inability of the AHIII TCR to bind p1058/A2 without undergoing a conformational change. These data also suggest that mutations made on the surface of the MHC molecule are better by the TCR tolerated than mutations in the peptide. This biophysical data presented in this chapter will be combined with a full spectrum of biological assays on AHIII T cells including cytolysis,

combined with a full spectrum of biological assays on AHIII T cells including cytolysis, proliferation, and cytokine secretion, as a means to evaluate any correlation between TCR-pMHC recognition and T cell activation.

3.2 INTRODUCTION

Cytotoxic T cells are a critical component of the adaptive immune response, responsible for clearing infected cells from the body. Recognition of these infected cells is mediated through the T cell receptor (TCR), which recognizes and binds to peptides presented in the context of the class I major histocompatibility complex (MHC) molecules on the surface of nearly all nucleated cells. While other T cell surface molecules are involved in cytotoxic T cell killing of antigen presenting cells, the TCR interaction with peptide/MHC ultimately determines if the cell is healthy or infected.

TCR triggering of T cell activation cannot be described in as a binary system, i.e. on or off. Instead, qualitatively different T cell signaling can lead to a range of responses from maximal activation to desensitization of the T cell (reviewed in (Bongrand and Malissen, 1998; Uhlin et al., 2006)). The cognate pMHC ligand of a TCR that leads to a full response is generally referred to as an agonist. Agonists elicit the full range of T cell responses, including cell proliferation, cytokine secretion, expression of activation markers, and cytotoxicity (for CTLs). Variants of the cognate pMHC, often called altered peptide ligands (APLs), can result in various responses. Partial agonists result in some, but not all, of these responses. Null agonists elicit no response. Other ligands, called antagonists, not only elicit no response, but actually seem to block T cell responses to agonist ligands, sometimes even resulting in T cell anergy (Sloan-Lancaster et al.,

1993). Importantly, these antagonist peptides must be co-presented with agonists on the same antigen presenting cell (APC) to mediate their suppressive effects.

Antagonistic peptides do not follow a simple competitive model, occupying the TCR-pMHC binding and dampening T cell signaling in a dose dependent manner. Rather, the qualitative differences in T cell signaling are the result of alternate patterns of phosphorylation in the signaling pathway. Pull down experiments have shown that agonistic peptides result in full phosphorylation of Lck, ZAP-70, CD3ε, and both p21-CD3ζ and p23-CD3ζ chains, where as null or antagonistic peptides resulted in phosphorylation of only p21-CD3ζ and not p23-CD3ζ, CD3ε, or ZAP-70 (reviewed in (Madrenas and Germain, 1996)). Importantly, this qualitative difference in phosphorylation cannot be reproduced by just stimulating T cells with lower concentrations of weak or full agonists (Reis e Sousa et al., 1996). It is theorized that this pattern is the result of incomplete activation, i.e. lack of the secondary activation signal from co-stimulatory receptors, primarily CD28 and LFA-1 (Schwartz, 2003). Partial agonists and antagonists also affect the downstream patterns of Ca^{2+} flux compared to full agonists (Chen et al., 1998).

The most extreme effect of antagonism is T cell anergy, where the cell becomes functionally inactive following encounter with antagonist pMHC (reviewed in (Schwartz, 2003)). Anergic T cells have a similar phosphorylation pattern described above for antagonists. Clonal anergy of CTLs often manifests itself in a somewhat normal secretion of IFNγ, but drastically reduced levels of IL-2 and an arrest in cell growth. These cells can sometimes be rescued from anergy with the addition of high levels of IL-2 (Schwartz, 2003).

The study of agonist, partial agonist, and antagonist peptides provide a means of deciphering the mechanisms of T cell activation. Better understanding of these activation phenomena could also lead to be treatment of certain diseases. Antagonist peptides have been encountered in viral infections and may aid in immune evasion. Mutations in HIV, Hepatitis B and C, and LCMV have been reported to produce antagonistic peptides; and even self-peptides presented by MHC have been shown to enhance or suppress immune response to certain antigens (Vukmanovic et al., 2003). Naturally processed antagonist peptides during a Listeria infection in mice were shown to suppress activation of naïve T cells by agonist peptide, suppress memory response upon challenge, and alter the hierarchy of immunodominance (Lau et al., 2005). These results suggest the need to study possible antagonistics associated with vaccine development. A clearer understanding of T cell antagonism could potentially allow for the use of antagonistic peptides as therapeutics; potentially down-regulating a cytotoxic T cell response in autoimmune disorders or transplantation (Garcia-Peydro et al., 2000).

The qualitatively different signals described above lead to a range of T cell responses. These stem from quantitative differences for TCR-pMHC molecular recognition. However, it is still unclear how that quantitative difference is determined by the TCR. It was hypothesized that the overall structure of a TCR bound to an agonist would differ from the same TCR bound to antagonist, thus relaying a signal into the cell through some allosteric mechanism. Unfortunately, it was found that the TCR-pMHC crystal structures of A6-tax/A2 (agonist) and A6-tax(P6A)/A2 (antagonist) are virtually identical, and another A6-tax(Y8A)/A2 (antagonist) structure showed only a small change in the CDR3β loop (Ding et al., 1999). Consequently, the structural (Rudolph et

al., 2006) and thermodynamic (Armstrong et al., 2008) mechanisms of TCR-pMHC molecular recognition vary greatly. It seems that each TCR finds a unique way in which to bind its respective pMHC targets. If a conformational change in the TCR structure does not relay the pMHC readout into the cell than some other biophysical mechanism must.

A few biophysical models exist to explain differences in TCR triggering and downstream T cell outcome. The kinetic model proposes that the level of T cell activation is dependent on the dissociation rate of the TCR-pMHC interaction; slower off-rate equals greater signal. Due to the two sets of signals required for full T cell activation the kinetic model proposes that the TCR-pMHC must be engaged long enough for both the first TCR initiated signal and the co-stimulatory signal to occur (McKeithan, 1995; Rabinowitz et al., 1996). This kinetic correlation has been supported by a number of experimental observations (Kersh et al., 1998; Lyons et al., 1996; Matsui et al., 1994; Rosette et al., 2001). Experiments with the class II MHC restricted 2B4 TCR measured lower affinities and faster dissociation rates when the TCR bound antagonist ligands compared to the agonist 2B4 target (Lyons et al., 1996). A more recent refinement of this basic off-rate model combines off-rate with a measure of conformational change upon binding (ΔCp) to predict T cell stimulation (Krogsgaard et al., 2003).

Another popular model is the affinity model, which states that T cell activation relates to the concentration or number of pMHC ligands engaged. The affinity model is also supported by an abundance of experimental data, which all show a correlation between determined TCR-pMHC affinities and activation (Alam et al., 1996; Baker et al., 2000; Buslepp et al., 2001; Garcia et al., 2001; Holler and Kranz, 2003; Miller et al.,

2007; Schodin et al., 1996; Sykulev et al., 1994; Sykulev et al., 1998; Tian et al., 2007). Agonist versus antagonist response of the class I MHC restricted A6 T cell correlates with the determined affinities (Baker et al., 2000; Ding et al., 1999). Another case supporting a correlation with affinity involves activation of the P14 T cell. Recently, two independent laboratories have determined the affinity to be consistent with other agonist pMHC interactions, but the shortest half-life of any other agonist TCR-pMHC interaction (k_{off} >1 s^{-1}) (Boulter et al., 2007; Tian et al., 2007).

The serial triggering model attempts to explain the paradox of high specificity of TCR-pMHC with a low affinity interaction. It does not compete with kinetic or affinity models, but rather incorporates them both. Following ITAM phosphorylation the TCR-CD3 complex is downregulated, or internalized, in the T cell. Lanzavecchia and colleagues measured this internalization following stimulation by agonist pMHC (Valitutti et al., 1995). They determined that a single pMHC complex could serially trigger ~200 TCR, due to the fast off-rate of TCR-pMHC binding. Partial agonists were shown to downregulate fewer TCR, suggesting that there exists an optimum affinity and off-rate (or dwell time) that allows TCR triggering and pMHC complex recycling. Without a full TCR trigger, antagonists could actually inhibit downregulation of TCR. Finally this model suggests that there is a threshold of "triggered" TCRs needed in order to fully activate the cell (Lanzavecchia et al., 1999; Valitutti et al., 1995).

Differences in kinetics or affinity should be able define the differences in response between agonist and antagonist peptides. However, there is still no concensus on which mechanisms connect TCR-pMHC molecular recognition to T cell activation. In an effort to address this, we undertook most extensive analysis of TCR-pMHC binding to

date. We have evaluated the affects of 24 variants of an agonist and antagonist peptides. Most studies of this nature have only evaluated a handful of pMHC ligands and a single readout of T cell activation, where we will have measured T cell proliferation, cytotoxicity, and cytokine secretion.

The work presented here attempts to answer if TCR-pMHC binding affinity or kinetics can be correlated with the T cell response measured against an agonist versus an antagonist pMHC ligand. To address this we relied on the AHIII12.2 (AHIII) T cell system. AHII is a murine T cell clone that recognizes class I H-2D^b (D^b) in complex with the synthetic peptide p1058 (FAPGFFPYL) and its variants (Loftus et al., 1997). AHIII is interesting in that it also recognizes a xenogenic human class I MHC, HLA-A2.1 (A2), when presenting the peptide p1049 (ALFGFFPVL) (Henderson et al., 1993). So, p1058/D^b and p1049/A2 both produce an agonistic response in AHIII. Interestingly, it was found that when p1058 is bound and presented by A2 it becomes antagonistic. Experiments using fluorescently labeled p1058/A2 tetramer also suggested that the AHIII TCR bound p1058/A2 with lower affinity than p1049/A2 (Buslepp et al., 2001). However, this affinity has never been directly measured.

We utilized surface plasmon resonance (SPR) to determine the affinity and kinetics of AHIII TCR binding to A2 complexed with a panel of 24 variants of p1058 and p1049 including wild-type. Based on the previous AHIII activation data (Buslepp et al., 2001), we find a trend between T cell activation and TCR-pMHC affinity. We show that the binding constants determined are not affected by the ability of A2 to bind the peptide variants. Additionally, analysis of the determined crystal structures of p1058/A2 (Buslepp et al., 2001) and AHIII TCR bound to p1049/A2 (Buslepp et al., 2003b)

revealed an unforeseen relationship between position 3 and position 5 of the peptides. Finally, our analysis suggests that the AHIII TCR must undergo a structural rearrangement, or must dock in an alternate manner in order to bind antagonistic p1058/A2.

3.3 MATERIALS AND METHODS

3.3.1 Protein Production and Purification

Soluble AHIII12.2 TCR was produced as previously described in Chapter 2 (Miller et al., 2007). Briefly, the ectodomains of AHIII TCR α and β chains were expressed as inclusion bodies in *E. coli*. Purified inclusion bodies, previously dissolved in 8M Urea, were rapidly injected into a folding buffer optimized for the AHIII TCR at a concentration of 50 μg/ml. After incubation for 36 hours at 10 °C and extensive dialysis against 0.1 M Urea and 50 mM Tris, pH 8, the native TCR was purified and concentrated by DE52 anion exchange (Whatman, Florham Park, NJ) followed by gel filtration chromatography (Phenomenex, Torrance, CA) on HPLC. Purified AHIII TCR for SPR experiments was concentrated to 200 μM and stored at -80 °C. Soluble AHIII TCR was tested for proper folding and activity through an ELISA using HLA-A2 tetramer made from streptavidin conjugated to horseradish peroxidase (Leinco Technologies, St. Louis MO). Typical yield for each 1 L *in vitro* fold is about 3-5 mg of active TCR. The P14 TCR (Tian et al., 2007) that was used as a negative control and reference in the surface plasmon resonance experiments was produced and purified identically to the AHIII TCR.

Similarly, soluble HLA-A2 was produced as inclusion bodies in *E. coli* and folded in vitro (Garboczi et al., 1992; Miller et al., 2007). Peptides p1049 (ALWGFFPVL) and

p1058 (FAPGFFPYL) and their variants were synthesized by both the UNC Peptide Synthesis Facility (Chapel Hill, NC), or by our collaborators in the laboratory of Dr. Ettore Appella at the NIH (Bethesda, MD). Peptide, β_2m, and heavy chain were then injected in that order into a folding buffer optimized for *in vitro* folding class I MHC at a concentration of 50 μg/ml. After incubation for 36 hours at 10 °C the folded pMHC was concentrated in an Amicon ultrafiltration cell (Millipore, Billerica, MA) and purified using gel filtration chromatography (Phenomenex) on HPLC. The purified pMHC were concentrated to approximately 10 mg/ml and stored at -80°C. Typical yield for each 1 L *in vitro* fold is about 5 mg of pMHC. Two to four folds of each pMHC variant were necessary to obtain the amount of protein needed for surface plasmon resonance experiments.

3.3.2 Surface Plasmon Resonance Experiments

The day of each surface plasmon resonance (SPR) experiment the frozen stocks of the pMHC being tested was removed from -80 °C and rerun over the gel filtration column to remove any aggregates from the freeze-thaw process. These pMHC were then extensively buffer-swapped with HBS-EP buffer (GE Healthcare, Piscataway, NJ) and concentrated to the concentrations listed here: p1049(A1G)/A2, 80 μM; p1049(A1F)/A2, 240 μM; p1049(L2A)/A2, 80 μM; p1049(W3F)/A2, 320 μM; p1049(W3L)/A2, 270 μM; p1049(W3P)/A2, 210 μM; p1049(G4A)/A2, 300 μM; p1049(F5V)/A2, 200 μM; p1049(F5A)/A2, 250 μM; p1049(F6V)/A2, 200 μM; p1049(F6A)/A2, 300 μM; p1049(P7A)/A2, 200 μM; p1049(V8Y)/A2, 200 μM; p1049(V8A)/A2, 80 μM; p1049(L9A)/A2, 250 μM; p1049(A1F/V8Y)/A2, 300 μM; p1058/A2, 300 μM;

p1058(P3L)/A2, 320 μM; p1058(F1A/P3W)/A2, 360 μM; p1058(P3W/Y8V), 340 μM. Two fold dilutions then resulted eight to nine concentrations for SPR.

SPR experiments were carried out on a Biacore 2000 (GE Healthcare, Piscataway, NJ). Approximately 2000-4000 resonance units (RU) of H57-597, anti-TCR Cβ antibody (eBioscience), were covalently bound to a Biacore CM5 sensor chip (GE Healthcare, Piscataway, NJ) using standard amine coupling. Soluble AHIII12.2 TCR was then added to the Ab at a concentration of 800 nM to generate 600–700 RU of bound TCR. Soluble pMHC was injected onto the surface at a flow rate of 50 μl/min in a 30 second pulse. TCR and MHC were removed from the surface with 0.1 M Glycine, pH 2, and the procedure was repeated until three curves were obtained for the different concentrations of pMHC. Curves obtained at each concentration were subtracted from a reference surface that contained immobilized P14 TCR as a negative control. The P14 TCR was loaded to generate the same ΔRU as the AHIII TCR. Data were processed using Scrubber 2.0 software (Center for Biomolecular Interaction Analysis, University of Utah). The suitability of the fit was measured based on χ^2 values and the appearance of residuals. In all cases, χ^2 was below 2, residuals were small and random, and the experimental curves visually matched the predicted curves. The data from each two-fold pMHC dilution series from each experiment were processed and fit separately and the resulting binding constants were then averaged. The mean values and their respective errors are presented in Table 1.

3.3.3 Peptide-MHC Affinity Assay

Peptide-A2 binding constants were determined by measuring surface stability of A2 varying concentrations of peptide as previously described (Buslepp et al., 2001;

Kuhns et al., 1999). Briefly, 2.0 x 10^5 T2 cells (ATCC #CRL-1992) were incubated overnight in AIM V serum-free media (Invitrogen) at 37 °C in 5% CO_2 in the presence of 100 nM soluble β_2m and variant peptides at concentrations ranging from 0.5 μM – 20 μM. Cells incubated in AIM V with a peptide (KTFGPIYKR) that binds HLA-Aw68 (Collins et al., 1999), but not HLA-A2 were used a negative control. Cells were then stained with PE conjugated BB7.2 anti-A2 monoclonal antibody (BD Pharmingen). Cells were analyzed by flow cytometry, and the mean fluorescence intensity (MFI) was determined using Summit software (Beckman Coulter). Equilibrium binding curves were fit to the MFI data to determine an EC50 for each peptide using GraphPad Prism software (La Jolla, CA).

3.4 RESULTS

3.4.1 Affects of Altered Peptide Ligands on Binding Paramters

The amino acid sequences of p1049 (ALWGFFPVL) and p1058 (FAPGFFPYL) are identical from positions 4-7 and at position 9. From the previously determined structure of the AHIII TCR bound to p1049/A2 (Buslepp et al., 2003b) we know that the majority of the peptide-TCR contacts occur in middle of the peptide, especially with F5 and F6. Yet, the T cell response to these two peptides is opposite: agonistic toward p1049 and antagonistic toward p1058 (Buslepp et al., 2001). To help elucidate the different mechanisms of recognition between these two targets, we assessed the binding of the AHIII TCR to p1058/A2, p1049/A2, and variants of each peptide. We employed surface plasmon resonance, which can determine both the affinity and the kinetics of the interaction in the same experiment. Surface plasmon resonance kinetic and equilibrium

binding sensorgram data and the curve fits are shown in Figure 1. The calculated binding constants are presented in Table 1.

SPR data had been previously collected on wild-type p1049/A2, determining a dissociation constant (K_d) of 9 μM and an off-rate (k_{off}) of 0.27 s^{-1} (see Table 2.1) (Miller et al., 2007). Mutations in the 1049 peptide all result in a weaker affinity except for one, V8A, where the increase in affinity can be attributed to an order of magnitude longer off-rate, 0.024 s^{-1}, which can be clearly seen in Figure 1. Not surprisingly, mutations of F5 and F6, which make van der Waals interactions with the CDR2 and CDR3 loops of the TCR, result in substantially weaker binding. The two surprising peptide positions that are significantly impacted by mutation are position 1 and position 3, both of which make no direct contact to the TCR. The A1F mutation decreases the affinity by over 200 μM, and ΔG by almost 2 kcal/mol. A conservative mutation at position 3 of Trp to Phe results in a K_d of 101 μM, but any smaller side chain substitution (Leu, Val, or Pro) at position 3 results in a K_d greater than 300 μM. Mutations at position 8 also affect binding in some unexpected ways. The valine at position 8 in p1049 points up toward the TCR, and makes a hydrophobic interaction with a Trp97 on the CDR3β loop. As mentioned above the V8A mutation results in a higher affinity and a substantially longer off-rate. The V8T substitution is well tolerated, but then V8Y likely causes steric problems because of its relative size and has a deleterious affect on the affinity. Importantly, the mutations A1F,

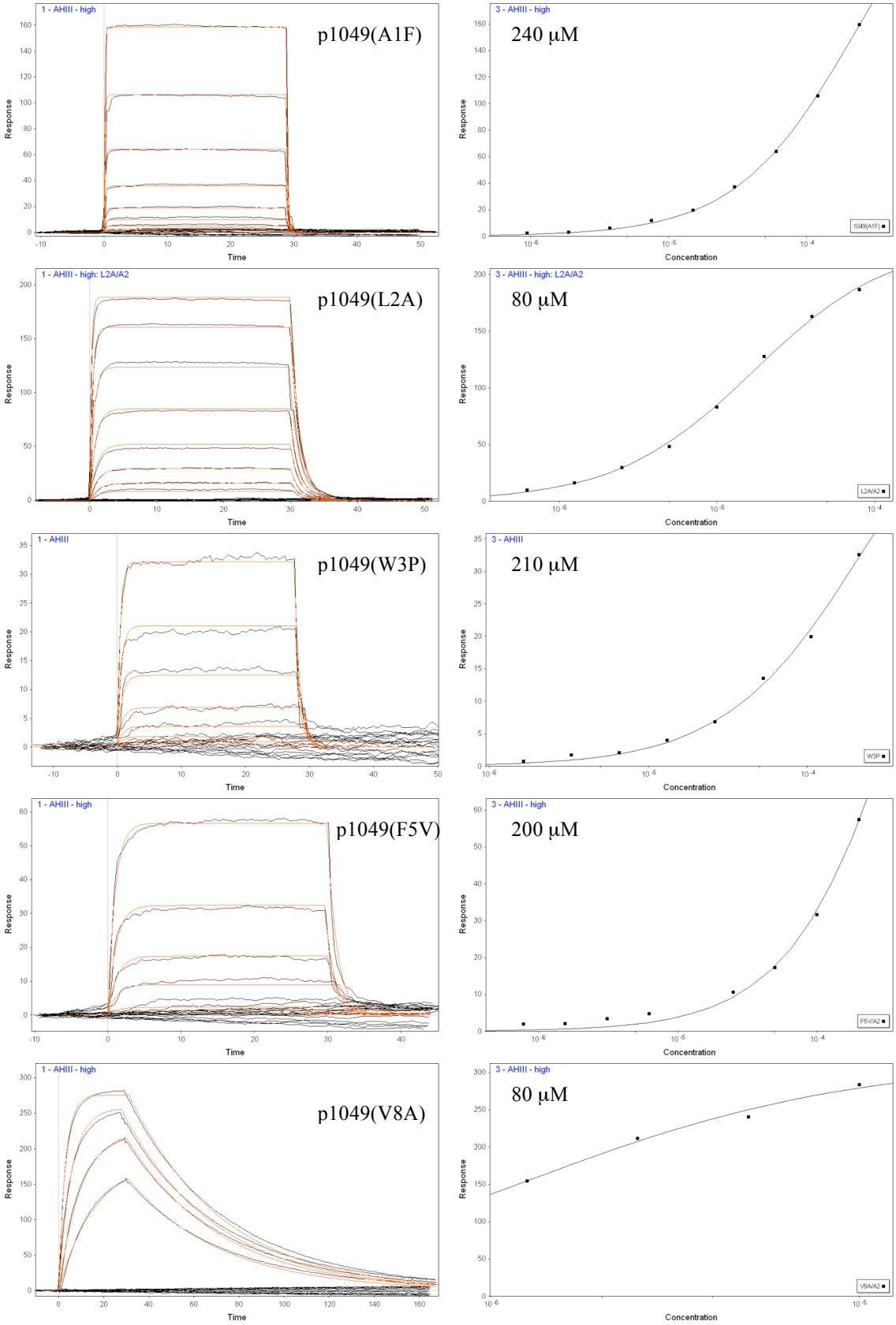
1 - AHIII - high
p1049(A1F)
Response
Time
3 - AHIII - high
240 µM
Response
Concentration
1049(A1F)
1 - AHIII - high: L2A/A2
p1049(L2A)
Response
Time
3 - AHIII - high: L2A/A2
80 µM
Response
Concentration
L2A/A2
1 - AHIII
p1049(W3P)
Response
Time
3 - AHIII
210 µM
Response
Concentration
W3P
1 - AHIII - high
p1049(F5V)
Response
Time
3 - AHIII - high
200 µM
Response
Concentration
F5V/A2
1 - AHIII - high
p1049(V8A)
Response
Time
3 - AHIII - high
80 µM
Response
Concentration
V8A/A2

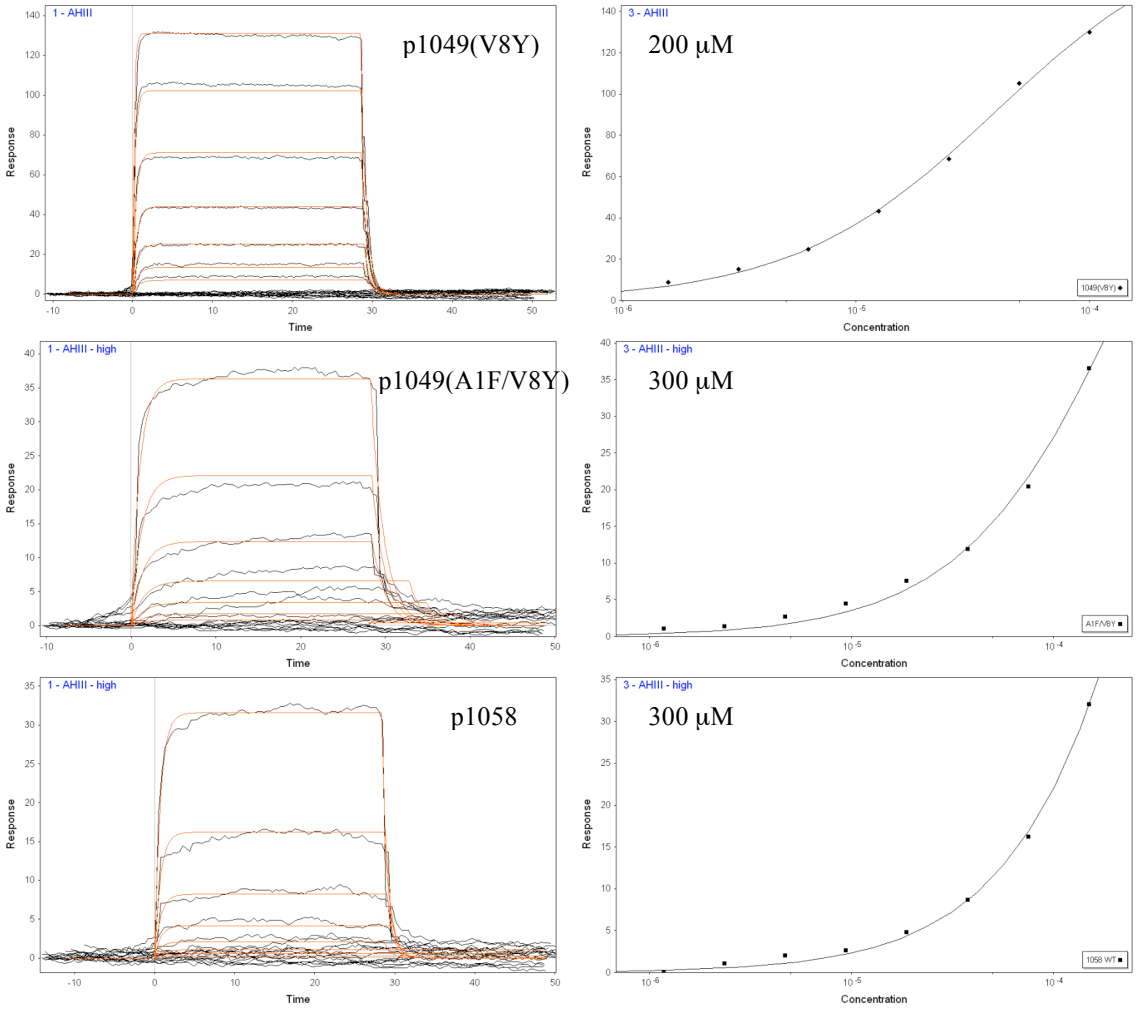

Figure 1. SPR sensorgram data and resulting kinetic and equilibrium curve-fits. AHIII TCR was immobilized on sensor chip using an anti-Cβ antibody (H57). Peptide/A2 at varying concentrations were then injected. SPR data was processed using Scrubber 2.0. Highest injected concentration is stated on equilibrium binding curve. Few mutations like p1049(L2A) have little affect on equilibrium binding and kinetics compared to wild-type. The increased half-life of p1049(V8A) can be clearly seen in the data. Most mutations at positions 1, 3, and in the middle of the peptide (5 and 6) have a deleterious affect on binding affinity and increase the off-rate. This is evident in the weak binding signal, the sharp drop after the injection, and the equilibrium binding curves that never reach an upper limit.

W3P, and V8Y individually have deleterious effects on AHIII binding to p1049/A2, and together essentially mutate p1049 into p1058. In fact, energetically these mutations add up to the difference between p1049/A2 and p1058/A2. Using the data in Table 1, the

ΔΔG for A1F, W3P, and V8Y is 4.88 kcal/mol, while the ΔΔG for p1049 to p1058 is 4.33 kcal/mol.

Combining these mutations has a dramatic impact, as seen by the constants determined for p1058/A2. The estimated affinity of 20 mM, according to the kinetically determined K_d, confirms previous tetramer binding experiments that the suggested AHIII

Table 1. TCR-pMHC Binding Constants Determined by Surface Plasmon Resonance

Peptide	Sequence	Equil. K_d (μM)	ΔG (kcal/mol)	σ ΔG	k_{on} ($M^{-1}s^{-1}$)	σ k_{on}	k_{off} (s^{-1})	σ k_{off}	$t_{1/2}$ (s)
p1049	ALWGFFPVL	9.0	-6.88		30000		0.270		2.57
p1049(A1G)	**G**LWGFFPVL	24.0	-6.30	0.04	30653	8766	0.710	0.17	0.98
p1049(A1F)	**F**LWGFFPVL	217.3	-5.00	0.06	20800	4689	4.647	0.38	0.15
p1049(L2A)	A**A**WGFFPVL	17.9	-6.47	0.03	39300	3100	0.707	0.02	0.98
p1049(W3F)	AL**F**GFFPVL	101.0	-5.45	0.10	14417	2766	1.440	0.08	0.48
p1049(W3L)	AL**L**GFFPVL	482.0	-4.53	0.12	5850	212	2.850	0.49	0.24
p1049(W3P)	AL**P**GFFPVL	324.0	-4.79	0.26	4839	228	1.580	0.59	0.44
p1049(G4A)	ALW**A**FFPVL	387.3	-4.66	0.13	8733	1955	3.367	0.38	0.21
p1049(F5V)	ALWG**V**FPVL	359.7	-4.75	0.30	2321	961	0.753	0.14	0.92
p1049(F5A)	ALWG**A**FPVL	698.0	-4.31	0.08	754	394	1.102	0.17	0.63
p1049(F6V)	ALWGF**V**PVL	221.0	-4.99	0.10	3847	1748	0.807	0.23	0.86
p1049(F6A)	ALWGF**A**PVL	363.7	-4.70	0.12	8186	2905	2.900	0.72	0.24
p1049(P7A)	ALWGFF**A**VL	58.4	-5.77	0.03	37307	13327	2.233	0.87	0.31
p1049(V8Y)	ALWGFFP**Y**L	42.5	-5.97	0.10	36733	3450	1.587	0.43	0.44
p1049(V8T)	ALWGFFP**T**L	12.3	-6.70	0.05	32533	2804	0.400	0.02	1.73
p1049(V8A)	ALWGFFP**A**L	1.5	-7.97	0.09	29194	1795	0.024	0.00	28.88
p1049(L9A)	ALWGFFPV**A**	15.4	-6.56	0.06	39167	1935	0.603	0.05	1.15
p1049(A1F/V8Y)	**F**LWGFFP**Y**L	950.0	-4.31	0.70	3593	4112	2.250	1.77	0.31
p1058	FAPGFFPYL	20000	-2.55	0.82	206	244	1.700	0.53	0.41
p1058(P3L)	FA**L**GFFPYL	800000	-0.11	0.02	5	1	4.150	1.06	0.17
p1058(F1A/P3W)	**A**A**W**GFFPYL	406	-4.64	0.16	3387	707	1.387	0.21	0.50
p1058(P3W/Y8V)	FA**W**GFFP**V**L	3550	-3.53	0.71	768	935	2.047	0.25	0.34

Constants were determined by fitting kinetic and equilibrium binding data shown in Figure 1 using Scrubber 2.0 software. Data from each series of peptide/A2 injections were processed and fit individually and then averaged to determine a mean value for K_d, ΔG, k_{on}, and k_{off}. Free energy was calculated using $\Delta G = -RT\ln(K_a)$. The standard deviation (σ) from each mean is listed. Half-life is calculated as $t_{1/2} = (\ln 2)/k_{off}$. The calculated kinetic affinity was within 5% of the equilibrium affinity for almost all experiments. Equilibrium affinities could not be determined for peptides p1058 and p1058(P3L), so kinetic K_d and ΔG is shown. Wild-type p1049 values from data in Chapter 2.

TCR binding to p1058/A2 was much weaker than p1049/A2 (Buslepp et al., 2001). Mutations made that turn p1058 into p1049 improves the affinity, as seen by p1058(P3W/Y8V)/A2 and p1058(F1A/P3W)/A2. The fact that the F1A/P3W mutation jumps to an affinity around 400 μM compared to P3W/Y8V, which stays above 1 mM, suggests that tyrosine at position 8 is tolerated by AHIII better than phenylalanine at position 1. This is further supported by the p1049 double mutant, A1F/V8Y, which has a calculated affinity of almost 1 mM.

In general mutants with lowered affinities also displayed increased off-rates. Mutations F5V and F6V, however, have only a slight increase in off-rate considering the determined affinities are greater than 300 μM and 200 μM, respectively. Similarly, mutants with decreased affinity also had slower on-rates, as shown by both p1049 and p1058 variants. The increased time required to bind these altered peptide ligands might reflect some conformational change that must occur prior to TCR-pMHC binding.

3.4.2 Peptide-MHC Binding

It is important to verify that the changes reflected in the binding constants determined by surface plasmon resonance (SPR) for all altered peptide ligands are due to differences in TCR-pMHC binding and not peptide-MHC binding. Interpretation of the SPR data assumes that mutations in the peptide do not affect peptide-MHC binding. To evaluate if the peptide mutations have any affect on peptide-MHC binding, we determined the peptide-MHC binding constants by measuring the pMHC complex stability on the surface of T2 cells. T2 cells express high levels of surface class I HLA-A2, yet are TAP deficient, which inhibits peptide-loading into the MHC while in the endoplasmic reticulum (Salter et al., 1985). MHC without a peptide is very unstable and

(a)

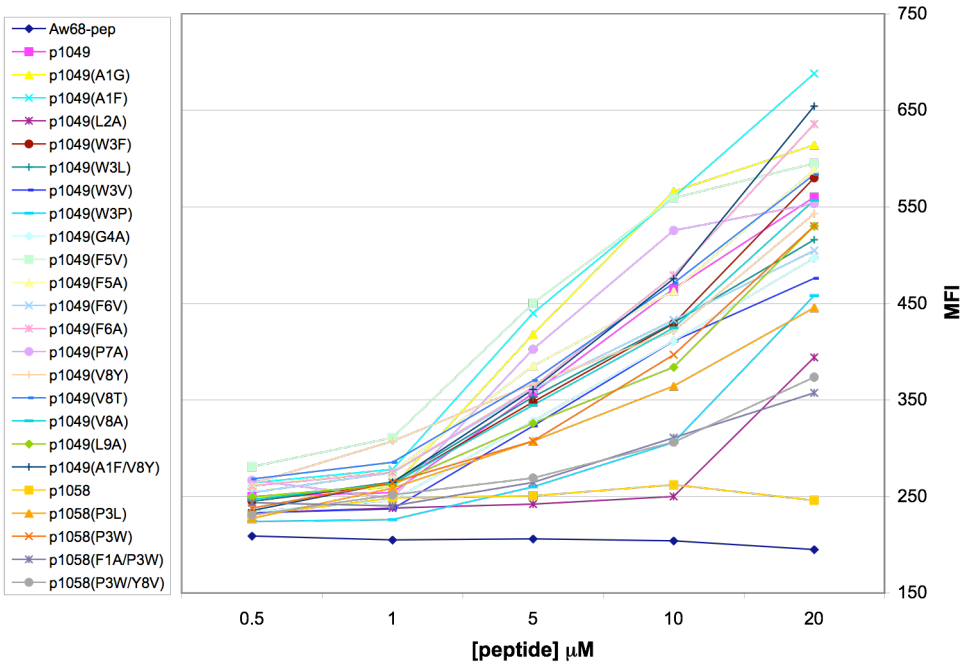

(b)

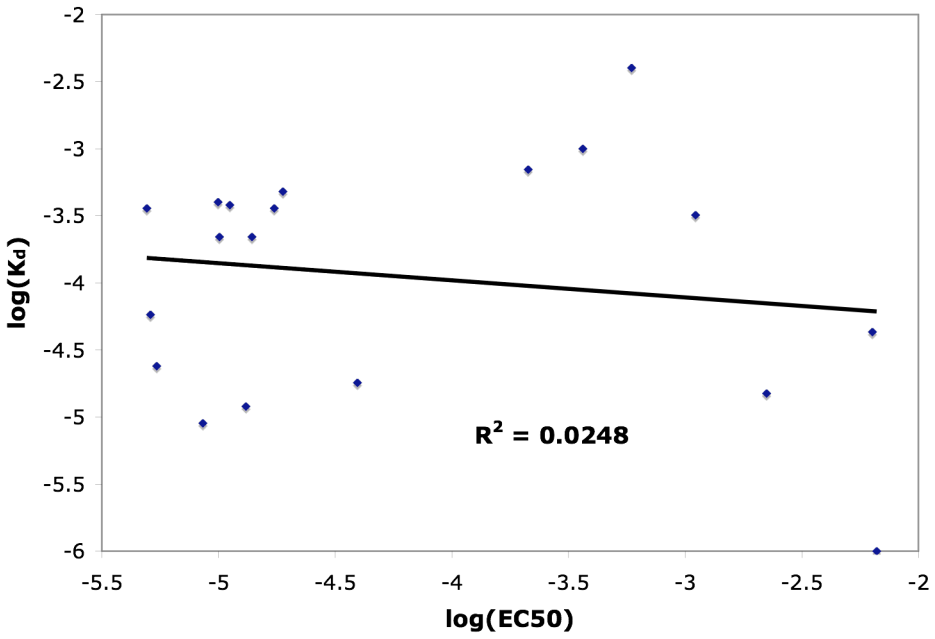

Figure 2. TCR-pMHC binding does not correlate with peptide binding to HLA-A2. (a) A2 expressing T2 cells were incubated overnight with peptide variants at various concentrations, and were stained with BB7.2 and analyzed flow cytometry. A peptide that binds Aw68 but not A2 was used as a negative control. (b) A scattergram of calculated EC50 for each peptide-A2 versus the determined AHIII-peptide/A2 affinities shows the lack of correlation ($R^2 = 0.025$).

surface half-lives are very short. By using T2 cells we can load peptide exogenously and study the stability of the peptide-A2 complex of any peptide.

All peptides listed in Table 1 were incubated with T2 cells and surface peptide-A2 levels were evaluated using flow cytometry. The tighter the peptide-MHC interaction, the more stable surface A2 will be, and the resulting mean fluorescence intensity (MFI) will be higher. Peptide titration curves are presented in Figure 2a. An influenza peptide, np91(G3F) (KTFGPIYKR), that binds to the HLA-Aw68 MHC (Collins et al., 1999) but not A2, was used as a negative control and provides a MFI baseline of approximately 200. The weakest binding peptide was p1058. This is not too surprising as two out of three MHC anchor residues for A2 (reviewed in section 1.2.2) are not ideal in p1058 (Ala at position 2 and Pro at position 3). These two mutations in p1049 (L2A and W3P) also drastically affect p1049 binding to A2, bringing their MFIs close to those of p1058 (Figure 2a).

An EC50 for each peptide titration curve was determined by fitting the data to an equilibrium binding curve (data not shown). The EC50 is effectively the peptide-MHC binding affinity. The determined EC50 for each peptide was plotted against the TCR-pMHC binding affinity values listed in Table 1 (Figure 2b). With a resulting correlation coefficient of 0.025, we can confidently state that the binding constants determined by SPR for TCR-pMHC do not correlate with the ability of the peptide variants to bind to A2.

3.4.3 Structural Prediction of AHIII TCR Docking on p1058/A2

So, why is AHIII TCR binding to these peptides so greatly affected by the peptide residues at positions 1, 3, and 8? The AHIII TCR does not even contact the p1049

peptide at positions 1 and 3, and makes a single weak van der Waals contact with position 8 (Buslepp et al., 2003b). While the co-crystal structure of AHIII-p1058/A2 is unknown, the apo structure of p1058/A2 has been determined (Buslepp et al., 2001). We superimposed the p1058/A2 structure onto the complex structure of AHIII-p1049/A2 (Buslepp et al., 2003b) (Figure 3) in attempt to explain the binding data we obtained in Table 1. The structures were superimposed using the "align" feature in PyMol (DeLano, 2002) restricting the alignment to the Cα of the peptide-binding cleft of the MHC.

Overall, the structure of the A2 MHC is identical (Figure 3a). Even though the sequence of the peptides is different, primarily at the N and C termini, the peptide backbone orientation is virtually unchanged. The only difference is seen within the side chains. When we take a look at position 1 of the peptide in relation to the AHIII TCR, it becomes clear why the A1F mutation in p1049 (and F1 in p1058) is so deleterious (Figure 3b). The Cε2 and Cζ atom of phenylalanine are less than 2.4 Å from the Cα and Cβ of Ser99 on the AHIII CDR3α, as well as Cζ being 2.1 Å from the backbone oxygen of Ser99. The phenylalanine has no other rotamer options available due to the location of MHC residues, especially Trp167. This suggests that the CDR3α loop must undergo some structural rearrangement to accommodate Phe at position 1. However, this "new conformation" is not likely to be as energetically favorable, hence the decrease in affinity.

Figure 3c shows the C-terminal end of the peptides and in particular, position 8. A Tyr at position 8 in its current orientation would be too close for the CDR3β loop of AHIII to maintain the same position. However, as shown by the binding data in Table 1,

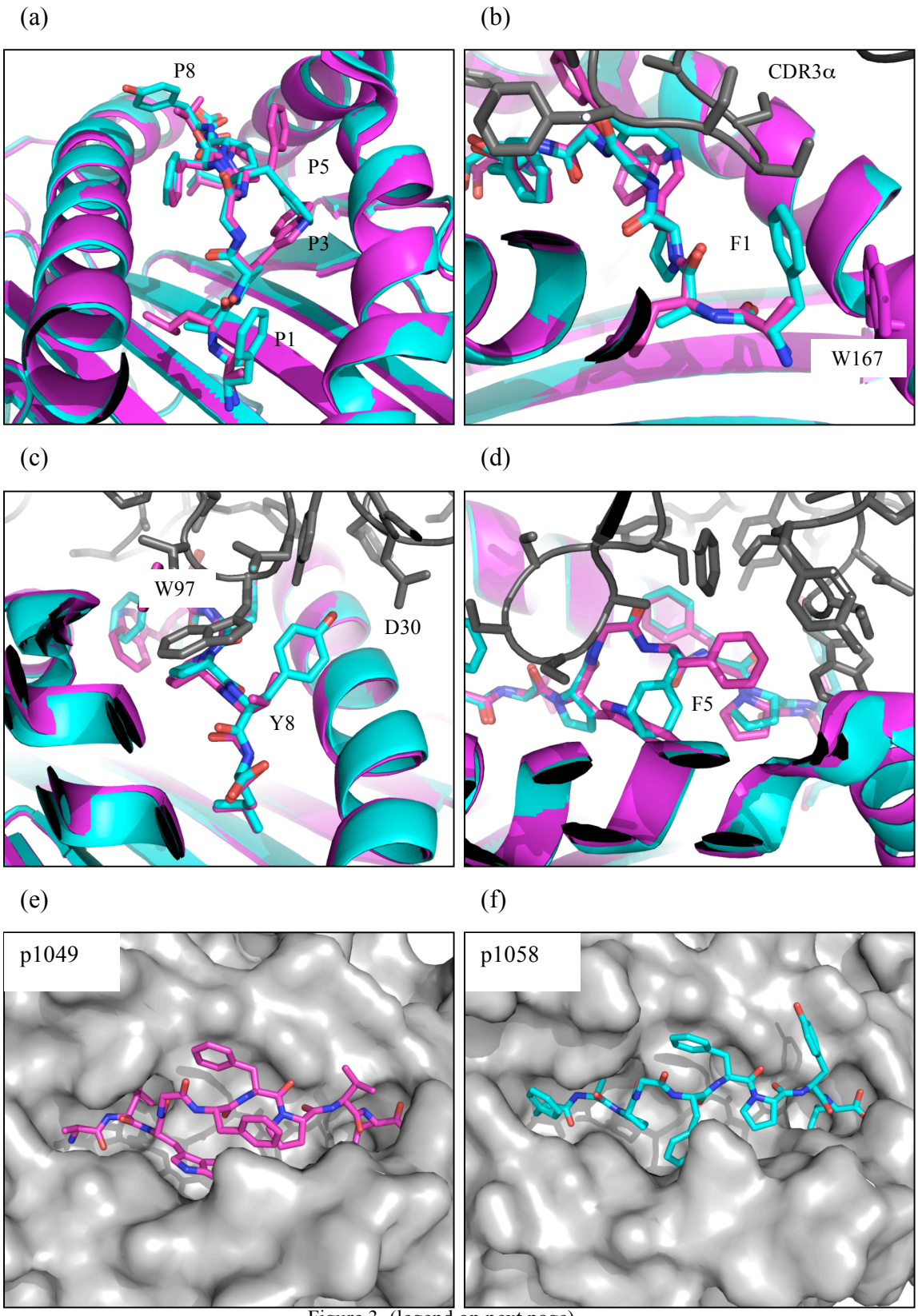

Figure 3. (legend on next page)

Figure 3. AHIII TCR cannot dock p1058/A2 in same manner as p1049/A2. The previously determined structures of p1058/A2 (cyan) alone (1I7R) is superimposed onto AHIII - p1049/A2 (magenta) complex (1LP9). (a) A2 MHC forces both peptides into same backbone conformation, difference occur only in peptide side chains. (b) Phe at position 1 (F1) of p1058 would clash with AHIII CDR3α (grey) if the TCR had the same conformation as when docked on p1049/A2. Other rotamer positions for F1 are not available due to local A2 MHC structure including W167. The CDR3α must change conformation or the TCR must dock differently. (c) The AHIII TCR as it binds p1049/A2 clashes with Tyr (Y8) of p1058. Y8 must take a different rotamer to avoid W97 of AHIII CDR3β (grey), or the TCR must bind in a different manner. (d) Phe (F5) of p1049 is involved in numerous van der Waals interactions with AHIII TCR. However, F5 of 1058 is forced to fill void left by removal of Trp at position 3, impeding interactions with the TCR. (e) Surface of A2 (grey) with p1049 shows L2, W3, and L9 filling peptide-binding pockets. F5 is available to interact with AHIII TCR. (f) Surface of A2 with p1058 clearly shows how F5 side chain is necessary to fill pocket and can no longer engage TCR. All figures were generated using PyMol (DeLano, 2002).

this residue is more easily accommodated than Phe1. This accommodation may occur through a slight movement of the CDR3β loop, the Trp97 on that loop, or perhaps a rotation about $\chi 2$ in Tyr8 itself to make a stacking interaction with Trp97. Asp30 on the CDR2β loop is also positioned close enough to provide a hydrogen-bonding partner with the hydroxyl on Tyr8 with little rearrangement. It is difficult to surmise any mechanism for the increased affinity and slower off-rate for the V8A mutation in p1049 based on the superimposition in Figure 3c.

Figure 3d helps demonstrate the critical role of F5 in p1049. It is involved in a number of van der Waals interactions with both CDR3 α and β loops. When the Trp in position 3 is removed either in p1058 (cyan) or p1049 mutants, the Phe at position 5 is recruited to fill the void, removing it from the TCR binding surface. A bulky hydrophobic residue at position 3 is critical for peptide binding to A2. Figures 3e and 3f clearly show the binding pocket filled by the Trp at position 3 in p1049 and how F5 swings down into it with p1058. This analysis suggests that a mutation placing a small side chain at position 3 simultaneously removes F5 from the TCR binding surface. Hence, the dramatic affects on binding data in Table 1 when position 3 is altered.

3.5 DISCUSSION

We present here a large body of TCR-pMHC binding data, which is the biophysical half of a larger study including biological T cell responses to these p1049 and p1058 chimeras. Previous work by Buslepp et al. suggested that mutations turning p1049 into p1058 made the peptide less and less of an agonist until it became antagonistic (Buslepp et al., 2001). That work included only a T cell lysis assay and an estimation of AHIII-peptide/A2 binding using pMHC tetramer. Here we have directly measured the affinity and the kinetics of the AHIII TCR binding to an extended panel of p1049 and p1058 variants presented in A2 using surface plasmon resonance (SPR). There seems to be a general correlation between low affinity binding and those peptides previously defined as antagonistic. However, it is still unclear how the antagonism is manifest by signaling inside the cell.

Peptide binding to various MHC allotypes including HLA-A2 has been studied extensively (reviewed in section 1.2). Each MHC allotype has unique binding pockets that prefer certain peptide side chains. For peptides binding to A2 the primary anchor residues occur at P2 and P9, with secondary anchors at P1, P3, and P7. P3 needs to be a large aromatic side chain to fill the large C-pocket in A2 (Falk et al., 1991; Ruppert et al., 1993). As we saw from our SPR experiments mutations at P1, P2, P3, P7, and P9 all had affects on AHIII-peptide/A2 binding. To ensure that the change in binding constants were only due to the effect the mutation had on the AHIII TCR binding and not due to the peptide binding to HLA-A2, we evaluated the ability of each peptide variant to bind A2. We found that p1049 variants at P1, P7, and P9 had no effect on the peptide binding to A2. Mutations at P2 and P3 were somewhat deleterious on peptide-A2 binding, but

binding of those mutants was still much stronger than the control peptide. The mean fluorescence intensities at varying concentrations allowed us to determine an EC50 for each peptide. Plotting these against the calculated AHIII-peptide/MHC affinities determined by SPR showed that there is no correlation between them. Therefore, we are confident that our binding constants presented in Table 1 represent the effect of the mutations on the AHIII TCR binding.

The crystal structure of p1058/A2 had been previously determined (Buslepp et al., 2001) in an effort to explain the antagonistic effects of the 1058 peptide presented in A2. However, as this was before the co-crystal structure of AHIII-p1049/A2 (Buslepp et al., 2003b) had been determined, it was difficult to interpret the consequences of changes seen in the p1058/A2 structure. As part of this body of work, we superimposed the structure of p1058/A2 onto the complex of AHIII-p1049/A2, and were able to get a much clearer idea of the impact that p1058 and p1049 variants have on the AHIII TCR upon binding. Peptide positions 1 and 3 in p1058 are particularly deleterious. Phe at position 1 cannot be accommodated by the AHIII TCR is its p1049/A2 conformation. Altering the Trp at position 3 also has the unexpected consequence of a compensatory movement of the Phe at position 5 to fill the pocket, thus removing it from the TCR binding surface. F5 is critical, as it makes a number of hydrophobic contacts to the CDR3 loops of both the TCR alpha and beta chains.

The only other structural study comparing a TCR docking on an agonist peptide/MHC versus two different antagonist peptide/MHC found no differences in the TCR between the two co-crystal structures in one, and a small change in the CDR3β loop of A6 in the other (Ding et al., 1999). Our analysis presented above suggests that a

conformational change or alternate docking mode is required for AHIII binding to p1058/A2 and to some of the "p1058-like" p1049 variants. However, we do not suggest that the conformational change has anything to do with T cell signaling, but more to do with CDR loop movements affecting binding. The requirement for a conformational change is further supported by slower on-rates determined for these peptides. A conformational change in the TCR required for binding has certainly been seen before for other TCR binding even their agonistic cognate peptide/MHC (Degano et al., 2000; Garcia et al., 1998; Kjer-Nielsen et al., 2003; Reiser et al., 2002), and movement has also been seen in the peptide itself (Tynan et al., 2007). However, without determining the co-crystal structure of AHIII-p1058/A2, it is impossible to be certain where the conformational change occurs.

The molecular events occurring upon substitution at position 8 of the peptides is also very interesting, and unfortunately not much information can be gleaned from the superimposed structures above. Exactly how does the V8A mutation in p1049 make the TCR-pMHC interaction so stable? As a continuation of this project, attempts at co-crystallization of the AHIII TCR bound to p1049(V8A)/A2 are underway. As this complex has a higher affinity and longer half-life than any other AHIII-p1409/A2 interaction measured, we are confident that we will be able to co-crystallize these molecules and determined the structure using molecular replacement. Aside from the crystal structure, isothermal titration calorimetry (ITC) will be used to evaluate changes to the enthalpy and entropy of binding in AHIII-p1049(V8A)/A2. We have previously used ITC to verify the loss of H-bonds upon the K66A mutation in A2 (see Chapter 2) (Miller et al., 2007). Even without the co-crystal structure, changes in ΔH and ΔS

between the wild-type complex and the V8A mutant will provide energetic details about how the AHIII-p1049(V8A)/A2 interaction achieves such tight binding and slow off-rate. Performing ITC or SPR experiments at various temperatures allows for the determination of the change in heat capacity (ΔC_p) upon binding, which has been used as a means to estimate conformational change taking place upon TCR-pMHC binding (Anikeeva et al., 2003; Armstrong and Baker, 2007; Boulter et al., 2007; Ely et al., 2006; Garcia et al., 2001; Krogsgaard et al., 2003; Lee et al., 2004; Mazza et al., 2007). As there is still no crystal structure of the AHIII TCR alone, determining the ΔC_p of AHIII binding to p1049/A2 and some p1049/A2 mutants including p1049(V8A) may provide more insight into the degree of conformational change that occurs.

The results presented in this chapter may also suggest something interesting regarding how the CDR loops are involved in AHIII-p1049/A2 molecular recognition. Chapter 2 focused on mutations made in the TCR binding surface of the A2 MHC and their effect on the TCR. While SPR data was presented for only three MHC mutants, data had been collected for an entire panel of MHC mutants. The A2(K66A) mutant had the worst binding affinity to the AHIII TCR of any of the mutants. We showed that the K66A mutation resulted in a conformational change in the CDR3α loop, eliminated a number of hydrogen bonds. Yet, the determined TCR-pMHC dissociation constant (K_d) was still approximately 30 μM. The data presented in this chapter involve mutations made in the peptides presented by A2. All the mutations to peptide residues between position 3 and position 7 result in binding affinities worse than that of the K66A mutation in A2. Any amino acid substitution at P3 through P6 results in a K_d of greater than 100 μM. This says that the contacts made between the AHIII TCR CDR3 loops and the

p1049 peptide are more critical than the contacts made to the A2 MHC. While the entire pMHC surface is recognized by the CDR loops of TCR, the discriminatory power of the TCR between agonist and antagonist comes from the interaction of CDR3 loops with the peptide.

As mentioned above, the work presented here will be combined with biological data looking at the T cell response to these same peptides presented in A2. T cell proliferation, cytokine secretion, and T cell killing will all be evaluated and correlated with the binding constants presented here. Importantly, the experiments involving these biological assays will done using AHIII T cells from the AHIII12.2 transgenic mouse recently generated by our collaborators in the laboratory of Dr. Ettore Appella at the NIH (Bethesda, MD). This has the advantage of having naïve AHIII T cells, and being able to use them directly *ex vivo* for functional experiments, providing a better measure of what might be occurring *in vivo*. Previous studies evaluating the biological outcome of AHIII T cells (Buslepp et al., 2003a; Buslepp et al., 2001; Loftus et al., 1997; Miller et al., 2007) used immortalized AHIII T cell lines coming form the original AHIII12.2 clone discovered in 1987 (Bernhard et al., 1987). These cells have been passaged for weeks, if not months at a time, continually being *in vitro* stimulated with irradiated splenocytes, and, of course, frozen and thawed. While they have provided information in the past, it is ideal to start with naïve T cells directly from the mouse.

This will be the most comprehensive analysis of TCR-pMHC binding and resultant T cell activation to date; over 20 different peptides evaluated using SPR and three separate aspects of T cell activation. Based on previously published (Chapter 2) (Buslepp et al., 2001; Miller et al., 2007) and preliminary data, we expect to see CTL

killing with p1049 and its variants the correlate with affinity. The antagonistic ability of p1058 should also increase as affinity decreases. As antagonistic peptides have been shown to have a differential cytokine profile of decreased IL-2 production, but normal IFNγ secretion (Schwartz, 2003), we expect to see this profile for p1058. Similarly, we expect no proliferation of AHIII T cells exposed to antagonist peptides.

3.6 REFERENCES

Alam S. M., Travers P. J., Wung J. L., Nasholds W., Redpath S., Jameson S. C. and Gascoigne N. R. (1996) T-cell-receptor affinity and thymocyte positive selection. *Nature* **381**, 616-20.

Anikeeva N., Lebedeva T., Krogsgaard M., Tetin S. Y., Martinez-Hackert E., Kalams S. A., Davis M. M. and Sykulev Y. (2003) Distinct molecular mechanisms account for the specificity of two different T-cell receptors. *Biochemistry* **42**, 4709-16.

Armstrong K. M. and Baker B. M. (2007) A comprehensive calorimetric investigation of an entropically driven T cell receptor-peptide/major histocompatibility complex interaction. *Biophys J* **93**, 597-609.

Armstrong K. M., Insaidoo F. K. and Baker B. M. (2008) Thermodynamics of T-cell receptor-peptide/MHC interactions: progress and opportunities. *J Mol Recognit* **21**, 275-287.

Baker B. M., Gagnon S. J., Biddison W. E. and Wiley D. C. (2000) Conversion of a T cell antagonist into an agonist by repairing a defect in the TCR/peptide/MHC interface: implications for TCR signaling. *Immunity* **13**, 475-84.

Bernhard E. J., Le A. X., Yannelli J. R., Holterman M. J., Hogan K. T., Parham P. and Engelhard V. H. (1987) The ability of cytotoxic T cells to recognize HLA-A2.1 or HLA-B7 antigens expressed on murine cells correlates with their epitope specificity. *J Immunol* **139**, 3614-21.

Bongrand P. and Malissen B. (1998) Quantitative aspects of T-cell recognition: from within the antigen-presenting cell to within the T cell. *Bioessays* **20**, 412-22.

Boulter J. M., Schmitz N., Sewell A. K., Godkin A. J., Bachmann M. F. and Gallimore A. M. (2007) Potent T cell agonism mediated by a very rapid TCR/pMHC interaction. *Eur J Immunol* **37**, 798-806.

Buslepp J., Kerry S. E., Loftus D., Frelinger J. A., Appella E. and Collins E. J. (2003a) High affinity xenoreactive TCR:MHC interaction recruits CD8 in absence of binding to MHC. *J Immunol* **170**, 373-83.

Buslepp J., Wang H., Biddison W. E., Appella E. and Collins E. J. (2003b) A correlation between TCR Valpha docking on MHC and CD8 dependence: implications for T cell selection. *Immunity* **19**, 595-606.

Buslepp J., Zhao R., Donnini D., Loftus D., Saad M., Appella E. and Collins E. J. (2001) T cell activity correlates with oligomeric peptide-major histocompatibility complex binding on T cell surface. *J Biol Chem* **276**, 47320-8.

Chen Y. Z., Lai Z. F., Nishi K. and Nishimura Y. (1998) Modulation of calcium responses by altered peptide ligands in a human T cell clone. *Eur J Immunol* **28**, 3929-39.

Collins E. J., Booth B. L., Jr. and Cerundolo V. (1999) Extensive alanine substitutions increase binding affinity of an influenza nucleoprotein peptide to HLA-Aw68 and do not abrogate peptide-specific CTL recognition. *J Immunol* **162**, 331-7.

Degano M., Garcia K. C., Apostolopoulos V., Rudolph M. G., Teyton L. and Wilson I. A. (2000) A functional hot spot for antigen recognition in a superagonist TCR/MHC complex. *Immunity* **12**, 251-61.

DeLano W. L. (2002) The PyMOL Molecular Graphics System. DeLano Scientific, San Carlos, CA, USA.

Ding Y. H., Baker B. M., Garboczi D. N., Biddison W. E. and Wiley D. C. (1999) Four A6-TCR/peptide/HLA-A2 structures that generate very different T cell signals are nearly identical. *Immunity* **11**, 45-56.

Ely L. K., Beddoe T., Clements C. S., Matthews J. M., Purcell A. W., Kjer-Nielsen L., McCluskey J. and Rossjohn J. (2006) Disparate thermodynamics governing T cell receptor-MHC-I interactions implicate extrinsic factors in guiding MHC restriction. *Proc Natl Acad Sci U S A* **103**, 6641-6.

Falk K., Rotzschke O., Stevanovic S., Jung G. and Rammensee H. G. (1991) Allele-specific motifs revealed by sequencing of self-peptides eluted from MHC molecules. *Nature* **351**, 290-6.

Garboczi D. N., Hung D. T. and Wiley D. C. (1992) HLA-A2-peptide complexes: refolding and crystallization of molecules expressed in Escherichia coli and complexed with single antigenic peptides. *Proc Natl Acad Sci U S A* **89**, 3429-33.

Garcia K. C., Degano M., Pease L. R., Huang M., Peterson P. A., Teyton L. and Wilson I. A. (1998) Structural basis of plasticity in T cell receptor recognition of a self peptide-MHC antigen. *Science* **279**, 1166-72.

Garcia K. C., Radu C. G., Ho J., Ober R. J. and Ward E. S. (2001) Kinetics and thermodynamics of T cell receptor- autoantigen interactions in murine experimental autoimmune encephalomyelitis. *Proc Natl Acad Sci U S A* **98**, 6818-23.

Garcia-Peydro M., Paradela A., Albar J. P. and Castro J. A. (2000) Antagonism of direct alloreactivity of an HLA-B27-specific CTL clone by altered peptide ligands of its natural epitope. *J Immunol* **165**, 5680-5.

Henderson R. A., Cox A. L., Sakaguchi K., Appella E., Shabanowitz J., Hunt D. F. and Engelhard V. H. (1993) Direct identification of an endogenous peptide recognized by multiple HLA-A2.1-specific cytotoxic T cells. *Proc Natl Acad Sci U S A* **90**, 10275-9.

Holler P. D. and Kranz D. M. (2003) Quantitative analysis of the contribution of TCR/pepMHC affinity and CD8 to T cell activation. *Immunity* **18**, 255-64.

Kersh G. J., Kersh E. N., Fremont D. H. and Allen P. M. (1998) High- and low-potency ligands with similar affinities for the TCR: the importance of kinetics in TCR signaling. *Immunity* **9**, 817-26.

Kjer-Nielsen L., Clements C. S., Purcell A. W., Brooks A. G., Whisstock J. C., Burrows S. R., McCluskey J. and Rossjohn J. (2003) A structural basis for the selection of dominant alphabeta T cell receptors in antiviral immunity. *Immunity* **18**, 53-64.

Krogsgaard M., Prado N., Adams E. J., He X. L., Chow D. C., Wilson D. B., Garcia K. C. and Davis M. M. (2003) Evidence that structural rearrangements and/or flexibility during TCR binding can contribute to T cell activation. *Mol Cell* **12**, 1367-78.

Kuhns J. J., Batalia M. A., Yan S. and Collins E. J. (1999) Poor binding of a HER-2/neu epitope (GP2) to HLA-A2.1 is due to a lack of interactions with the center of the peptide. *J Biol Chem* **274**, 36422-7.

Lanzavecchia A., Lezzi G. and Viola A. (1999) From TCR engagement to T cell activation: a kinetic view of T cell behavior. *Cell* **96**, 1-4.

Lau L. L., Jiang J. and Shen H. (2005) In vivo modulation of T cell responses and protective immunity by TCR antagonism during infection. *J Immunol* **174**, 7970-6.

Lee J. K., Stewart-Jones G., Dong T., Harlos K., Di Gleria K., Dorrell L., Douek D. C., van der Merwe P. A., Jones E. Y. and McMichael A. J. (2004) T cell cross-reactivity and conformational changes during TCR engagement. *J Exp Med* **200**, 1455-66.

Loftus D. J., Chen Y., Covell D. G., Engelhard V. H. and Appella E. (1997) Differential contact of disparate class I/peptide complexes as the basis for epitope cross-recognition by a single T cell receptor. *J Immunol* **158**, 3651-8.

Lyons D. S., Lieberman S. A., Hampl J., Boniface J. J., Chien Y., Berg L. J. and Davis M. M. (1996) A TCR binds to antagonist ligands with lower affinities and faster dissociation rates than to agonists. *Immunity* **5**, 53-61.

Madrenas J. and Germain R. N. (1996) Variant TCR ligands: new insights into the molecular basis of antigen-dependent signal transduction and T-cell activation. *Semin Immunol* **8**, 83-101.

Matsui K., Boniface J. J., Steffner P., Reay P. A. and Davis M. M. (1994) Kinetics of T-cell receptor binding to peptide/I-Ek complexes: correlation of the dissociation rate with T-cell responsiveness. *Proc Natl Acad Sci U S A* **91**, 12862-6.

Mazza C., Auphan-Anezin N., Gregoire C., Guimezanes A., Kellenberger C., Roussel A., Kearney A., van der Merwe P. A., Schmitt-Verhulst A. M. and Malissen B. (2007) How much can a T-cell antigen receptor adapt to structurally distinct antigenic peptides? *EMBO J* **26**, 1972-83.

McKeithan T. W. (1995) Kinetic proofreading in T-cell receptor signal transduction. *Proc Natl Acad Sci U S A* **92**, 5042-6.

Miller P. J., Pazy Y., Conti B., Riddle D., Appella E. and Collins E. J. (2007) Single MHC mutation eliminates enthalpy associated with T cell receptor binding. *J Mol Biol* **373**, 315-27.

Rabinowitz J. D., Beeson C., Lyons D. S., Davis M. M. and McConnell H. M. (1996) Kinetic discrimination in T-cell activation. *Proc Natl Acad Sci U S A* **93**, 1401-5.

Reis e Sousa C., Levine E. H. and Germain R. N. (1996) Partial signaling by CD8+ T cells in response to antagonist ligands. *J Exp Med* **184**, 149-57.

Reiser J. B., Gregoire C., Darnault C., Mosser T., Guimezanes A., Schmitt-Verhulst A. M., Fontecilla-Camps J. C., Mazza G., Malissen B. and Housset D. (2002) A T cell receptor CDR3beta loop undergoes conformational changes of unprecedented magnitude upon binding to a peptide/MHC class I complex. *Immunity* **16**, 345-54.

Rosette C., Werlen G., Daniels M. A., Holman P. O., Alam S. M., Travers P. J., Gascoigne N. R., Palmer E. and Jameson S. C. (2001) The impact of duration versus extent of TCR occupancy on T cell activation: a revision of the kinetic proofreading model. *Immunity* **15**, 59-70.

Rudolph M. G., Stanfield R. L. and Wilson I. A. (2006) How TCRs bind MHCs, peptides, and coreceptors. *Annu Rev Immunol* **24**, 419-66.

Ruppert J., Sidney J., Celis E., Kubo R. T., Grey H. M. and Sette A. (1993) Prominent role of secondary anchor residues in peptide binding to HLA-A2.1 molecules. *Cell* **74**, 929-37.

Salter R. D., Howell D. N. and Cresswell P. (1985) Genes regulating HLA class I antigen expression in T-B lymphoblast hybrids. *Immunogenetics* **21**, 235-46.

Schodin B. A., Tsomides T. J. and Kranz D. M. (1996) Correlation between the number of T cell receptors required for T cell activation and TCR-ligand affinity. *Immunity* **5**, 137-46.

Schwartz R. H. (2003) T cell anergy. *Annu Rev Immunol* **21**, 305-34.

Sloan-Lancaster J., Evavold B. D. and Allen P. M. (1993) Induction of T-cell anergy by altered T-cell-receptor ligand on live antigen-presenting cells. *Nature* **363**, 156-9.

Sykulev Y., Brunmark A., Jackson M., Cohen R. J., Peterson P. A. and Eisen H. N. (1994) Kinetics and affinity of reactions between an antigen-specific T cell receptor and peptide-MHC complexes. *Immunity* **1**, 15-22.

Sykulev Y., Vugmeyster Y., Brunmark A., Ploegh H. L. and Eisen H. N. (1998) Peptide antagonism and T cell receptor interactions with peptide-MHC complexes. *Immunity* **9**, 475-83.

Tian S., Maile R., Collins E. J. and Frelinger J. A. (2007) CD8+ T cell activation is governed by TCR-peptide/MHC affinity, not dissociation rate. *J Immunol* **179**, 2952-60.

Tynan F. E., Reid H. H., Kjer-Nielsen L., Miles J. J., Wilce M. C., Kostenko L., Borg N. A., Williamson N. A., Beddoe T., Purcell A. W., Burrows S. R., McCluskey J. and Rossjohn J. (2007) A T cell receptor flattens a bulged antigenic peptide presented by a major histocompatibility complex class I molecule. *Nat Immunol* **8**, 268-76.

Uhlin M., Masucci M. and Levitsky V. (2006) Is the activity of partially agonistic MHC:peptide ligands dependent on the quality of immunological help? *Scand J Immunol* **64**, 581-7.

Valitutti S., Muller S., Cella M., Padovan E. and Lanzavecchia A. (1995) Serial triggering of many T-cell receptors by a few peptide-MHC complexes. *Nature* **375**, 148-51.

Vukmanovic S., Neubert T. A. and Santori F. R. (2003) Could TCR antagonism explain associations between MHC genes and disease? *Trends Mol Med* **9**, 139-46.

CHAPTER 4

Rapid Production of Soluble Recombinant TCR from Singly Isolated T cells

4.1 ABSTRACT

Cytotoxic T cell (CTL) response to self and non-self peptides presented in the context of the MHC molecule (pMHC) relies on the molecular recognition of those pMHC ligands by the T cell receptor (TCR). After years of study it is still unclear exactly how the TCR can discriminate between self and non-self. There are an estimated 10^8 clonal T cells in the body, each with a unique TCR, but most of what we know about TCR-pMHC binding is based on the study of only two dozen T cell receptors. The paucity of TCRs studied may be due to the fact that the task of isolating a T cell specific for a particular pMHC target, determing the DNA sequences of its αβTCR, and recombinantly expressing its TCR for *in vitro* study, is technically arduous and time consuming, taking months to years. To be able to answer fundamental questions about TCR-pMHC recognition that still exist, and identify and produce TCR that could be used as potential therapeutics, the rate of TCR identification and production needs to increase. We present here a TCR production scheme that allows for the production of soluble, recombinant TCR from singly isolated T cells in less than two months.

4.2 INTRODUCTION

Cytotoxic T lymphocytes (CTL), or $CD8^+$ T cells, are a critical component of the adaptive immune response to infection. They are required for the elimination of infected host cells, which are harboring virus or intracellular bacteria. The critical step required for T cell activation is the recognition of peptides derived from these pathogens when presented by the Major Histocompatibility Complex (MHC) molecule. Recognition of foreign peptide, or antigen, bound to MHC is achieved through the clonotypic T cell receptor (TCR). Upon TCR recognition of a peptide bound to MHC (pMHC) cytotoxic T cells kill the antigen presenting cell, thereby eliminating the means for pathogen replication. Recognition of pMHC by the TCR heterodimer is accomplished using the three complementarity determining region (CDR) loops from each chain. The CDR1 and CDR2 loops are germ-line encoded within the variable gene segment of each TCRα and TCRβ chain. The CDR3 loop of each chain is unique and arises through V(D)J recombination (Schatz and Spanopoulou, 2005; Spicuglia et al., 2006). While recognition of the pMHC is carried out using all the CDR loops of each chain, generally the CDR3 makes more contacts with the bound peptide than CDR1 and CDR2 (Rudolph et al., 2006).

Considering the immense number of T cells generated in the body and the subsequent unique clonal TCR on those T cells (estimated 10^8), relatively few clones have been isolated for study. Only 23 unique TCR have been studied structurally (presented in Chapter 1). All the models we have regarding TCR-pMHC engagement and subsequent T cell activation, or inactivation, rely in some way on these few structures. Fundamental questions surrounding TCR-pMHC interactions still exist, such

as: how a TCR discriminates between a self and non-self pMHC ligand, whether conserved TCR-pMHC contacts exist, and why the TCR seems to dock all pMHC molecules in a canonical diagonal orientation. To accurately answer these questions a greater number of structural studies involving new and disparate TCR are required. Clinically, isolation of a T cell clone specific for an antigenic peptide-MHC followed by rapid production and purification of that TCR is essential to realistically use recombinant TCR for diagnostic or therapeutic purposes (Abad et al., 2008; Johnson et al., 2006; Zhao et al., 2007).

Traditionally, T cell clones are isolated using multiple rounds of limiting dilution followed by clonal expansion (Engelhard and Benjamin, 1982). This techniques has two drawbacks: 1) it takes months and consumes lots of money for reagents, media, and cells for *in vitro* stimulation; 2) the population of T cells that actually survive and can grow under these conditions may not be a good representation of the original T cell population. Once the T cell of interest is selected to acceptable clonality, its αβTCR genes can be determined. Then these genes must be placed into a suitable expression system, which is another major technically challenging, time consuming step. Production in mammalian expression systems, are traditionally expensive and do not produce the quantities of protein necessary for biophysical and structural studies. Expression in *E. coli* is generally easier and more cost effective, but soluble expression again usually does not produce gram quantities of protein. Expressing proteins as inclusion bodies allows for gram quantities, but then *in vitro* folding conditions and subsequent purification steps still need to be worked out. We, therefore, sought to design a system to rapidly go from mouse to recombinant TCR production for TCR-pMHC studies or clinical applications.

In order to make recombinant TCR we must first obtain the nucleotide sequence of the V, D (for β chain), and J gene segments, which encode the TCR α and β chains. Single cell reverse transcription polymerase chain reaction (RT-PCR) has been used previously to identify alpha and beta variable gene usage, as well as specific CDR loop sequences of TCR to analyze the repertoire present in specific diseases (Baker et al., 2002; Wong et al., 2006; Wong et al., 2007). Using single cell RT-PCR we developed a strategy to generate TCR variable gene segments that could be quickly subcloned into an *E. coli* expression vector.

To obtain the large quantities of protein necessary for structural biology and many other biophysical analyses, many laboratories, including ours, employ *in vitro* folding of proteins produced as inclusion bodies in *E. coli*. Inclusion bodies are aggregated, insoluble proteins commonly formed upon over-expression of recombinant proteins in *E. coli*. Once isolated and purified these inclusion body proteins can be solublized and folded *in vitro*. As every protein has a unique amino acid sequence and unique three dimensional surface characteristics, each protein may require a unique *in vitro* folding condition in order to "find" its native fold (reviewed in (Rudolph and Lilie, 1996).

The methods presented here are the result of our goal to develop a streamlined protocol to isolate T cells specific for one particular pMHC, determine the DNA sequences of the TCR α and β chains from those T cells, and generate soluble TCR *in vitro* from those T cells to use for structural, biochemical, and biophysical study. We used molecules on which we currently work as our models for assay development, specifically H-2K^{b} MHC and the AHIII12.2 TCR. We describe a TCR production scheme involving single-cell sorting of T cells, amplification of the TCR variable

domains, recombinant expression of the TCR chains in *E. coli*, and a means of testing successful *in vitro* folding using a novel folding screen and a pMHC-tetramer based ELISA.

4.3 MATERIALS AND METHODS

4.3.1 Expression Optimization of H-2K^b and Tetramer Production

Peptide/MHC-tetramers are necessary to stain and sort pMHC specific T cells. In order to sort H-2K^b (K^b) specific TCR in the future, it was essential that we had a stock of K^b MHC inclusion bodies ready for *in vitro* folding. Initial expression of K^b heavy chain in BL21-RIL *E. coli* (Stratagene) was poor. Analysis of the heavy chain nucleotide sequence revealed a number of codons that were not used in *E. coli* as well as possible high-energy hairpins in the resulting mRNA transcript. We optimized the codon usage for *E. coli* expression, and rebuilt the gene using two oligos with overlapping sequence, which were spliced together using Klenow. The forward K^b oligo has the sequence of 5′-GAATTCAGGAGGAATTTAAAAATGGGTCCACACTCTCTGCGTTACTTCGTTACTGCTGTT-3′ and a reverse primer of 5′-AAGCAATGACGACAAAGAGCAGGCCCGGACCCACTCGGCGCAATGTAC CTTCAGCCGATG-3′ (Invitrogen). This new segment consisting of the first 84 base-pairs of the gene was then spliced with the remaining portion of the K^b heavy chain using PCR. The final K^b heavy chain was then subcloned into the inducible pLM1 expression vector (Zhao et al., 1999). To facilitate tetramer formation the K^b heavy chain contains a 3' biotinylation sequence (GLNDIFEAQKIEWHE) recognized by BirA enzyme (Avidity, LLC). Test expressions were performed and the best K^b heavy chain expressing clone was selected for scale-up. Heavy chain and β_2m were recombinantly expressed in *E. coli*

as inclusion bodies, purified, and folded *in vitro* as previously described in Chapter 2 (Miller et al., 2007). Peptides were provided by the University of North Carolina Peptide Synthesis Facility (Chapel Hill, NC). Folded and purified K^b monomer was then biotinylated using BirA enzyme (Avidity, LLC) following the manufacturer's protocol. Biotinylated pMHC can then be mixed with streptavidin conjugated with a variety of fluorophores or enzymes to create pMHC-tetramers for flow cytometry or ELISA.

4.3.2 Isolation of T cells

Spleens and lymph nodes from mice were harvested and cells were kept separate thru sorting. Ideally cells are sorted directly *ex vivo*. In preparation for fluorescence-activated cell sorted (FACS), splenocytes and lymphocytes were treated with Fc block (2.4G2 supernatant), stained using a cocktail of CD19-PE-Cy7, CD11b-PE-Cy7, CD11c-PE-Cy7, NK1.1-PE-Cy7, CD4-PacOrange, and pMHC-tetramer-APC, followed by a PBS wash step. Staining with this cocktail allowed for $CD19^+$ (B cells), $CD11b^+$, $CD11c^+$ (Dendritic cells, macrophages, and other leukocytes), and $NK1.1^+$ (NK cells) to be shuttled directly to waste. $CD4^+$ cells (helper T cells) were gated out as well. Single T cells (pMHC-tetramer-positive, CD4-negative) were FACS sorted on a Dako MoFlo (Beckman Coulter) at the University of North Carolina Flow Cytometry Core Facility into 96 well PCR plates containing lysis buffer consisting of RT/PCR reaction mix (Invitrogen), PBS, nuclease-free water, 100 mM DTT, and RNAse OUT (Invitrogen). Plates were immediately covered with adhesive sealing foil (Research Products International) and stored at -80 °C.

4.3.3 Single-cell PCR

TCR variable gene sequences were determined by methods previously described (Baker et al., 2002; Riddle et al., 2008; Wong et al., 2006; Wong et al., 2007) with the following changes. To each of the 96 wells described above, a cocktail containing Cα and Cβ primers and Super Script II Reverse Transcriptase (Invitrogen) was added. All primers were purchased through Invitrogen. The Reverse Transcription (RT) PCR reaction was carried out following the manufacturer's protocol. The resulting cDNA was divided into two new 96 well PCR plates for the external and nested PCR to obtain the sequence of the TCR α and β chain variable regions. A panel of external and internal primers specific for all murine TCR α and β chain variable regions were used along with the Cα and Cβ primers and Taq polymerase. Wells were inactivated with exonuclease I and shrimp alkaline phosphatase and then sequenced at the University of North Carolina Genome Analysis Facility (Chapel Hill, NC).

Variable gene sequences obtained were then trimmed and aligned against a basic database of variable (V) genes, J segments, and constant domains for both α and β chain of the TCR using Sequencher 4.5 (Gene Codes Corp.). These "cleaned" sequences were then analyzed using V-QUEST (Giudicelli et al., 2004) for complete V gene, D, and J segment identification.

4.3.4 Cloning and Protein Expression

Lymphocyte RNA was purchased from Sigma and cDNA was obtained using the Cα and Cβ internal primers. This cDNA was used to obtain additional upstream variable region sequence not amplified by the primers described above. Once the variable gene had been determined from sequencing, we designed a 5' primer unique to the start of framework 1 of each TCR variable gene with a 5' EcoRI restriction site added.

Additionally, the reverse-complement of the internal variable gene primers used above provided the 3' primer necessary to acquire the remaining upstream sequence of each TCR variable gene. The entire variable region was then spliced together and unique restriction sites were placed at the 5' and 3' ends. In order to rapidly go from variable gene sequence and identification to expressed TCR α and β chains, TCR expression constructs were generated using the pLM1 expression vector. The alpha and beta constant regions, which contained unique 5' restriction sites, Sac II and SnaB I, respectively, were cloned into pLM1. The 3' end of the Cα and Cβ regions also encoded a streptavidin binding peptide (SBP) tag and a hexa-histidine (HIS) tag, respectively, to aid in TCR protein purification. The TCR variable regions obtained from single-cell PCR could then be easily subcloned into the Cα or Cβ TCR-pLM1 constructs using EcoR I and Sac II or EcoR I and SnaB I, respectively. The TCR alpha and beta chains were then expressed recombinantly in *E. coli* as inclusion bodies.

As a means to test this expression system, the variable domains of the AHIII12.2 (AHIII) TCR α and β chains were PCR amplified using primers that added the unique SacII and SnaBI sites, respectively. These AHIII constructs in the pLM1 expression vector were then transformed into BL21-RIL cells (Stratagene). AHIII TCR α and β chains were expressed as inclusion bodies in *E. coli* in a 5 liter fermenter vessel. Inclusion bodies were then cleaned and solublized in 8M Urea.

4.3.5 TCR Folding Screen

A TCR folding screen was developed to determine the best *in vitro* folding conditions for any new TCR that we are able to isolate. The folding "matrix" of 48 different folding conditions is described in Table 1. Using the AHIII TCR chains as our

model, a 1:1 (α:β) ratio of TCR chains were diluted into an injection buffer consisting of 10 mM Tris, pH 8, 6M Guanidine HCl, and 0.2 mM DTT. 20 μL of this TCR mixture was distributed into the bottom of each well a 96 deep-well (2 mL/well) plate, resulting in 50 μg of protein per well.

Table 1. TCR *in vitro* Folding Matrix

		1	2	3	4	5	6	7	8	9	10	11	12
	Sucrose	-	-	+	+	-	-	+	+	-	-	+	+
	PEG	-	-	-	+	+	+	-	-	-	+	+	+
	Na:K	-	+	-	+	-	+	-	+	-	+	-	+
A/B	GuHCl	-	-	-	-	-	-	+	+	+	+	+	+
	Glutathione	-	-	-	+	+	+	-	-	-	+	+	+
	CHAPS	-	-	-	-	-	-	-	-	-	-	-	-
	Arginine	-	-	-	-	-	-	+	+	+	+	+	+
	pH	-	-	-	-	-	-	-	-	-	-	-	-
	Sucrose	-	-	+	+	-	-	+	+	-	-	+	+
	PEG	-	-	-	+	+	+	-	-	-	+	+	+
	Na:K	-	+	-	+	-	+	-	+	-	+	-	+
C/D	GuHCl	-	-	-	-	-	-	+	+	+	+	+	+
	Glutathione	-	-	-	+	+	+	-	-	-	+	+	+
	CHAPS	+	+	+	+	+	+	+	+	+	+	+	+
	Arginine	-	-	-	-	-	-	+	+	+	+	+	+
	pH	-	-	-	-	-	-	-	-	-	-	-	-
	Sucrose	-	-	+	+	-	-	+	+	-	-	+	+
	PEG	+	+	+	-	-	-	+	+	+	-	-	-
	Na:K	-	+	-	+	-	+	-	+	-	+	-	+
E/F	GuHCl	+	+	+	+	+	+	+	-	-	-	-	-
	Glutathione	-	-	-	+	+	+	-	-	-	+	+	+
	CHAPS	-	-	-	-	-	-	-	-	-	-	-	-
	Arginine	-	-	-	-	-	-	+	+	+	+	+	+
	pH	+	+	+	+	+	+	+	+	+	+	+	+
	Sucrose	-	-	+	+	-	-	+	+	-	-	+	+
	PEG	+	+	+	-	-	-	+	+	+	-	-	-
	Na:K	-	+	-	+	-	+	-	+	-	+	-	+
G/H	GuHCl	+	+	+	+	+	+	-	-	-	-	-	-
	Glutathione	-	-	-	+	+	+	-	-	-	+	+	+
	CHAPS	+	+	+	+	+	+	+	+	+	+	+	+
	Arginine	-	-	-	-	-	-	+	+	+	+	+	+
	pH	+	+	+	+	+	+	+	+	+	+	+	+

Sucrose: (+) 0.4 M; (-) 0 M. PEG: (+) 0.05% PEG 3350, (-) 0%. Na:K: (+) 0.25 M NaCl, 0.01 M KCl; (-) 0 M NaCl, 0 M KCl. GuHCl: (+) 0.5 M; (-) 0 M. Glutathione: (+) 5 mM reduced, 0.5 mM oxidized; (-) 1 mM reduced, 0.1 mM oxidized. CHAPS: (+) 0.06%; (-) 0%. Arginine: (+) 1 M; (-) 0.5 M. pH: (+) 100 mM Tris, pH 8.6; (-) 100 mM Tris, pH 8.2. All conditions also contain 2mM EDTA and 0.01% sodium azide.

To this, 1 mL of the folding buffer was added to the well and aspirated to mix the protein with the buffer. The plate was incubated at 10 °C for 36 hours. In order to rapidly dialyze all 96 wells, the wells were first diluted 1:2 with 10 mM Tris, pH 8. Then

aliquots from all 96 wells were transferred to a 10 kDa cutoff 96 well filter plate (Pall Corporation). Liquid was pulled through the plate using a vacuum plate manifold (Eppendorf). A total volume of 600 μL from each folding condition was concentrated. The volume of each well was then brought up to 400 μL with 10 mM Tris, pH 8. This dialysis step is necessary as the ELISA assay is inhibited by components in the folding buffers (data not shown).

To quickly determine if the condition resulted in correctly folded, active TCR, an ELISA using horseradish peroxidase conjugated pMHC-tetramer was employed. Two dilutions, 1:2 and 1:50, of the samples from the filter plate were added to ELISA plates that had been previously incubated with anti-Cβ antibody, H57 (eBioscience). The appropriate pMHC tetramer was then added, followed by ABTS single solution (Invitrogen), and colorimetric readout was quantified on a plate reader at 415 nm. Background was determined and subtracted using a pMHC tetramer formed with a non-specific peptide.

4.3.6 Folded TCR purification

Following identification of ideal TCR folding condition, folding was then scaled-up to one liter. TCR α and β chains were diluted into 20 mL of injection buffer described above, and rapidly diluted into one liter of folding buffer (as determined from the folding screen) for a total mass of approximately 50 mg of TCR. Following an incubation period of 36 hours at 10 °C, the fold was then dialyzed against 10 liters of 100 mM Urea for 24 hours, followed by another 24 hours of dialysis against 10 liters of 100 mM Urea and 10 mM Tris, pH 8. The dialyzed TCR fold was first batch purified and concentrated using DE52 ion exchange resin (Whatman). The protein was eluted off the DE52 with 20 mL

of 2 M NaCL in 10 mM Tris, pH 8. This was then further concentrated down to 2 mL using Amicon Ultra Centrifugal concentrators (Millipore). This TCR concentrate was then purified using a Biosep SEC S3000 column (Phenomenex) on a Waters HPLC in 250 μL injections.

4.4 RESULTS

4.4.1 Expression Optimization of H-2K^b

Both single cell FACS sorting and the ELISA in the TCR folding screen require pMHC-tetramer as a reagent. Initial attempts to over-express K^b heavy chain as inclusion bodies were unsuccessful (Figure 1a). We examined both the codon usage of our K^b gene and any possible RNA secondary structure as these often effect expression levels. Codon usage of the K^b heavy chain was analyzed using the program "*E. coli* Codon Usage Analysis 2.0" (www.biology.ualberta.ca/pilgrim.hp/links/usage2.0c.html). As shown in Figure 1b, eight of the first 25 codons were rarely used in *E. coli*. Secondary RNA structure analysis using the GeneBee server (Brodsky L.I., 1992) predicted two high-energy RNA hairpins early in the mRNA transcript, one of which started already at the third nucleotide (Figure 1c). Based on these findings the first 28 codons of the K^b heavy chain were rebuilt with ideal *E. coli* expressing codons (Henaut, 1996), which also resulted in removing the high-energy RNA hairpins early in the transcript (Figures 1b and 1c). These changes in the gene resulted in abundant over-expression of the K^b heavy chain (Figure 1a). Following inclusion body clean-up K^b heavy chain was folded *in vitro* with β_2m and peptide. HPLC purified K^b monomers were then biotinylated using the BirA enzyme (Avidity LLC).

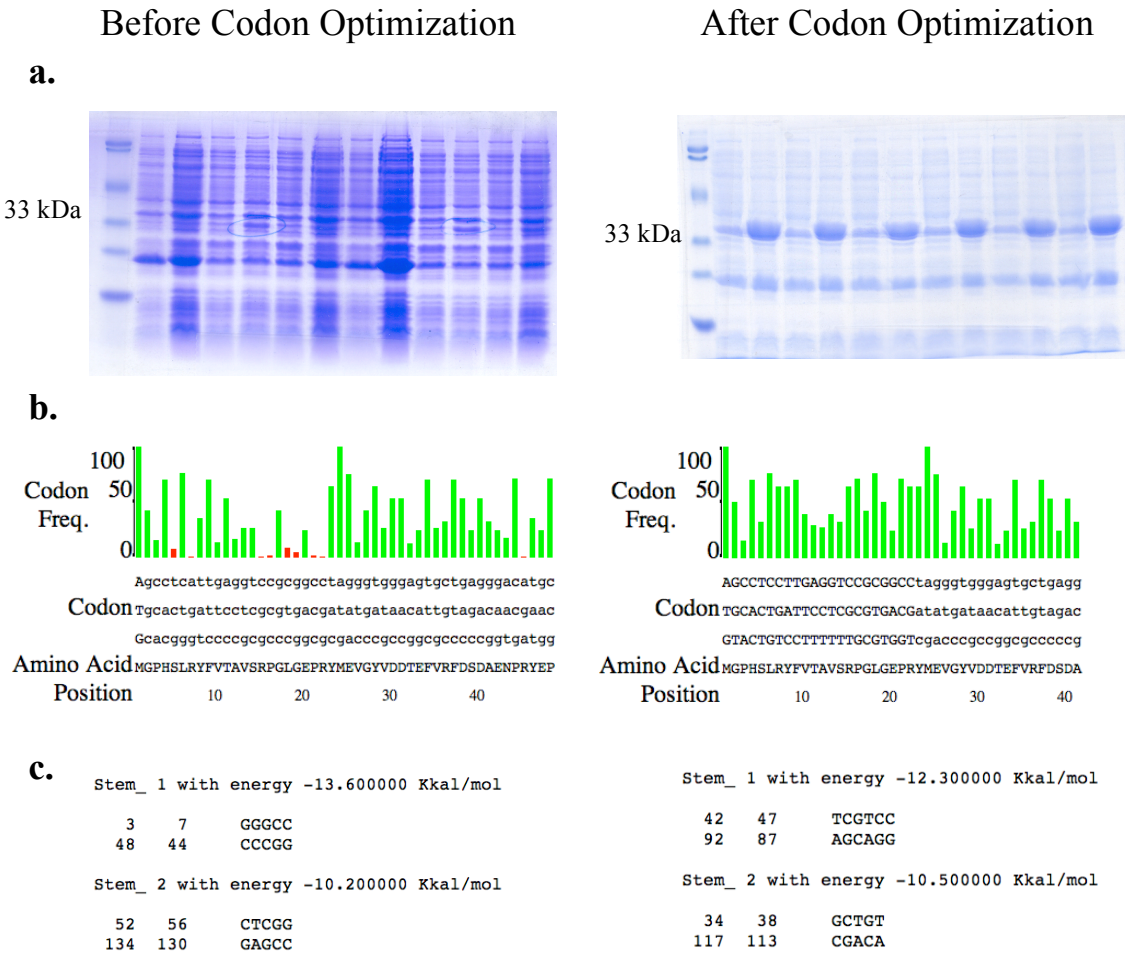

Figure 1. Codon optimization results in successful over-expression of H-2K^b heavy chain. (a) IPTG induced test expressions of K^b heavy chain in pLM1 vector in BL21-Codon Plus cells run on SDS-PAGE gels show almost no expression of K^b with original murine codons. After codon optimization, every colony picked over-expresses heavy chain. (b) Codon analysis determines 8 of the first 25 codons in the original K^b gene are rarely used in *E. coli*, and are subsequently fixed. (c) A high energy RNA hairpin is predicted to start at the third nucleotide of the gene, and is gone following codon optimization.

4.4.2 T cell Isolation, RT-PCR, and TCR Sequencing

As proof of principle, single cell sorting of cytotoxic T cells from Lymphocytic Choriomeningitis Virus (LCMV) infected double konckout mice, CD8α$^{-/-}$ x MHC II$^{-/-}$ (II-/8-) (Riddle et al., 2008), was performed. Infection of mice with LCMV has been used extensively as a model system to study cytotoxic T cell response to viral infection.

LCMV infection in mice provides a number of dominant and subdominant epitopes presented in the context of murine class I MHC H-2D^b (van der Most et al., 1998; van der Most et al., 1996). RT-PCR reactions from individual T cells was performed, run on an agarose gel, and sequences were obtain for the TCR α and β chains (data not shown).

4.4.3 Cloning and Expression of TCR

In order to move quickly from sequence analysis of any TCR α and β chain to expression of protein, TCR expression constructs were created. These TCR α or β specific pLM1 expression constructs already encoded the Cα and Cβ domains, as well as streptavidin binding peptide (SBP) and hexa-histidine (HIS) purification tags, respectively. The variable domains of any TCR with the appropriate restriction sites can be quickly subcloned into these vectors and recombinant TCR chains can be expressed. The variable genes of the AHIII TCR were amplified and subcloned into these expression constructs, and AHIII TCR α and β chains were expressed as inclusion bodies in *E. coli*.

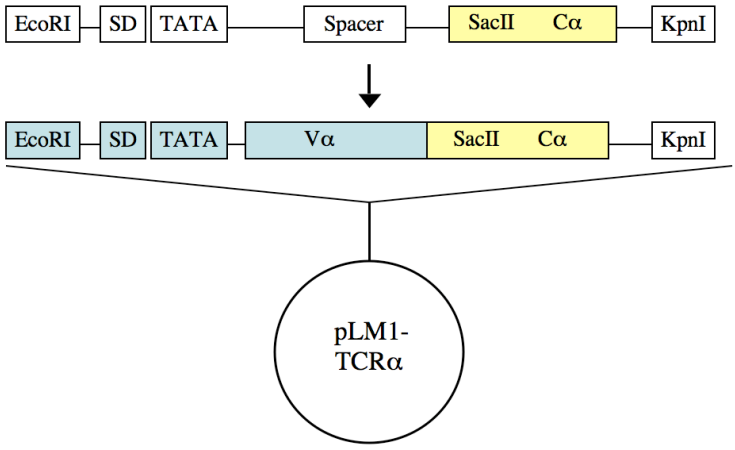

Figure 2. TCR expression vector. TCR Cα and Cβ gene segments were cloned into pLM1 expression vector. The 3' regions of the Cα and Cβ domains contained unique restriction sites allowing for fast subcloning of TCR Vα and Vβ genes into plasmids.

4.4.4 TCR Folding Screen and ELISA

Solubilized inclusion bodies of TCR α and β chains then needed to be folded *in vitro*. We developed a unique TCR folding screen to quickly identify each new TCR's ideal folding conditions. As each TCR has a unique amino acid sequence, it consequently has a unique surface chemistry, and prefers different conditions to fold optimally. The screen matrix contains a random combination of reagents that have been used successfully to fold proteins *in vitro* (Armstrong et al., 1999; Chen and Gouaux, 1997; Heiring and Muller, 2001), as well as reagents for specific considerations of TCR folding, i.e. reducing and oxidizing reagents for disulfide formation in the TCR Ig folds. Our TCR folding screen consists of 48 different conditions listed in Table 1. 48 conditions allows for the sample TCR to be in the same condition twice on a 96 well plate, and be tested using the relevant pMHC tetramer and an irrelevant, negative control, pMHC tetramer.

Proof-of-concept of the folding screen was tested using the AHIII TCR, which has been extensively characterized by our lab (Buslepp et al., 2003a; Buslepp et al., 2003b; Buslepp et al., 2001; Miller et al., 2007; Zhao et al., 1999). The plot in Figure 3a clearly shows that there are conditions in which the AHIII TCR folds well (E12 and G12) and others where it does not. We then wanted to see if the conditions determined in the screen were any better than the existing *in vitro* folding conditions we had previously been using to fold AHIII TCR (Buslepp et al., 2003b; Miller et al., 2007). We did a side-by-side one liter fold of the AHIII TCR using our original folding condition and the E12 folding condition. The E12 folding condition resulted in a cleaner fold (Figure 3b) and doubled our yield of natively folded, active AHIII TCR.

a.

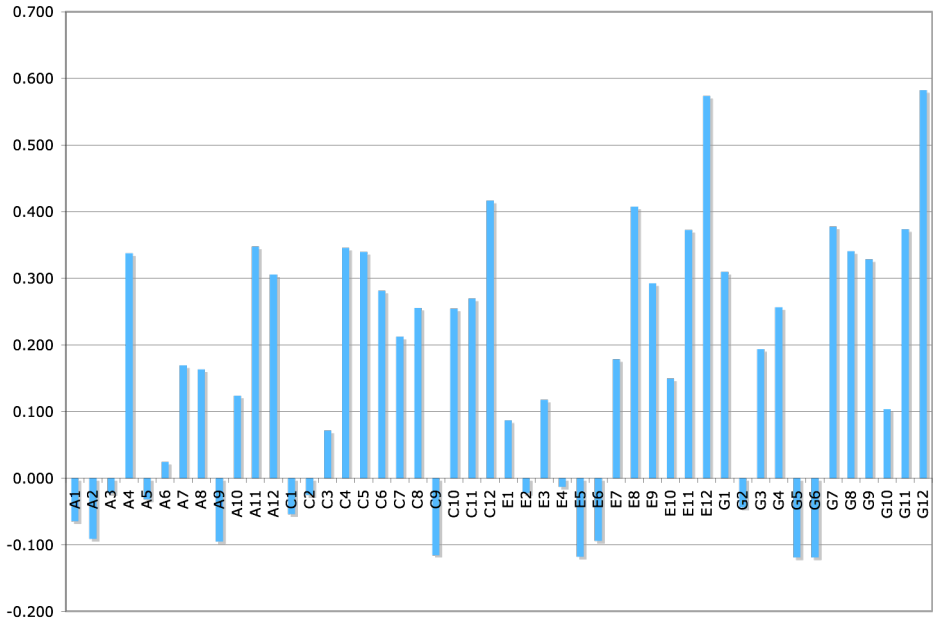

b.

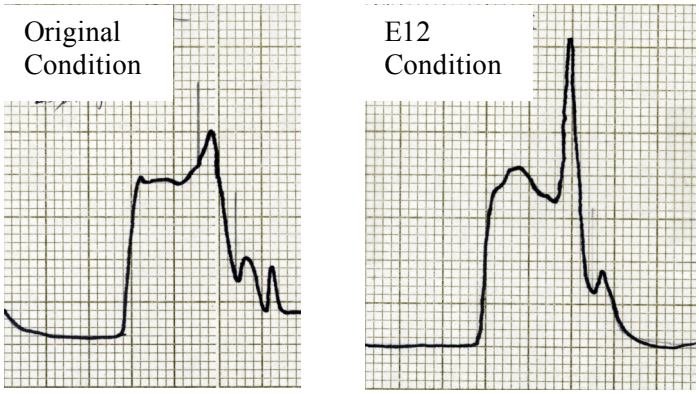

Figure 3. Folding of AHIII TCR is improved as a result of folding screen. (a) ELISA results from AHIII folding screen with p1049/A2 tetramer. Non-specific MLL/A2 tetramer used as negative control. Conditions E12 and G12 resulted in highest amount of functionally folded AHIII TCR. (b) Chromatogram showing size-exclusion purification of AHIII TCR following 1 liter *in vitro* fold. 58 kDa AHIII TCR comes out just before 10 minutes on SEC column. Fold on the left was done with folding conditions traditionally used for AHIII TCR. Fold on the right was done using E12 folding condition. Total yield at the end of purification was doubled using E12 condition.

The functional activity of this AHIII TCR was confirmed using surface plasmon resonance (SPR). All of the SPR experiments performed in Chapter 3 of this dissertation utilized AHIIII TCR generated using these new expression constructs and E12 folding conditions. The TCR was clean, active, and bound its pMHC ligand.

4.5 DISCUSSION

Further study of TCR recognition of pMHC, and the development of TCR mediated therapeutics in a realistic timeframe requires the rapid production of soluble TCR from T cells specific to a pMHC of interest. We present here a means to quickly isolate single T cells directly *ex vivo*, amplify their TCR V genes, subclone those V genes into *E. coli* expression vectors, and rapidly identify the best TCR folding conditions. We have already successfully used this screen to improve the folding yield of our AHIII TCR. We are currently using this scheme to isolate and express TCRs from our double knockout mouse, CD8$\alpha^{-/-}$ x MHC II$^{-/-}$ (Riddle et al., 2008).

Traditional clonal T cell isolation and identification is a long arduous processing taking weeks if not months. Splenocytes or lymphocytes are removed from the mouse and must be cultured and *in vitro* stimulated using irradiated target cells. The surviving T cells are plated out using limiting dilution in hopes to isolate a single clone per well. These are then again *in vitro* stimulated using irradiated target cells (Engelhard and Benjamin, 1982). Most T cells are not happy and do not survive. If they do survive and proliferate, then after weeks of culturing and hopeful clonal expansion, enough cells are present to verify lysis of specific pMHC targets using a cytolysis assay, and isolate RNA and perform RT-PCR to identify the $\alpha\beta$TCR genes.

Most of the T cell systems studied and the determined TCR-pMHC structures have originated from T cells that have been isolated in a traditional limiting dilution manner. In addition to the time that it takes to finally characterize the TCR from these cells, we must ask ourselves an important question. Are these immortalized T cells that survived weeks of abuse, truly good representatives of T cells as a whole? Perhaps the affinities we have measured, kinetics we have determined, and TCR-pMHC docking orientations that we have seen are characteristic of these "super" T cells that were able to outlast all others *in vitro*, but not characteristic of most T cells. A rapid method allowing isolation of T cells directly ex vivo, without weeks of culturing and in vitro stimulation, may permit the isolation and characterization of T cells with unique properties not yet seen.

4.6 REFERENCES

Abad J. D., Wrzensinski C., Overwijk W., De Witte M. A., Jorritsma A., Hsu C., Gattinoni L., Cohen C. J., Paulos C. M., Palmer D. C., Haanen J. B., Schumacher T. N., Rosenberg S. A., Restifo N. P. and Morgan R. A. (2008) T-cell receptor gene therapy of established tumors in a murine melanoma model. *J Immunother* **31**, 1-6.

Armstrong N., de Lencastre A. and Gouaux E. (1999) A new protein folding screen: application to the ligand binding domains of a glutamate and kainate receptor and to lysozyme and carbonic anhydrase. *Protein Sci* **8**, 1475-83.

Baker F. J., Lee M., Chien Y. H. and Davis M. M. (2002) Restricted islet-cell reactive T cell repertoire of early pancreatic islet infiltrates in NOD mice. *Proc Natl Acad Sci U S A* **99**, 9374-9.

Brodsky L.I. A. V. V., Ya.L. Kalaydzidis, Yu.S. Osipov, A.R.L. Tatuzov, S.I. Feranchuk. (1992) GeneBee: the Program Package for Biopolymer Structure Analysis. *Dimacs* **8**, 127-139.

Buslepp J., Kerry S. E., Loftus D., Frelinger J. A., Appella E. and Collins E. J. (2003a) High affinity xenoreactive TCR:MHC interaction recruits CD8 in absence of binding to MHC. *J Immunol* **170**, 373-83.

Buslepp J., Wang H., Biddison W. E., Appella E. and Collins E. J. (2003b) A correlation between TCR Valpha docking on MHC and CD8 dependence: implications for T cell selection. *Immunity* **19**, 595-606.

Buslepp J., Zhao R., Donnini D., Loftus D., Saad M., Appella E. and Collins E. J. (2001) T cell activity correlates with oligomeric peptide-major histocompatibility complex binding on T cell surface. *J Biol Chem* **276**, 47320-8.

Chen G. Q. and Gouaux E. (1997) Overexpression of a glutamate receptor (GluR2) ligand binding domain in Escherichia coli: application of a novel protein folding screen. *Proc Natl Acad Sci U S A* **94**, 13431-6.

Engelhard V. H. and Benjamin C. (1982) Isolation and characterization of monoclonal mouse cytotoxic T lymphocytes with specificity for HLA-A,B or -DR alloantigens. *J Immunol* **129**, 2621-9.

Giudicelli V., Chaume D. and Lefranc M. P. (2004) IMGT/V-QUEST, an integrated software program for immunoglobulin and T cell receptor V-J and V-D-J rearrangement analysis. *Nucleic Acids Res* **32**, W435-40.

Heiring C. and Muller Y. A. (2001) Folding screening assayed by proteolysis: application to various cystine deletion mutants of vascular endothelial growth factor. *Protein Eng* **14**, 183-8.

Henaut D. (1996) Analysis and Predictions from Escherichia coli sequences. In *Escherichia coli and Salmonella* (Edited by Neidhardt F. C.), Vol. 2, p. 2047-2066. ASM Press, Washington, D.C.

Johnson L. A., Heemskerk B., Powell D. J., Jr., Cohen C. J., Morgan R. A., Dudley M. E., Robbins P. F. and Rosenberg S. A. (2006) Gene transfer of tumor-reactive TCR confers both high avidity and tumor reactivity to nonreactive peripheral blood mononuclear cells and tumor-infiltrating lymphocytes. *J Immunol* **177**, 6548-59.

Miller P. J., Pazy Y., Conti B., Riddle D., Appella E. and Collins E. J. (2007) Single MHC mutation eliminates enthalpy associated with T cell receptor binding. *J Mol Biol* **373**, 315-27.

Riddle D. S., Miller P. J., Vincent B. G., Kepler T. B., Maile R., Frelinger J. A. and Collins E. J. (2008) Rescue of cytotoxic function in the CD8alpha knockout mouse by removal of MHC class II. *Eur J Immunol* **38**, 1511-21.

Rudolph M. G., Stanfield R. L. and Wilson I. A. (2006) How TCRs bind MHCs, peptides, and coreceptors. *Annu Rev Immunol* **24**, 419-66.

Rudolph R. and Lilie H. (1996) In vitro folding of inclusion body proteins. *FASEB J* **10**, 49-56.

Schatz D. G. and Spanopoulou E. (2005) Biochemistry of V(D)J recombination. *Curr Top Microbiol Immunol* **290**, 49-85.

Spicuglia S., Franchini D. M. and Ferrier P. (2006) Regulation of V(D)J recombination. *Curr Opin Immunol* **18**, 158-63.

van der Most R. G., Murali-Krishna K., Whitton J. L., Oseroff C., Alexander J., Southwood S., Sidney J., Chesnut R. W., Sette A. and Ahmed R. (1998) Identification of Db- and Kb-restricted subdominant cytotoxic T-cell responses in lymphocytic choriomeningitis virus-infected mice. *Virology* **240**, 158-67.

van der Most R. G., Sette A., Oseroff C., Alexander J., Murali-Krishna K., Lau L. L., Southwood S., Sidney J., Chesnut R. W., Matloubian M. and Ahmed R. (1996) Analysis of cytotoxic T cell responses to dominant and subdominant epitopes during acute and chronic lymphocytic choriomeningitis virus infection. *J Immunol* **157**, 5543-54.

Wong C. P., Li L., Frelinger J. A. and Tisch R. (2006) Early autoimmune destruction of islet grafts is associated with a restricted repertoire of IGRP-specific CD8+ T cells in diabetic nonobese diabetic mice. *J Immunol* **176**, 1637-44.

Wong C. P., Stevens R., Long B., Li L., Wang Y., Wallet M. A., Goudy K. S., Frelinger J. A. and Tisch R. (2007) Identical beta cell-specific CD8(+) T cell clonotypes typically reside in both peripheral blood lymphocyte and pancreatic islets. *J Immunol* **178**, 1388-95.

Zhao R., Loftus D. J., Appella E. and Collins E. J. (1999) Structural evidence of T cell xeno-reactivity in the absence of molecular mimicry. *J Exp Med* **189**, 359-70.

Zhao Y., Bennett A. D., Zheng Z., Wang Q. J., Robbins P. F., Yu L. Y., Li Y., Molloy P. E., Dunn S. M., Jakobsen B. K., Rosenberg S. A. and Morgan R. A. (2007) High-affinity TCRs generated by phage display provide CD4+ T cells with the ability to recognize and kill tumor cell lines. *J Immunol* **179**, 5845-54.

CHAPTER 5

DISCUSSION AND FUTURE DIRECTIONS

5.1 Introduction

TCR discrimination between self and non-self pMHC is the critical event in determining whether or not the CTL will be activated and lyse the antigen presenting cell. T cell activation through the cognate pMHC generates an agonist T cell response, including clonal proliferation, cytokine production, and ultimately cytolysis. Altered peptide ligands, generated through mutations of the peptide or MHC, can result in a range of T cell responses. It remains unclear how the TCR recognition of these different pMHC surfaces translates into qualitatively different signals in the T cell. The goal of my project was to dissect and investigate the interaction between TCR and pMHC to determine what mechanism(s) exists to differentiate between agonist, partial agonist, and antagonist ligands.

The AHIII12.2 (AHIII) TCR recognizes and is activated by its cognate pMHC, p1049 in HLA-A2(A2), while activation is inhibited by the peptide p1058 when presented by A2. Through mutation of residues in both the peptides and MHC, we present here further support for the affinity model of T cell triggering, that AHIII T cell activation correlates with TCR-pMHC binding affinity. Interestingly, mutations in the peptide seem to be more deleterious to binding than mutations in the MHC. Crystal structures of A2 mutants bound to the AHIII TCR were determined, and showed that the

K66A mutation in the MHC can influence the conformation of a TCR CDR3 loop, which is generally thought of as being restricted to peptide recognition. Thermodynamic analysis of p1049/A2(K66A) binding confirmed that the loop movement results in a loss H-bonds. Thermodynamic analysis of the AHIII TCR binding to wild-type p1049/A2 determined that binding occurs through favorable enthalpy and favor entropy, which contradicts the favored thermodynamic TCR-pMHC binding model of an enthalpically driven and entropically apposed binding. Finally, we present here a streamlined protocol to express and purify soluble TCR from singly isolated T cells directly *ex vivo*.

5.2 Mutation in MHC Results in CDR3 Movement in TCR and Loss of Binding Enthalpy

Based on the co-crystal structure of the AHIII TCR bound to p1049/A2 (Buslepp et al., 2003), we chose to mutate residues in A2 that either made contacts to the AHIII TCR or residues that had high sequence identity in HLA MHC allotypes. The main goal of the project presented in Chapter 2 was to determine what is happening on the molecular level between the AHIII TCR and these mutated p1049/A2 molecules to better understand how TCR-pMHC molecular recognition occurs. Using these MHC mutants we first measured the resulting T cell response in the form of cytolysis. From the range of responses observed, three representative A2 mutants, T163A, W167A, and K66A, were selected for further study. Binding constants and co-crystal structures of the AHIII TCR and the three mutants were determined. K66 in wild-type p1049/A2 makes contacts with both peptide and TCR and had previously been identified as a critical residue for recognition in other TCRs (Baker et al., 2001; Baxter et al., 2004; Gagnon et al., 2005; Wang et al., 2002); however, the affect of K66A on a bound TCR has never been seen structurally. The K66A mutation resulted in the lowest AHIII T cell response and the

lowest binding affinity. These data along with the binding and activation data for the other A2 mutants, suggests that T cell response may correlate with affinity. Importantly, the K66A mutation in A2 does not affect the conformation of the peptide. The decrease in affinity for AHIII-p1049/A2(K66A) appears to be due to a loss in hydrogen bonds in the interface as a result of a conformational change in the TCR CDR3α loop. The resolution to which the AHIII-p1049/A2(K66A) structure was determined was too low to confidently place residue side chains and H-bonds. Therefore, isothermal titration calorimetry (ITC) was able to confirm the loss of hydrogen bonding by a measured loss in enthalpy (ΔH). Our findings in Chapter 2 are inconsistent with the notion that the CDR1 and CDR2 loops of the TCR are responsible for MHC restriction, while the CDR3 loops interact solely with the peptide. Instead, we found a MHC mutation in the peptide binding cleft that does not change the conformation of the peptide, yet results in an altered conformation of a CDR3 loop.

5.3 The AHIII TCR Binds Antagonist pMHC with Very Weak Affinity

T cell activation is not binary, as a full range of T cell responses have been reported, which stem from the discriminatory ability of the TCR to recognize self from non-self pMHC ligands. Variants of a fully activating peptide, or altered peptide ligands (APL), can produce this range of responses, including antagonism, whereby the T cell response is actually inhibited. TCR engagement with antagonist pMHC complexes actually results in unique phosphorylation events with T cell activation signaling molecules inside the cell (Schwartz, 2003). It remains unclear through which biophysical mechanism this altered signaling event occurs. Previous work by our lab has suggested that the p1058 peptide, when presented by A2, acts as an antagonist peptide on the AHIII

T cell (Buslepp et al., 2001). This p1058 peptide (FAPGFFPYL) differs from the agonist p1049 (ALWGFFPVL) peptide by only a few residues. The goal of the project presented in Chapter 3 was to identify which TCR-pMHC binding parameter(s) is important for determining the difference between an agonist and antagonist pMHC. A panel of over 20 variants of p1049 and p1058 presented in A2 was used in surface plasmon resonance experiments to determine binding constants to the AHIII TCR. The data presented here suggest that the antagonism of p1058 correlates with a very weak binding affinity and this weak binding is due to the inability of the AHIII TCR to bind p1058/A2 without undergoing a conformational change. These data also suggest that mutations made on the surface of the MHC molecule are better tolerated by the TCR than mutations in the peptide.

5.4 Improved Expression, Folding, and Purification of TCR

There are an estimate 10^8 clonal T cells in the body, each with a unique TCR, but most of what we know about TCR-pMHC binding is based on the study of only two dozen T cell receptors (reviewed Chapter 1). Traditionally the task of isolating a T cell specific for a particular pMHC target, identifying the DNA sequences of its αβTCR, and recombinantly expressing these TCR, has been incredible arduous and can take years. To be able to answer fundamental questions about TCR-pMHC recognition that still exist, and identify and produce TCR that could be used as potential therapeutics, the rate of TCR identification and production needs to increase. During my time here working on the projects presented in Chapter 2 and 3, I was able to develop methods to improve the TCR isolation, folding, and purification. The work in Chapter 4 presents a TCR production scheme that can go from infection of mice to purified, soluble, recombinant

TCR in less than two months. All of the AHIII TCR used for SPR studies in Chapter 3 was generated following this new protocol. This TCR production scheme is currently being employed on a project involving a double knockout mouse generated by our lab (Riddle et al., 2008) to isolate T cells and generate soluble TCR for biophysical and structural studies.

5.5 Contributions to the Understanding of TCR-pMHC Molecular Recognition

Although exceptions exist, the two-step binding model (Wu et al., 2002) is favored to depict TCR-pMHC molecular recognition. As the name implies, this model describes the TCR-pMHC binding event in two discrete steps. First, the CDR1 and CDR2 loops of the TCR make contact with the α helices of the MHC, followed by the CDR3 loops contacting the peptide after finding the right conformation. The data presented in Chapter 2 is inconsistent with this model. The K66A mutation in the α helix of the MHC induces a conformational change in the CDR3 loop of AHIII TCR. This finding and data from other sources (Davis-Harrison et al., 2007; Kjer-Nielsen et al., 2003) suggest that the pMHC should be thought of as one surface that the TCR recognizes using all of its CDR loops; peptide and MHC should not be thought of as two separate pieces.

Between the work presented in Chapter 2 and 3, we have mutated a full spectrum of residues on the pMHC surface, which contact the TCR. Combining this large data set, the data suggest something interesting regarding how the CDR loops are involved in AHIII-p1049/A2 molecular recognition. Chapter 2 focused on mutations made in the TCR binding surface of the A2 MHC and their effect on the TCR. While SPR data was presented for only three MHC mutants, data had been collected for an entire panel of A2

mutants. The A2(K66A) mutant had the worst binding affinity to the AHIII TCR compared with any of the other A2 mutants. We showed that the K66A mutation resulted in a conformational change in the CDR3α loop, eliminated a number of hydrogen bonds. Yet, the determined TCR-pMHC dissociation constant (K_d) was still approximately 30 μM. All of the mutations presented in Chapter 3 take place in the peptides presented by A2. All the mutations to peptide residues between position 3 and position 7 result in binding affinities worse than that of the K66A mutation in A2. Any amino acid substitution at P3 through P6 results in a K_d of greater than 100 μM. This says that the contacts made between the AHIII TCR CDR3 loops and the p1049 peptide are more critical than the contacts made to the A2 MHC. While the entire pMHC surface is recognized by the CDR loops of TCR, the discriminatory power of the TCR between agonist and antagonist comes from the interaction of CDR3 loops with the peptide.

When we set out to analyze the energetics of AHIII-p1049/A2 binding using ITC, few thermodynamic experiments had been performed and it was generally accepted that TCR-pMHC binding was enthalpically driven and entropically unfavorable (Anikeeva et al., 2003; Boniface et al., 1999; Garcia et al., 2001; Krogsgaard et al., 2003; Lee et al., 2004; Willcox et al., 1999). These results were satisfying considering polar interactions should provide the specificity seen with TCR-pMHC recognition, compared to relying on van der Waals contacts. In addition, entropically unfavorable binding seems to correlate well with the idea that flexible CDR loops are being constricted upon TCR-pMHC binding. Our thermodynamic data presented in Chapter 2 show that this is enthalpically driven TCR-pMHC binding model is not generalizable to all TCR-pMHC. The AHIII TCR binds to p1049/A2 with a small enthalpic contribution and is entropically favorable.

As we prepared our manuscript for publication, other groups began reporting similar data proving entropically favorable, and sometimes entropically driven, TCR-pMHC binding does occur (Colf et al., 2007; Davis-Harrison et al., 2005; Ely et al., 2006).

Finally, the AHIII TCR and its recognition of p1049/A2 brings into question the concept that H-bonds and enthalpically driven binding drive high specificity interactions. As mentioned above our thermodynamic data and data of others have shown that TCR-pMHC binding can be achieved with little or no enthalpic contribution. Additionally, as seen by our SPR data in Chapter 3, the critical residues for AHIII-p1049/A2 binding recognition are positions 5 and position 6 in the p1049 peptide, which are hydrophobic phenylalanine residues at both positions. Only 21 H-bonds occur in the AHIII-p1049/A2 interface (Buslepp et al., 2003), and the recently determined structure of 2C-QL9/L^d (Colf et al., 2007) reveals an interface with less than 10 hydrogen bonds. What does this say about specificity? If there are no hydrogen bonds determining specificity, the only way the TCR can be sure to only recognize the foreign complex must be complementarity of fit. Not surprisingly perhaps, AHIII-p1049/A2 (Buslepp et al., 2003) and 2C-QL9/L^d (Colf et al., 2007) have the greatest complementarity of fit of all TCR-pMHC structures determined to date. Perhaps we should be more careful ruling out the importance of van der Waals contacts in conferring specificity.

5.6 Future Experiments

While I have completed a large body of work over the last five years, by no means is this dissertation an exhaustive analysis of TCR-pMHC interactions. The Collins lab will continue to probe the AHIII T cell system and is in the process of expressing new TCR from other model systems to look at fundamental questions like whether conserved

TCR-pMHC contacts exist and why the TCR seems to dock all pMHC molecules in a canonical diagonal orientation.

Specifically, the biophysical data presented in Chapter 3 will be combined with a full spectrum of biological assays on AHIII T cells including cytolysis, proliferation, and cytokine secretion, as a means to evaluate any correlation between TCR-pMHC recognition and T cell activation. This will be the most comprehensive analysis of TCR-pMHC binding and resultant T cell activation to date; over 20 different peptides evaluated using SPR and three separate aspects of T cell activation. Based on previously published (Chapter 2) (Buslepp et al., 2001; Miller et al., 2007) and preliminary data, we expect to see CTL killing with p1049 and its variants to correlate with affinity. The antagonistic ability of p1058 should also increase as affinity decreases. As antagonistic peptides have been shown to have a differential cytokine profile of decreased IL-2 production, but normal IFNγ secretion (Schwartz, 2003), we expect to see this profile for p1058. Similarly, we expect no proliferation of AHIII T cells exposed to antagonist peptides.

Also from Chapter 3, the enormous decrease in the off-rate measured for the p1049(V8A) mutant using SPR cannot be explained through analysis of the existing co-crystal structure of AHIII-p1049/A2 (Buslepp et al., 2003). We are already in the process of screening for crystal conditions in the hopes of determining the co-crystal structure of the AHIII TCR bound to p1049(V8A)/A2. We feel confident this will be successful as other mutant structures presented in Chapter 2 were crystallized with AHIII, and the V8A mutation actually results in a higher affinity and long half-life, theoretically increasing the chances of the complex to crystallize. Aside from the crystal structure, isothermal

titration calorimetry (ITC) will be used to evaluate changes to the enthalpy and entropy of binding in AHIII-p1049(V8A)/A2. Changes in ΔH and ΔS between the wild-type complex and the V8A mutant will provide energetic details about how the AHIII-p1049(V8A)/A2 interaction achieves such tight binding and slow off-rate.

Finally, the T cell isolation scheme and TCR folding screen will be utilized heavily in the future here in the Collins lab. Our lab recently generated a double knockout mouse, without class II MHC and CD8 (Riddle et al., 2008), to determine the effect of not having the CD8 coreceptor present during thymic selection (reviewed in Chapter 1). This mouse has functional cytotoxic T cells and attempts are underway using the isolation scheme and TCR folding screen to isolate TCR for biophysical and structural studies.

5.7 REFERENCES

Anikeeva N., Lebedeva T., Krogsgaard M., Tetin S. Y., Martinez-Hackert E., Kalams S. A., Davis M. M. and Sykulev Y. (2003) Distinct molecular mechanisms account for the specificity of two different T-cell receptors. *Biochemistry* **42**, 4709-16.

Baker B. M., Turner R. V., Gagnon S. J., Wiley D. C. and Biddison W. E. (2001) Identification of a crucial energetic footprint on the alpha1 helix of human histocompatibility leukocyte antigen (HLA)-A2 that provides functional interactions for recognition by tax peptide/HLA-A2-specific T cell receptors. *J Exp Med* **193**, 551-62.

Baxter T. K., Gagnon S. J., Davis-Harrison R. L., Beck J. C., Binz A. K., Turner R. V., Biddison W. E. and Baker B. M. (2004) Strategic mutations in the class I major histocompatibility complex HLA-A2 independently affect both peptide binding and T cell receptor recognition. *J Biol Chem* **279**, 29175-84.

Boniface J. J., Reich Z., Lyons D. S. and Davis M. M. (1999) Thermodynamics of T cell receptor binding to peptide-MHC: evidence for a general mechanism of molecular scanning. *Proc Natl Acad Sci U S A* **96**, 11446-51.

Buslepp J., Wang H., Biddison W. E., Appella E. and Collins E. J. (2003) A correlation between TCR Valpha docking on MHC and CD8 dependence: implications for T cell selection. *Immunity* **19**, 595-606.

Buslepp J., Zhao R., Donnini D., Loftus D., Saad M., Appella E. and Collins E. J. (2001) T cell activity correlates with oligomeric peptide-major histocompatibility complex binding on T cell surface. *J Biol Chem* **276**, 47320-8.

Colf L. A., Bankovich A. J., Hanick N. A., Bowerman N. A., Jones L. L., Kranz D. M. and Garcia K. C. (2007) How a single T cell receptor recognizes both self and foreign MHC. *Cell* **129**, 135-46.

Davis-Harrison R. L., Armstrong K. M. and Baker B. M. (2005) Two different T cell receptors use different thermodynamic strategies to recognize the same peptide/MHC ligand. *J Mol Biol* **346**, 533-50.

Davis-Harrison R. L., Insaidoo F. K. and Baker B. M. (2007) T Cell Receptor Binding Transition States and Recognition of Peptide/MHC. *Biochemistry* **46**, 1840-50.

Ely L. K., Beddoe T., Clements C. S., Matthews J. M., Purcell A. W., Kjer-Nielsen L., McCluskey J. and Rossjohn J. (2006) Disparate thermodynamics governing T cell receptor-MHC-I interactions implicate extrinsic factors in guiding MHC restriction. *Proc Natl Acad Sci U S A* **103**, 6641-6.

Gagnon S. J., Borbulevych O. Y., Davis-Harrison R. L., Baxter T. K., Clemens J. R., Armstrong K. M., Turner R. V., Damirjian M., Biddison W. E. and Baker B. M. (2005) Unraveling a hotspot for TCR recognition on HLA-A2: evidence against the existence of peptide-independent TCR binding determinants. *J Mol Biol* **353**, 556-73.

Garcia K. C., Radu C. G., Ho J., Ober R. J. and Ward E. S. (2001) Kinetics and thermodynamics of T cell receptor- autoantigen interactions in murine experimental autoimmune encephalomyelitis. *Proc Natl Acad Sci U S A* **98**, 6818-23.

Kjer-Nielsen L., Clements C. S., Purcell A. W., Brooks A. G., Whisstock J. C., Burrows S. R., McCluskey J. and Rossjohn J. (2003) A structural basis for the selection of dominant alphabeta T cell receptors in antiviral immunity. *Immunity* **18**, 53-64.

Krogsgaard M., Prado N., Adams E. J., He X. L., Chow D. C., Wilson D. B., Garcia K. C. and Davis M. M. (2003) Evidence that structural rearrangements and/or flexibility during TCR binding can contribute to T cell activation. *Mol Cell* **12**, 1367-78.

Lee J. K., Stewart-Jones G., Dong T., Harlos K., Di Gleria K., Dorrell L., Douek D. C., van der Merwe P. A., Jones E. Y. and McMichael A. J. (2004) T cell cross-reactivity and conformational changes during TCR engagement. *J Exp Med* **200**, 1455-66.

Miller P. J., Pazy Y., Conti B., Riddle D., Appella E. and Collins E. J. (2007) Single MHC mutation eliminates enthalpy associated with T cell receptor binding. *J Mol Biol* **373**, 315-27.

Riddle D. S., Miller P. J., Vincent B. G., Kepler T. B., Maile R., Frelinger J. A. and Collins E. J. (2008) Rescue of cytotoxic function in the CD8alpha knockout mouse by removal of MHC class II. *Eur J Immunol* **38**, 1511-21.

Schwartz R. H. (2003) T cell anergy. *Annu Rev Immunol* **21**, 305-34.

Wang Z., Turner R., Baker B. M. and Biddison W. E. (2002) MHC allele-specific molecular features determine peptide/HLA-A2 conformations that are recognized by HLA-A2-restricted T cell receptors. *J Immunol* **169**, 3146-54.

Willcox B. E., Gao G. F., Wyer J. R., Ladbury J. E., Bell J. I., Jakobsen B. K. and van der Merwe P. A. (1999) TCR binding to peptide-MHC stabilizes a flexible recognition interface. *Immunity* **10**, 357-65.

Wu L. C., Tuot D. S., Lyons D. S., Garcia K. C. and Davis M. M. (2002) Two-step binding mechanism for T-cell receptor recognition of peptide MHC. *Nature* **418**, 552-6.